

# Development of new antimicrobial peptides against *Mycobacterium* *tuberculosis*

Sara Cristina Pinto Silva

Molecular and Cellular Biology Master's  
Dissertation presented to Faculty of Sciences,  
University of Porto

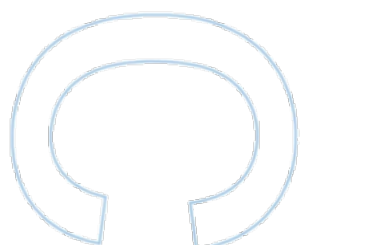
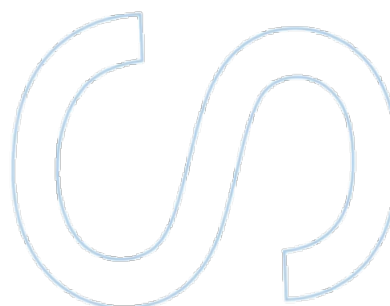
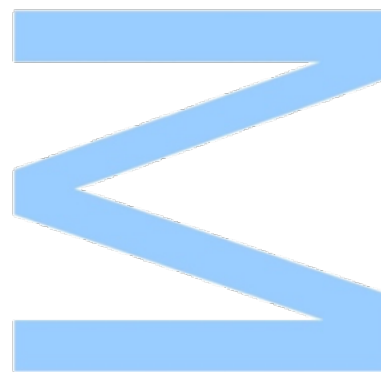
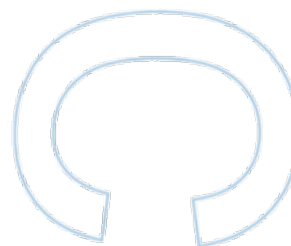
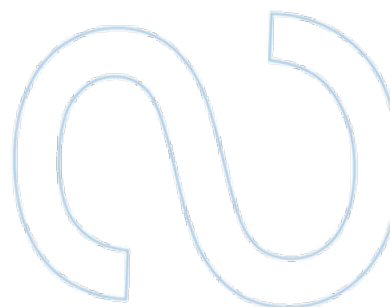
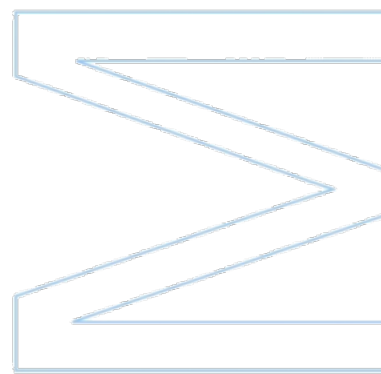
2017

## Supervisor

Prof. Dr. Nuno Filipe de Sousa Vale,  
*FCT Researcher, UCIBIO/REQUIMTE*  
*Invited Professor of Pharmacology,*  
*Faculty of Pharmacy, University of Porto*

## Laboratório de acolhimento:

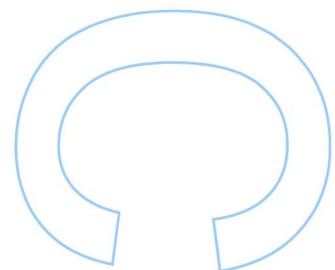
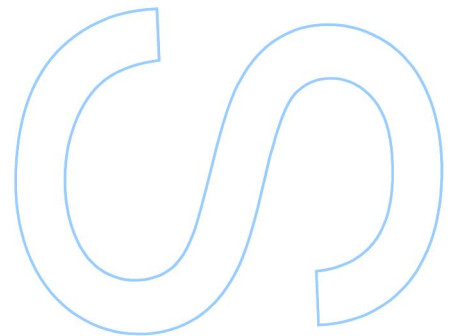
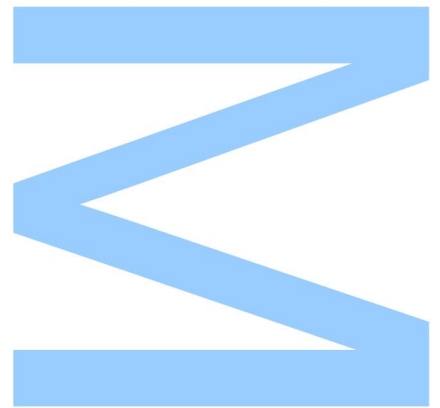
Laboratório nacional de referência de mycobacterias, Porto  
Instituto Nacional de saúde Ricardo Jorge





Todas as correções determinadas  
pelo júri, e só essas, foram efetuadas.  
O Presidente do Júri,

Porto, \_\_\_\_/\_\_\_\_/\_\_\_\_



# Declaração

Eu, Sara Cristina Pinto Silva, aluno/a com o número 201502152 do mestrado de Biologia Celular e Molecular da edição de 2016/2017, declaro por minha honra que sou a autora da totalidade do texto apresentado, não apresento texto plagiado, e tomei conhecimento das consequências de uma situação de plágio.

Faculdade de Ciências da Universidade do Porto

13-09-2017

Assinatura

# ACKNOWLEDGEMENTS

I want to acknowledge Professor Nuno Vale, for accepting to supervise and reviewing my thesis and for providing all the support, facilities and contacts necessary to perform the work. I also want to thank Dr. Anabela Santos Silva, Cristina Ferro and Professor José Manuel Correia da Costa, for all the support, care and access to the Laboratório nacional de referência de Mycobacterias in order to performed experiments with *Mycobacterium tuberculosis*. Thanks also for Alexandra Fraga from University of Minho for cytotoxicity study.

In addition, I express my gratitude to Ana Cristina Silva and Fernando Silva, my mother and father, without them none of this would be possible, I am truly blessed.

Finally, I acknowledge, Rui Ferreira and all my friends for their insatiable support and love.

I thank you all.



## Abstract

Tuberculosis (TB) is known as one of the 10 causes of death by infectious agent, worldwide. It affects around 10.4 million people per year and is still associated with a high number of deaths. Although the incidence of TB has declined in recent years, with HIV coinfection and the increasing appearance of multiple antibiotic resistance (MDR-TB) or cases of extensive resistance to antibiotics (XDR-TB), it's necessary the development of new effective TB therapy. Cationic antimicrobial peptides (CAMPs) emerge in the research as safe and effective against a variable range of bacterial and fungi pathogens, including *Mycobacterium tuberculosis* (*Mtb*). In addition, cinnamic acid had shown an interesting antimicrobial activity, particularly against TB. In the present project we synthesized, purified and characterized 10 peptides CAMP, which five present an N-terminal modification with addition of a cinnamic acid derivate, and also studied the antimicrobial activity against clinical isolates of *Mtb* and MDR-TB. In order to determine the cytotoxicity of AMPs towards eukaryotic cells, we performed a MTS assay in TPH-1 cells as the macrophage model. Almost all modified CAMP presented a enhance activity against both *Mtb* strains and were capable to disrupt heavily clumping of mycobacteria in culture. Moreover, all modified CAMPs were able to substantial inhibit the intra cellular growth of both strain at low concentrations.

**Keywords:** *Mycobacterium tuberculosis*; Peptides; antimicrobial activity; MIC

## Resumo

A Tuberculose (TB) caracteriza-se por ser uma doença infecciosa grave que, a nível global, afeta por ano cerca de 10,4 milhões de pessoas, estando ainda associada a um grande número de mortes. Apesar de nos últimos anos a taxa de incidência de TB ter diminuído, com a coinfeção com HIV e o aparecimento crescente de casos com resistência múltipla a antibióticos (MDR-TB) ou casos de resistência extensa a antibióticos (XDR-TB), tornaram urgente o desenvolvimento de terapias efetivas contra a TB. Os péptidos catiónicos antimicrobianos (CAMPs) surgem na investigação como sendo seguros e eficazes contra diversos patógenos, incluído *Mycobacterium tuberculosis* (*Mtb*). Para além disso, os ácidos cinâmicos têm demonstrado um potencial antimicrobiano, também contra a TB. No presente projeto, foram sintetizados, purificados e caracterizados 10 péptidos CAMPs, nos quais 5 apresentavam modificação N-terminal com adição de um derivado ácido cinâmico, e foi igualmente estudada a atividade antimicrobiana contra *Mtb* e MDR-TB. O grau de citotoxicidade provocado por estes 10 CAMPs foi calculado por MTS em células TPH-1 previamente diferenciadas em macrófagos. Quase todos os CAMPs modificados apresentaram um aumento da atividade contra *Mtb* e MDR. Todos os CAMPs modificados foram capazes, em cultura, de quebrar agregados de *Mtb* e inibir substancialmente, em concentrações baixas, o crescimento celular de ambas as estirpes estudadas.

# Index

Declaração .....	3
ACKNOWLEDGEMENTS.....	4
Abstract .....	5
Resumo .....	6
List of figures.....	9
List of tables.....	13
LIST OF ABBREVIATIONS .....	14
Objectives .....	16
1. Introduction.....	17
1.1. History .....	17
1.2. <i>Mycobacterium tuberculosis</i> .....	17
1.3. Transmission and Pathogenesis of <i>Mtb</i> .....	18
1.4. Current treatment.....	20
1.5. Development of resistant strains .....	23
1.6. New drugs.....	24
1.7. The impact of <i>Mtb</i> in the world.....	25
1.8. CAMPs .....	27
1.9. Natural occurring CAMPs .....	27
1.10. Mechanism of action.....	28
1.11. Antimicrobial potential.....	30
1.12. CAMPS against <i>Mtb</i> . .....	31
1.13. Cinnamic acids .....	36
1.14. Cinnamic acids against <i>Mtb</i> .....	36
1.15. Solid Phase Peptide Synthesis (SPPS) .....	38
2. Materials and Methods.....	40
2.1. Reagents, Solvents and Equipment .....	40
2.2. Peptide Synthesis by SPPS.....	40
2.2.1. Manual Synthesis developed in this Project.....	40
2.2.2. Preparation of the resin .....	41
2.2.3. Kaiser Test .....	42
2.2.4. Coupling of Amino Acids and Deprotection Cycles .....	43
2.2.5. Structural modification of CAMPs.....	43
2.2.6. Cleavage and deprotection of side chains of the peptide.....	44
2.3. Purification of the conjugates .....	44

2.3.1.	Antimicrobial peptides .....	44
<b>2.4.</b>	<b><i>In vitro</i> assays .....</b>	<b>46</b>
2.4.1.	Mycobacterial strains, growth conditions and inoculum preparation .....	46
2.4.2.	Preparation of Resazurin .....	47
2.4.3.	Anti-Mycobacterium tuberculosis assays .....	47
2.5.	Cell culture .....	48
2.6.	Cytotoxicity assay .....	49
<b>2.7.</b>	<b>Statistical analysis .....</b>	<b>49</b>
<b>3.</b>	<b>Results .....</b>	<b>49</b>
<b>3.1.</b>	<b>Peptide synthesis and characterization .....</b>	<b>49</b>
3.1.1.	CAMP1 .....	49
3.1.2.	CAMP2 .....	50
3.1.3.	CAMP3 .....	51
3.1.4.	CAMP5 .....	52
3.1.5.	CAMP7 .....	53
<b>3.2.</b>	<b>Structural modification of CAMP with cinnamic derivates .....</b>	<b>55</b>
3.2.1.	Cin+CAMP1 .....	55
3.2.2.	Cin+CAMP2 .....	56
3.2.3.	Cin+CAMP3 .....	58
3.2.4.	Cin+CAMP5 .....	59
3.2.5.	Cin+CAMP7 .....	60
<b>3.3.</b>	<b>Peptide Purification values .....</b>	<b>62</b>
<b>3.4.</b>	<b><i>In vitro</i> anti-tuberculosis assay .....</b>	<b>63</b>
<b>3.5.</b>	<b>Determination of peptide cytotoxicity .....</b>	<b>69</b>
<b>4.</b>	<b>Discussion .....</b>	<b>70</b>
<b>5.</b>	<b>Conclusions and Future perspectives .....</b>	<b>72</b>
<b>6.</b>	<b>Supplementary Information .....</b>	<b>73</b>
<b>6.1.</b>	<b>Work Plan .....</b>	<b>73</b>
<b>6.2.</b>	<b>Peptides purification analysis .....</b>	<b>75</b>
<b>7.</b>	<b>References .....</b>	<b>80</b>

## List of figures

Figure 1- Cell wall structure of: a) Mycobacteria consist of thin layers of peptidoglycan covalently bond with arabinogalactan, and a thick layer of mycolic acids. b) Gram-positive bacteria have a single lipid membrane surrounded by a thick layer of peptidoglycan and lipoteichoic acid. (Adapted from Brown et al. 2015).....	18
Figure 2 - Chronological events after inhalation of <i>M. tuberculosis</i> . Schematized the different possible scenarios of Tuberculosis disease. (Adapted from van Crevel et al. 2002).....	20
Figure 3 - General scheme of FAS-II system involved in mycolic acids biosynthesis Orange frame enzyme targets of INH. (adapted from Yoya 2009).....	22
Figure 4 - The molecular structures of first line drugs used against TB (A - Rifampin; B - Isoniazid; C - Pirazinamide; D - Etambutol). ....	23
Figure 5 - Molecular structures of (A) Bedaquiline and (B) Delamanid.....	25
Figure 6 - Estimated TB incidence rates, 2015. Adapted from (WHO 2016) .....	25
Figure 7 - Percentage of new TB cases with MDR-TB. Adapted from (WHO 2016) .....	26
Figure 8 - Schematic models of mechanism of action of CAMPs. (A) The carpet mechanism (B) The barrel-stave mechanism (c) The toroid pore. (adapted from Brogden 2005).....	29
Figure 9 - Molecular structure of trans-cinnamic acid. ....	36
Figure 10 - General scheme of SPPS. X=O,NH; AA= amino acid; PG=protecting group; TPG=temporary group; P - resin.....	39
Figure 11 - Manual SPPS development in this project. ....	41
Figure 12 - Ninhydrin reaction with primary amines, resulting in the formation of chromophore (deep blue). ....	42
Figure 13 - schematized the 96 well-plate, was performed serial two-fold dilutions (0,25-128 µg/mL); CAMP(n): CAMP without modification N-terminal; Cin+CAMP(n), CAMP with modification in N-terminal coupling cinnamic acid; Positive control (180µL medium + 20µL bacterial suspension + 1.04 µg/mL).....	48
Figure 14 – Chromatogram of the product of the manual synthesis of the peptide CAMP1, acquired with a HPLC system, with a C18 column, using ACN in water with 0.05% TFA as eluent, in gradient mode (0 – 100%), for 30 minutes, at a flow of 1 mL/min and detection at λ = 220 nm. ....	50
Figure 15 - Mass spectrum (LC-ESI/Orbitrap MS, positive mode) of the peptide CAMP1 (manual synthesis). ....	50
Figure 16 - Chromatogram of the product of the manual synthesis of the peptide CAMP2, acquired with a HPLC system, with a C18 column, using ACN in water with 0.05% TFA as eluent, in gradient mode (0 – 100%), for 30 minutes, at a flow of 1 mL/min and detection at λ = 220 nm. ....	51
Figure 17 - Mass spectrum (LC-ESI/Orbitrap MS, positive mode) of the peptide CAM2 (manual synthesis). ....	51
Figure 18 - Chromatogram of the product of the manual synthesis of the peptide CAMP3, acquired with a HPLC system, with a C18 column, using ACN in water with 0.05% TFA as eluent, in gradient mode (0 – 100%), for 30 minutes, at a flow of 1 mL/min and detection at λ = 220 nm. ....	52
Figure 19 - Mass spectrum (LC-ESI/Orbitrap MS, positive mode) of the peptide CAMP3 (manual synthesis). ....	52

Figure 20 - Chromatogram of the product of the manual synthesis of the peptide CAMP5, acquired with a HPLC system, with a C18 column, using ACN in water with 0.05% TFA as eluent, in gradient mode (0 – 100%), for 30 minutes, at a flow of 1 mL/min and detection at $\lambda = 220$ nm. ....	53
Figure 21 - Mass spectrum (LC-ESI/Orbitrap MS, positive mode) of the peptide CAMP5 (manual synthesis). ....	53
Figure 22 - Chromatogram of the product of the manual synthesis of the peptide CAMP7, acquired with a HPLC system, with a C18 column, using ACN in water with 0.05% TFA as eluent, in gradient mode (0 – 100%), for 30 minutes, at a flow of 1 mL/min and detection at $\lambda = 220$ nm. ....	54
Figure 23 - Mass spectrum (LC-ESI/Orbitrap MS, positive mode) of the peptide CAMP7 (manual synthesis). ....	54
Figure 24 - Chromatogram of the product of the manual synthesis of the peptide Cin+CAMP1, acquired with a HPLC system, with a C18 column, using ACN in water with 0.05% TFA as eluent, in gradient mode (0 – 100%), for 30 minutes, at a flow of 1 mL/min and detection at $\lambda = 220$ nm. ....	56
Figure 25 - Mass spectrum (LC-ESI/Orbitrap MS, positive mode) of the peptide Cin+CAMP1 (manual synthesis). ....	56
Figure 26 - Chromatogram of the product of the manual synthesis of the peptide Cin+CAMP2, acquired with a HPLC system, with a C18 column, using ACN in water with 0.05% TFA as eluent, in gradient mode (0 – 100%), for 30 minutes, at a flow of 1 mL/min and detection at $\lambda = 220$ nm. ....	57
Figure 27 - Mass spectrum (LC-ESI/Orbitrap MS, positive mode) of the peptide Cin+CAMP2 (manual synthesis). ....	57
Figure 28 - Chromatogram of the product of the manual synthesis of the peptide Cin+CAMP3, acquired with a HPLC system, with a C18 column, using ACN in water with 0.05% TFA as eluent, in gradient mode (0 – 100%), for 30 minutes, at a flow of 1 mL/min and detection at $\lambda = 220$ nm. ....	58
Figure 29 - Mass spectrum (LC-ESI/Orbitrap MS, positive mode) of the peptide Cin+CAMP3 (manual synthesis). ....	59
Figure 30 - Chromatogram of the product of the manual synthesis of the peptide Cin+CAMP5, acquired with a HPLC system, with a C18 column, using ACN in water with 0.05% TFA as eluent, in gradient mode (0 – 100%), for 30 minutes, at a flow of 1 mL/min and detection at $\lambda = 220$ nm. ....	59
Figure 31 - Mass spectrum (LC-ESI/Orbitrap MS, positive mode) of the peptide Cin+CAMP5 (manual synthesis). ....	60
Figure 32 - Chromatogram of the product of the manual synthesis of the peptide Cin+CAMP7, acquired with a HPLC system, with a C18 column, using ACN in water with 0.05% TFA as eluent, in gradient mode (0 – 100%), for 30 minutes, at a flow of 1 mL/min and detection at $\lambda = 220$ nm. ....	60
Figure 33 - Mass spectrum (LC-ESI/Orbitrap MS, positive mode) of the peptide Cin+CAMP7 (manual synthesis). ....	61
Figure 34 - MIC activities of CAMP1, Cin+CAMP1, CAMP3, Cin+CAMP3 against susceptible Mtb expressed in $\mu$ M. ....	64
Figure 35 - MIC50 activities of CAMP(n) and Cin+CAMP(n) against susceptible Mtb expressed in $\mu$ M. ....	65

Figure 36 - In vitro anti-TB screening of D-AMPs activity against <i>Mtb</i> clinical isolates susceptible strain H37Rv; Representative light microscope images show the growth condition of the bacteria at various concentrations of CAMP(n) and Cin+CAMP(n) after 7 days of incubation. The framed images indicate the lowest concentrations of each peptide to inhibit 95% of bacterial growth compared with the growth control and further confirmed through REMA assay.....	67
Figure 37 - MIC50 activities of CAMP(n) and Cin+CAMP(n) against Resistance <i>Mtb</i> MDR (INH,RIF and STR) expressed in $\mu$ M. ....	68
Figure 38 - Cytotoxicity of CAMP1 and Cin+CAMP(n) on THP-1 cells. Values expressed in $\mu$ g/mL, in collaboration with University of Minho. ....	69
Figure 39 - Chromatogram of the CAMP1 purified peptide, acquired with a HPLC system, with a C18 column, using ACN in water with 0.05% TFA as eluent, in gradient mode (0 – 100%), for 30 minutes, at a flow of 1 mL/min and detection at $\lambda = 220$ nm. ....	75
Figure 40 - Chromatogram of the Cin+CAMP1 purified peptide, acquired with a HPLC system, with a C18 column, using ACN in water with 0.05% TFA as eluent, in gradient mode (0 – 100%), for 30 minutes, at a flow of 1 mL/min and detection at $\lambda = 220$ .....	75
Figure 41 - Chromatogram of the CAMP2 purified peptide, acquired with a HPLC system, with a C18 column, using ACN in water with 0.05% TFA as eluent, in gradient mode (0 – 100%), for 30 minutes, at a flow of 1 mL/min and detection at $\lambda = 220$ . ....	76
Figure 42 - Chromatogram of the Cin+CAMP2 purified peptide, acquired with a HPLC system, with a C18 column, using ACN in water with 0.05% TFA as eluent, in gradient mode (0 – 100%), for 30 minutes, at a flow of 1 mL/min and detection at $\lambda = 220$ .....	76
Figure 43 - Chromatogram of the CAMP3 purified peptide, acquired with a HPLC system, with a C18 column, using ACN in water with 0.05% TFA as eluent, in gradient mode (0 – 100%), for 30 minutes, at a flow of 1 mL/min and detection at $\lambda = 220$ . ....	77
Figure 44 - Chromatogram of the Cin+CAMP3 purified peptide, acquired with a HPLC system, with a C18 column, using ACN in water with 0.05% TFA as eluent, in gradient mode (0 – 100%), for 30 minutes, at a flow of 1 mL/min and detection at $\lambda = 220$ .....	77
Figure 45 - Chromatogram of the CAMP5 purified peptide, acquired with a HPLC system, with a C18 column, using ACN in water with 0.05% TFA as eluent, in gradient mode (0 – 100%), for 30 minutes, at a flow of 1 mL/min and detection at $\lambda = 220$ .....	78
Figure 46 - Chromatogram of the Cin+CAMP5 purified peptide, acquired with a HPLC system, with a C18 column, using ACN in water with 0.05% TFA as eluent, in gradient mode (0 – 100%), for 30 minutes, at a flow of 1 mL/min and detection at $\lambda = 220$ . ....	78
Figure 47 - Chromatogram of the CAMP7 purified peptide, acquired with a HPLC system, with a C18 column, using ACN in water with 0.05% TFA as eluent, in gradient mode (0 – 100%), for 30 minutes, at a flow of 1 mL/min and detection at $\lambda = 220$ .....	79

Figure 48 - Chromatogram of the Cin+CAMP7 purified peptide, acquired with a HPLC system, with a C18 column, using ACN in water with 0.05% TFA as eluent, in gradient mode (0 – 100%), for 30 minutes, at a flow of 1 mL/min and detection at  $\lambda = 220$  .....79



## List of tables

Table 1 - Recommended treatment regimen against new TB cases. ....	21
Table 2 - Examples of AMPs showing in vitro or in vivo activity against <i>M. tuberculosis</i> and respective mechanisms of action. ....	32
Table 3 - Sequence of synthesized CAMP(n) in this project. ....	45
Table 4 - Sequence of synthesised Cin+CAMP(n) in this project. ....	45
Table 5 - The exact mass and molecular mass observed of the CAMP(n) peptides detected by LC-MS and retention time determined by HPLC. ....	55
Table 6 - The exact mass and molecular mass observed of the Cin+CAMP(n) peptides detected by LC-MS and retention time determid by HPLC. ....	61
Table 7 - Percentage of purification and amount of the manual synthesis CAMP(n) and Cin+CAMP(n). Purification step was performed as previously described in Experimental Procedures by RP-MPLC (purification analysis and quantification was made by HPLC, results in Supplementary information). ....	62
Table 8 - Reduction of MIC50 of Cin+CAMP(n) compared with IC50 of parental CAMP(n) against <i>Mtb</i> . ....	64
Table 9 - Reduction of MIC50 of Cin+CAMP(n) compared with IC50 CAMP(n) against MDR-TB. ....	67
Table 10 - Minimum inhibitory concentrations (MIC) of synthetic peptides against <i>Mtb</i> H37Rv and MDR <i>Mtb</i> (resistant to INH, RIF and STR) expressed in µg/m and µM. ....	68
Table 11 - Summary of IC50 of CAMP(n) and Cin+CAMP(n) of the MTS assay performed in THP-1 cells. Results are an average of two independent repeated experiments. (1) Value of reference previously describe in (Ramón-García et al. 2013). ....	69

# LIST OF ABBREVIATIONS

AAn -  $\alpha$ -amino acids  
 ACN – acetonitrile  
 ACP - enoyl-acyl carrier protein  
 AIDS - acquire immune deficiency syndrome  
 AMP – antimicrobial peptide  
 CAMP – cationic antimicrobial peptide  
 Cin+CAMP – cinnamic acid conjugated cationic antimicrobial peptide  
 DCM – Dichloromethane  
 DIAE – Diisopropylethylamine  
 DMF – Dimethylformamide  
 EMB – Ethambutol  
 FAS- fatty acid synthase  
 FCS - fetal calf serum  
 Fmoc – fluorenylmethoxycarbonyl  
 H<sub>2</sub>O<sub>dd</sub> – sterile distilled Water  
 HBD - human beta-defensins  
 HBTU - O-(benzotriazol-1-yl)-N,N,N',N'- tetramethyluronium hexafluorophosphate  
 HNP - human neutrophil defensins  
 HPLC - high-performance liquid chromatography  
 IC<sub>50</sub> - half maximal inhibitory concentration  
 INH - isoniazid  
 KasA - Ketoacyl-ACP synthase A  
 LC/MS - mass spectrometry  
 LJ - Lowenstein-Jensen  
 MB 7H9 - Middlebrook 7H9 brot medium  
 MDR-TB- multi drug resistant tuberculosis  
 MIC - minimum inhibitory concentration  
*Mtb* – *Mycobacterium tuberculosis*  
 MTS - 3-(4,5-dimethylthiazol-2-yl)-5-(3-carboxymethoxyphenyl)-2-(4-sulfophenyl)-2H-tetrazolium  
 PC - Phosphatidylcholine  
 PE -Phosphatidylethanolamine  
 PEG - Polyethylene glycol  
 PG - Phosphatidylglycerol

PMA - phorbol-myristate actate

PZA - Pyrazinamide

REMA – Resazurin Microtiter Assay Plate

RIF - Rifampin

RR-MPLC - Reverse Phase Medium-Pressure Liquid Chromatography

R<sub>t</sub> - retention time

SM - Sphingomyelin

SPPS - Solid Phase Peptide Synthesis

STR – streptomycin

TB- Tuberculosis

TBTU - N,N,N',N'-Tetramethyl-O-(benzotriazol-1-yl)uronium tetrafluoroborate

tBu - tert-butyl

TFA - trifluoroacetic acid

TIS – Triisopropylsilane

WHO – World health organization

XDR-TB – Extensive drug resistant tuberculosis

## Objectives

The main goal of the work developed in this thesis was the synthesises of new cationic antimicrobial peptides using cinnamic acids.

CAMP(n):

- 1 – WKWLKKWIK
- 2 – WRKFWKYLK
- 3 – RLWWWWRRR
- 4 – RIRRWKFRW
- 5 – RQRRVVIWW

Cin+CAMP(n):

- 1 - trans cinnamic+WKWLKKWIK
- 2 - p-methoxycinnamic+WRKFWKYLK
- 3 - 3,4-Dimethoxycinnamic+RLWWWWRRR
- 4 - o-Nitrocinnamic+RIRRWKFRW
- 5 - trans cinnamic+RQRRVVIWW

Furthermore, the work aimed the study of the respective antimicrobial activity against *Mtb* and MDR-TB, as well to evaluate the cytotoxicity against TPH-1 cells differentiated into macrophages.

# 1. Introduction

## *Human Tuberculosis*

### 1.1. History

In the study of tuberculosis, René Laennec a French physician holds an important position in medical history being one of the pioneers of clinical-pathological correlations and his descriptions of pulmonary lesions in patients. In this work, published in 1821 entitled 'A treatise on diseases of the chest', Laennec demonstrated drawn images of tuberculosis cavities and detailed descriptions of the pathologic changes ceasing with now known necrosis of the tissues. Through the examination of a patient body, he observed pathological similar lesions diffuse in different organs due to the same causative illness. However, he didn't find the cause behind the disease. Nevertheless, in 1868 a French military physician, Jean-Antoine Villemin, made a landmark study entitled 'Etudes sur la tuberculosis', on this research he described the transmissibility capability of tuberculosis infect throughout species such as from human to rabbits, from cows to rabbits and so on. Villemin exemplified the transmission of the disease to a rabbit with an injection of purulent liquid of tuberculosis cavities, yet he didn't found the responsible agent. The cause of tuberculosis was not found until Robert Koch contribution, being the first to identify and isolate the tubercle bacilli. Koch continued his work with the discovery of a substance, now known as tuberculin, and though that could have a potential impact on tuberculosis cure. Unfortunately for Koch, research tuberculin didn't cure tuberculosis, even so, he was capable to report cell-mediated immune responses for the first time (Schluger 2005; Smith 2003).

### 1.2. *Mycobacterium tuberculosis*

*Mycobacterium tuberculosis* (*Mtb*) is an aerobic obligate pathogen with G+C rich content and rod shape morphology of 0.3-0.5  $\mu\text{m}$  of diameter (Cole et al. 1998; Niederweiss 2013). Even though *Mtb* is classified as gram-positive bacteria, the composition of the cell wall differs from other gram-positive bacteria (Figure 1). The composition of the mycobacterial cell wall is determined by the presence of peptidoglycan layer which is covalently attached to arabinogalactans linked to mycolic acids (Brown et al. 2015). Mycolic acids structure is defined by a long chain  $\alpha$ -alkyl  $\beta$ -hydroxy fatty acids and corresponds to around 60% of the cell wall size. The biosynthesis of these structures

occurs with carboxylation of acetyl-CoA into acetyl-CoA carboxylase which is incorporated into the growing acyl chain during the repetitive cycle of fatty acid synthase (FAS) I and II reactions. FAS I catalyse the production of c24/C26-coA (alfa-branch) and FAS II elongates into meromycolic acid (C54/C56 – AcpM) (Pawelczyk and Kremer 2014). The complexity lipid-rich cell wall provides protection to chemical injury, dehydration and contributes to the extended persistence of *Mtb* bacilli within the host cells.

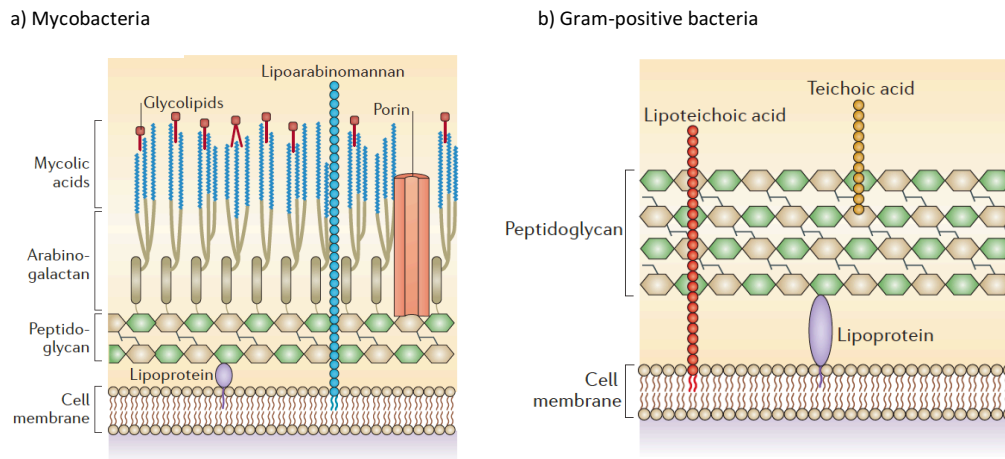


**Figure 1- Cell wall structure of: a) Mycobacteria consist of thin layers of peptidoglycan covalently bond with arabinogalactan, and a thick layer of mycolic acids. b) Gram-positive bacteria have a single lipid membrane surrounded by a thick layer of peptidoglycan and lipoteichoic acid. (Adapted from Brown et al. 2015)**

### 1.3. Transmission and Pathogenesis of *Mtb*

*Mtb* is transmitted through the air in airborne droplet nucleic when patients with active disease cough, sneeze, speak or sing. Tuberculosis disease is characterised by four major stages.

The first stage of infection occurs when the inhaled tuberculosis droplet reaches the alveolus, further implantation preferentially affect the middle and lower zones of the lungs (Leung 1999). Once lodged in the alveolus, *Mtb* bind to macrophage through mannose, complement and scavenger receptors and the bacilli are phagocytosis (van Crevel, et al. 2002). *Mtb* is kept in macrophage phagosome and is able to block the normal fusion with lysosome which is responsible for the creation of a stress environment conditions (acid pH, ROS, enzymes and peptides). The protection capability of *Mtb* which inhibits phagosome-lysosome fusion has been associated with different mechanism of

response. One side is consider that affect  $\text{Ca}^{2+}$  response by preventing the increase of  $\text{Ca}^{2+}$  levels and is also postulated that mycobacterial phagosome is capable of recruit large amounts of Rab5 proteins which are associated with endosome trafficking of early endosome (Delogu et al. 2015; Smith 2003). Within 3 to 8 weeks the bacillus has multiply causing the host macrophage to burst forming the Ghon complex and free bacilli through lymphatic circulation are able to disseminate to more distant tissues and organs.

The second stage, lasting about 3 months or delayed for up 2 years, is marked by the spread of *Mtb* throughout the body. When tuberculosis disease only affects the lungs is referred as pulmonary TB but can affect other organs such as larynx, the lymph nodes, pleural, the brain, the kidneys, or the bones and joints and is referred as extrapulmonary TB. In some infected individuals, an acute and fatal disease can occur in the form meningitis, if *Mtb* reach the nervous system. The case of miliary TB (when *Mtb* is disseminate through the all body) is normally associated with infants and children and severely immunocompromised individuals (Canadian Thoracic Society and The Public Health Agency of Canada and Licensor 2014). Clinical symptoms associated with TB reflect in systemic manifestations such as fever, anorexia, night sweats and cough from weeks to months. In approximately 5% of adult patients have a complete absence of symptoms (Leung 1999).

On the last stage (resolution) the primary complex is associated with the stagnation of the disease up to 3 years and characterized by the continuous development of granulomatous focal lesions and extra pulmonary lesions. The diversity of clinical manifestations between TB patients is influenced by age and immune strength. The success of tuberculosis infection in the early stage is determined by the strength of the host immune response. Around 90-95% of cases of *Mtb* are restricted and arrest in its latent form where infected patients do not show any signs or symptoms. The ability of *Mtb* of resisting immune responses in periods of latent infection is an essential feature. *Mtb* is able to switch between dormant and active state replicating bacilli as constantly stimulates T-cell responses which prevent the emergence of TB disease (Delogu et al. 2015). The maintenance of this persistent state is due to the incredible sensorial perception of the surrounding conditions and the composition of the extracellular matrix (Cole et al. 1998; Niederweiss 2013) (Figure 2).

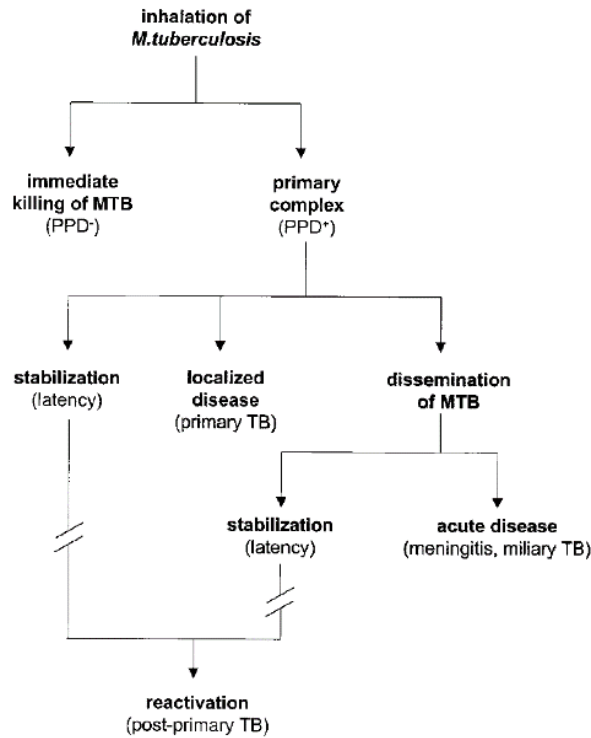


Figure 2 - Chronological events after inhalation of *M. tuberculosis*. Schematized the different possible scenarios of Tuberculosis disease. (Adapted from van Crevel et al. 2002)

## 1.4. Current treatment

The standard treatment for new TB patient with the active TB disease, recommended by the World Health Organization (WHO 2016), is characterise by a 6 month regiment divided in intensive phase of isoniazida (INH), rifampin (RIF), pyrazinamide (PZA) and Etanbutol (EMB) for 2 months, followed by INH and RIF for further 4 months. The standard treatment rate of cure is 83%. In cases of latent *Mtb* infections treatment with antibiotic is indicated for prevention of the development of active TB. The treatment can be administrated with drug alone treatment of INH or RIF for 9 months or through drug combination by 2 months of RIF followed by 2 or 3 months of PZA (Table 1) (Gleeson and Decker 2006; Ormerod 2005).



**Table 1 - Recommended treatment regimen against new TB cases.**

Active Disease		
Treatment	Time	Drugs
Intense phase	2 months	INH+RIF+PZA+EMB
Continuous Phase	4 months	INH+RIF
Latent Disease		
Treatment	Time	Drugs
Drug Alone	9 months	INH or RIF
Drug Combination	2 months	RIF
	2-3 months	PZA

INH introduced for the treatment of TB in 1952, was a high selectivity and antimicrobial activity against *Mtb*. The mechanism of action is composed by three steps: starting with activation of pro-drug into active drug, then INH binds to the target molecule and terminates with inhibition of mycolic acid synthesis. INH active form binds to the enoyl-acyl carrier protein (ACP) reductase one of FAS II system enzyme and it also targets the enzyme Ketoacyl-ACP synthase A (KasA) responsible to elongate fatty acids chain (Figure 3). Unfortunately, INH is only active against growing *Mtb* and possess adverse drug reactions in some patients such as hepatotoxicity, rash, fever or arthralgia (Figure 4).

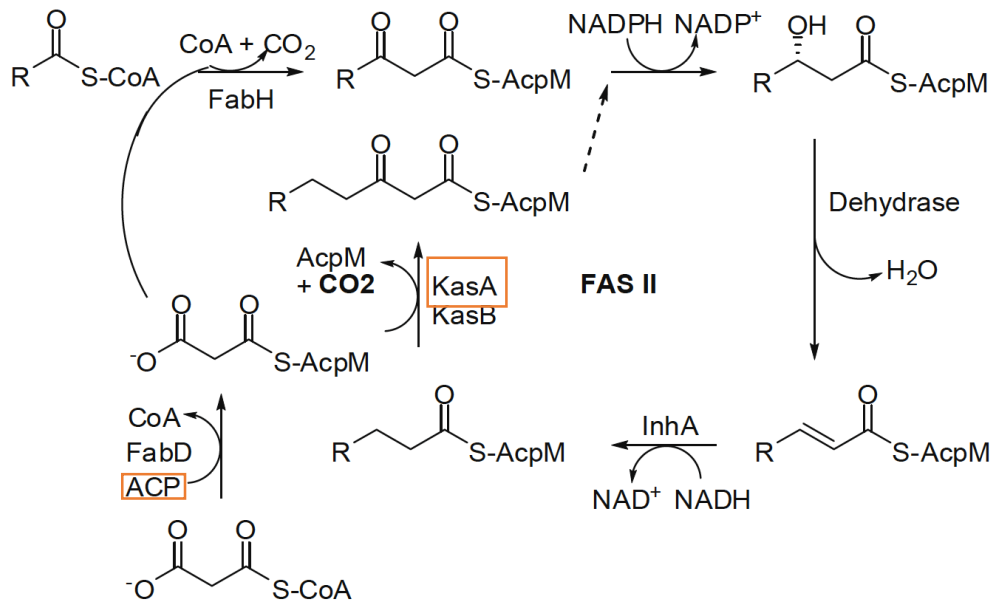


**Figure 3 - General scheme of FAS-II system involved in mycolic acids biosynthesis. Orange frame enzyme targets of INH. (adapted from Yoya 2009).**

RIF applied on treatment regimens since 1968, not only target intracellular, semi dormant *Mtb* present in Necrotic granuloma lesions but also replicating *Mtb*. RIF are associated with inhibition of transcription. The drug binds to the  $\beta$ -subunit of the DNA-dependent RNA polymerase resulting on alteration of conformation which leads to protein mistranslation through the incorporation of mismatch codons. The side effects are associated with hepatotoxicity effects, gastrointestinal and hypersensitivity reactions (Kohanski et al. 2010) (Figure 4).

EMB was first introduced in 1961 and is active against only to replicating *Mtb*. Responsible for inhibition of cell wall synthesis by targeting Arabinosyl transferase, EMB presents a bacteriostatic effect rather than bactericidal as the other compounds (Figure 4).

PZA, as excellent sterilizing effect on growing and not growing bacilli and is only active in acidic pH, reaching the *Mtb* in the interior of macrophages. (Somoskovi et al, 2001; Woods et al. 2012) (Figure 4).

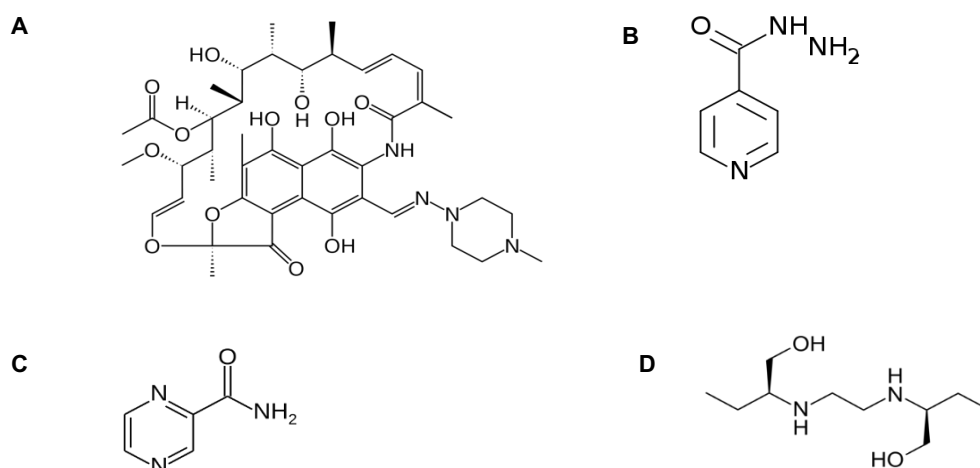


Figure 4 - The molecular structures of first line drugs used against TB (A - Rifampin; B - Isoniazid; C - Pirazinamide; D - Etambutol).

## 1.5. Development of resistant strains

*Mtb* is known as one of the most successful pathogens caused by an infectious organism. The discovery of streptomycin (STR) in 1945 for the treatment of TB made possible the cure of TB disease and boosted the development of new compounds. Over the years TB incidence decreased significantly, unfortunately the increasing epidemic acquire immune deficiency syndrome (AIDS) and the emergence of drug resistant consequently led to the recidivism of TB. Exposure to a drug induces stress responses that lead to both genetic and physiological mechanisms in order to survive (Reviewed in Chevalier et al. 2014 and Nguyen 2016).

The drug resistant *Mtb* is acquired through spontaneous chromosomal mutations that gives advantage of the strain to resist an antibiotic. For each antibiotic resistance, *Mtb* can present mutation on gene or group genes which reflects with alteration on composition of the cell wall or with an effect on the antibiotic target (Hoagland et al. 2016). The highly hydrophobic membrane cell wall of *Mtb* act as a selective barrier against antibiotic. Many mutated genes reported consequently changes in the membrane composition and fluidity (Cole et al. 1998).

The effect on the antibiotic target mechanism consists in modifying the structure (e.g Mutations on *rpoB* are responsible for conformational change at beta-subunit of RNA polymerase leading to a decrease in binding affinity of Rif) suppression or overexpression (The suppression of the antibiotic target such as Catalase peroxidase which results in a decrease on prodrug activation of INH), inactive drugs through

chemical modification (Mutations in *pncA* reducing conversion to active acid form of PZA), drug efflux (Tap, a transporter responsible for mycobacterial efflux of aminoglycosides, spectinomycin, tetracycline ) (Hoagland et al. 2016; Nguyen 2016; Sarathy et al. 2012).

The *Mtb* resistant strain can be divided into three major group based on the level of antibiotic resistance: Multi-drug resistant tuberculosis (MDR-TB) with drug resistance to at least the first-line drugs INH and RIF, extensively drug-resistant tuberculosis (XDR-TB) with drug resistance to the first line drugs INH and RIF and to specific second-line drug (resistant to quinolones and injectable drugs) and totally drug resistant tuberculosis (TDR-TB) drug resistance to all first and second line drugs.

## 1.6. New drugs

The development of new anti-tubercular drugs stagnated in time for over 50 years but with the synergy of TB with HIV, crescent multi drug resistances cases associated with exacerbate population growth culminated in an urgent need for new compounds. In the past few years, two new synthesis compounds have been approved for treatment of MDR-TB.

Bedaquiline, the family of diarylquinolones are the most advance anti-tubercular drugs currently available in the market. This drug is active from both replicating and not replicating *Mtb*. The prime target of bedaquiline is  $F_0 F_1$  ATP synthase main site of ATP production in non-replicating state. This mechanism of bedaquiline results in a new method to kill latent *Mtb* and MDR-TB strains. Bedaquiline shows a minimum inhibitory concentration (MIC) of 0.12  $\mu\text{g/mL}$  for drug resistant isolates (Andries et al. 2005; Hoagland et al. 2016) (Figure 5).

Delamanid is a nitro-dihydro-imidazooxazole derivative with a MIC of 0.012  $\mu\text{g/ml}$  for drug resistant isolates. The mechanism of action is incompletely understood but involve inhibition of mycolic acid synthesis possibly via radical intermediate (Matsumoto et al. 2006) (Figure 5).

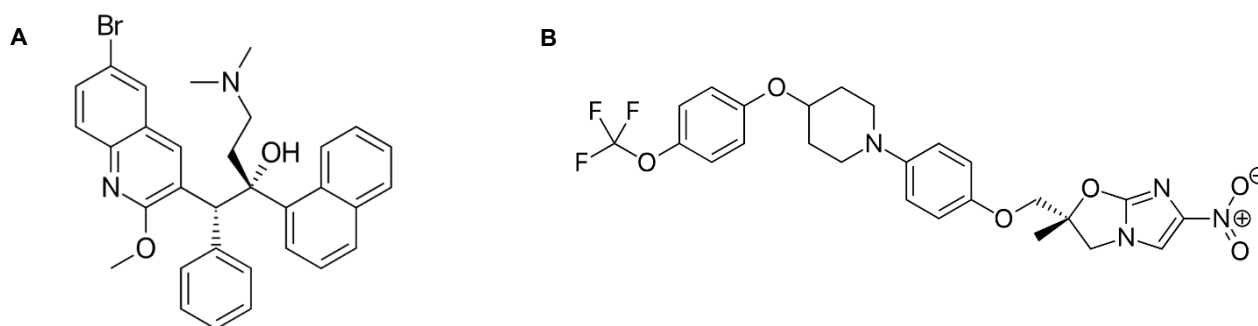


Figure 5 - Molecular structures of (A) Bedaquiline and (B) Delamanid.

## 1.7. The impact of *Mtb* in the world

TB is considered one of the 10 top leading causes of disease and mortality due to an infection agent. In 2015, according to the World Health Organization (WHO 2016) report, there was 10.4 million new cases and 1.8 million of deaths caused by TB (1.4 million TB and 0.4 million resulting from coexistence with HIV), worldwide.

Six countries accounted for 60% of new cases: India, Indonesia, China, Nigeria, Pakistan and South Africa (Figure 6).

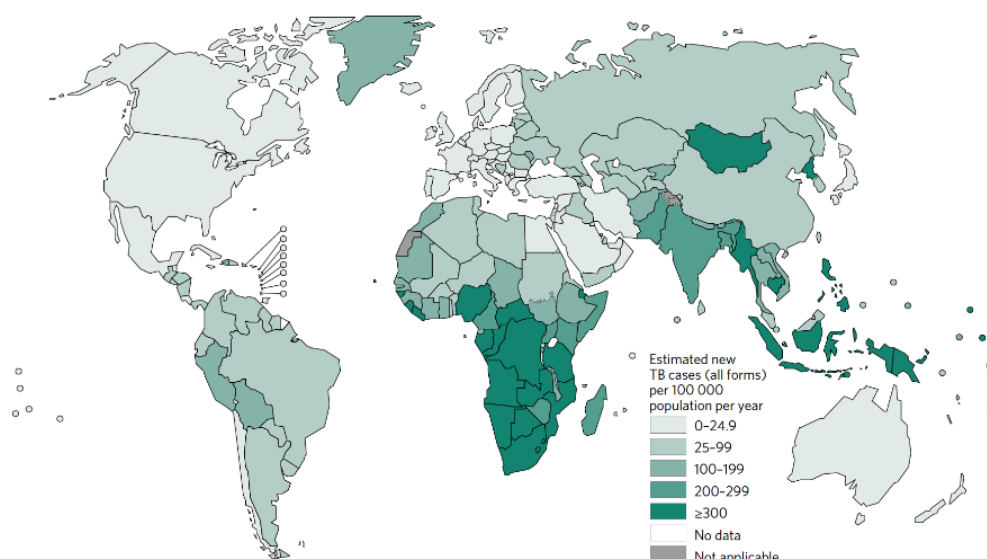
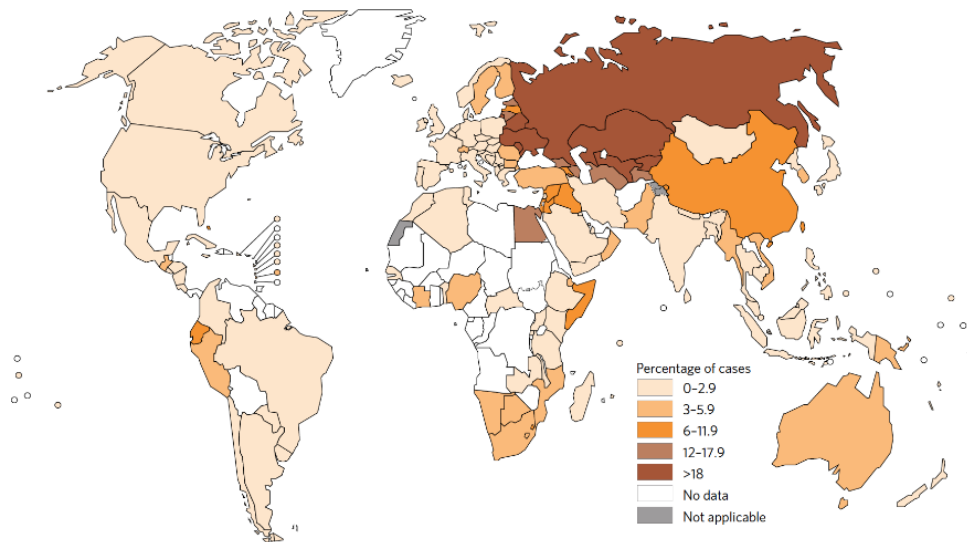


Figure 6 - Estimated TB incidence rates, 2015. Adapted from (WHO 2016)

Although, in the last few years incidence rate as decreased to 22%, cases of MDR-TB are growing, striking almost 480.000 in 2015 (Figure 7). Main countries accounted for 45% cases were India, China and the Russian Federation. The average proportion of MDR-TB cases with XDR-TB is 9.6%.



**Figure 7 - Percentage of new TB cases with MDR-TB. Adapted from (WHO 2016)**

Treatment of TB has become more difficult to achieve due in part to the duration of therapy and the crescent number of multiple drug resistance (MDR-TB and XDR-TB). Which leads to poor treatment outcomes and increased rate of mortality, reflecting in the urgent need to development new active drugs against drug resistance strains.

## 1.8. CAMPs

The global health concern of emergence of TB resistance to current antibiotic has triggered the development of new more effective compounds. Cationic antimicrobial peptide (CAMP) based therapies are interesting candidates as alternative or adjuvant to antibiotic treatments. CAMP are considered ancient defensive weapons with a wide spectrum of activity against gram-positive and gram-negative bacteria, fungus, parasites and virus and extending used against cancer. Through interaction with the negatively charged membrane which creates a displacement of lipids, alteration of membrane structure and possibility internalization (Lakshmaiah et al. 2015). CAMPs often possess a selectivity towards microbial membranes due to this anionic composition which differs from eukaryotic cells. Eukaryotic membranes are usually composed by zwitterionic phospholipids such as phosphatidylcholine (PC) and phosphatidylethanolamine (PE), sphingomyelin (SM) and cholesterol (increase of membrane stability) creating a neutral charged membrane ( -15 mV electrochemical gradient). In contrast the composition of prokaryotic membranes its characterise by the present of net negative charge/highly electronegative composed by hydroxylated phospholipids phosphatidylglycerol (PG), cardiolipin and phosphatidylserine (130 to 150 mV electrochemical gradient) (Robert E W Hancock et al. 1998; Yeaman and Yount 2003).

CAMPs are often small size (12-15 amino acid residue), cationic character (composed with positively charge Arginine and lysine residues) and amphipathic. (Robert E W Hancock et al. 1998) There are four major groups based on CAMP structure:  $\alpha$ -helical usually amphipathic in nature (e.g. LL37, cecropins or magainins);  $\beta$ -sheet characterised by the presence of two or more disulphide bonds (e.g. human defensins, plectasin or protegrins); extended associated with lack of secondary structure rich in proline, histidine, arginine or glycine residues (e.g. indolicidin); and  $\beta$ -hairpin are highly stable due to the presence of disulphide bonds between  $\beta$ -strands (e.g. Bactenecin) (Hancock and Sahl 2006).

## 1.9. Natural occurring CAMPs

CAMPs are usually found in bacteria, insects, plants and animals as host defence mechanism. In addition, CAMPs are considered multifunctional molecules with enormous proprieties such as anti-inflammatory, immunomodulatory, wound healing, cytokine release, chemoattraction and antimicrobial activity.

Natural CAMPs in mammals are encoded through a specific gene, being constitutively expressed (basal levels) or rapidly transcribed triggered with exposition to pathogens (Jenssen et al. 2006; McPhee et al. 2005).

Defensins and cathelicidins are the two major class of CAMPs present in the mammalian defence mechanism.

Cathelicidin is expressed in macrophages, epithelial cells and mainly store within granules of neutrophil expressed in mucosal surfaces (mouth, lung, genitourinary tract and skin). Beyond antibacterial activity, cathelicidin exhibits chemotactic, endotoxin-neutralizing, angiogenic, and wound healing proprieties (Jenssen et al. 2006).

Defensins are class of cyclic peptides with antimicrobial activity and immunomodulatory responses as mediators between innate and adaptive immune system. Defensins are divided in 3 groups:  $\alpha$ ,  $\beta$  defensins and  $\theta$ -defensins (Jenssen et al. 2006). Four  $\alpha$  human neutrophil defensins (HNP 1-4) are present in neutrophils being constitutive produce and HNP5 and 6 are found in Paneth cells of the gastrointestinal system (Kang et al. 2014). While human  $\beta$ -defensins (HBDs- 1-4) are produce in epithelial cells of the mucosa. Both cathelicidin and  $\beta$ -defensins are in constant surveillance against pathogen acting as the first defence barrier (Robert E W Hancock et al. 1998). In some individuals the lack of CAMP secretion through the body results with a higher susceptibility towards infection. Another feature of CAMPs is characterised by its immunomodulatory capacity, for example  $\alpha$ -defensins present in neutrophil are responsible to attract T cells expressing CD4 and CD8 antigens.  $\beta$ -defensin HBD(1-3) and LL37 is responsible to attract both neutrophils, monocytes and T cells to the site of the infection (Zasloff 2002).

## 1.10. Mechanism of action

Several studies with the membrane models were conducted in order to clarify the possible mechanism of action of CAMPs. Different models of mechanism associated with the interaction between peptides and membrane surface have been discussed and proposed over the years. The initial step results in electrostatic interactions between cationic peptide and positively charged membrane (Powers and Hancock 2003).

The carpet mechanism: CAMPs bond to the membrane surface and form a 'carpet' structure which destabilize hydrophobic interactions of phospholipids. When reach critical concentration of peptide the membrane integrity is lost and results in membrane disruption (e.g. cecropins, melittin, caerin) (Figure 8A) (Melo et al. 2009).



The barrel-stave mechanism: the attached CAMPs aggregate and insert into the membrane so that hydrophobic part of the peptide aligns with lipid core region and hydrophilic portion of the forms the interior region of the “barrel-like” pore (e.g. Pardaxin, alamethicin.) (Figure 8B).

The toroid pore: CAMPs bind parallel with membrane, hydrophobic residues disassociate the polar head group of phospholipids creating a breach in the hydrophobic region. Once reach the threshold of peptide-to-lipid ration, CAMPs make a transition to perpendicular orientation culminating on toroidal pore (e.g. magainins, protegrins and melittin) (Figura 8C) (Brogden 2005).

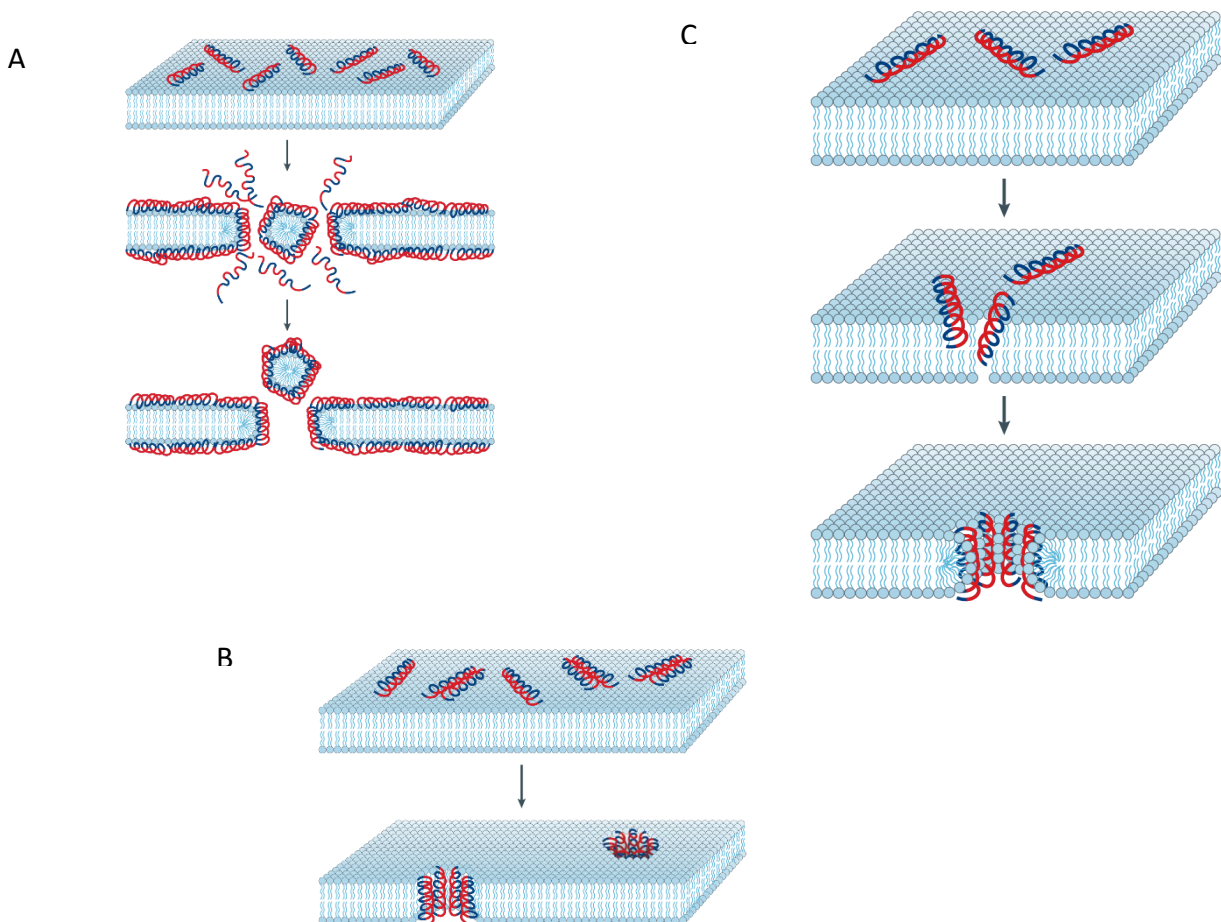


**Figure 8 - Schematic models of mechanism of action of CAMPs. (A) The carpet mechanism (B) The barrel-stave mechanism (c) The toroid pore. (adapted from Brogden 2005).**

Microbial cell membranes are responsible for many essential functions including permeability barrier, oxidative phosphorylation, synthesis of biopolymers and virulence

determinants. The creation of pores contributes to depolarization of the membrane, leakage of ions and metabolites which leads to cell death. Although, some CAMPs can enter into the cell without disrupting the membrane and then inhibited intracellular targets (Yeaman and Yount 2003).

### 1.11. Antimicrobacterial potencial

The antimicrobial proprieties of CAMPs hold in future a promising therapeutically approach. Many CAMPs are already available in the market as topical drugs such as Pexiganan for diabetic foot ulcers, Iseganan for oral mucosaitis, Neuprex for sepsis and Omiganan for catheter-associated infections (Hancock and Sahl 2006; Kang et al. 2014). Regarding this advances, CAMPs for systemic administration face some obstacles that reduced its full effectiveness such as degradation by proteolytic enzymes, low bioavailability and inhibition of activity by physiological conditions. Several studies present possible solutions with use of non-natural amino acid or D-enantiomer in the peptide sequence displaying an increase on stability to the proteases (Ong et al. 2014). In addition, delivery approaches with use of synthetic carries, scaffolds (liposomes and polymers) and nanoparticles emerged as promising solution to enhance antimicrobial activities, decrease toxicities, increase salt stability and reduce protease degradation (Schmidtchen et al. 2015).

Another obstacle facing is the high manufacturing value of large-scale productions of CAMPs, about 50 to 400 dollars per gram comparing with antibiotic that only cost 1\$ per gram. However, different approaches can be used to overcome this problem such as chemical synthesis (on solid-phase, solution phase and hybrid) provides the ability of incorporate unnatural amino acids (terms of isolation, purification and characterization), recombinant DNA, cell-free expression systems (*Escherichia coli*), transgenic plants (*Nicotiana benthamiana* using viral vectors based on TMV and potato virus X (PVX)) and fungi with enhance protein synthesis (da Cunha et al. 2017). The optimization approach selected should be carefully considered in the context on the nature of end application (e.g. topical or systemic), safety, the degree of antimicrobial potencies required and cost.

## 1.12. CAMPS against *Mtb*.

The rise of global health concern due to the increased number of multidrug-resistant tuberculosis reported has potentiated the research, in order to development of new effective drugs. CAMPs show a potential use, for administration as a monotherapy or as combined with other drugs. In the present, there is no CAMP admitted to clinical trials for the treatment of TB. Although, many studies *in vitro* and *in vivo* conducted so far have demonstrated inherent antimicrobial activity against either *Mtb* or MDR-TB. Some examples of CAMPs against *Mtb* studies are summarized in Table 2.

For instance, VpAmp, derivate from *Vaejovis punctatus* proved effective against both *Mtb* and MDR strain demonstrated a similar MIC range (Ramírez-Carretero et al. 2015). Ramón-García et al 2013 tested the MIC of 49 synthetic peptides W-R rich against *Mtb* presenting a 90 % decrease with 1,1  $\mu$ M (Ramón-García et al. 2013). The LL-37 and CRAMP derivate peptides, *in vivo*, were successful in reducing the loads in the lungs of both *Mtb* and MDR-TB strain, at 32 g/mouse reduced 53% and ate 32 ug/mouse reduced 45%, respectively (Rivas-Santiago et al. 2013). The synthetic IK8-all D proved an inhibition of growth in *Mtb* strain with the MIC of 15,6 mg/L (Ong et al. 2014). Yun Lan and co-workers, observed the benefits of combining synthesis D-LAK with INH which resulted in decreased of MIC of 10  $\mu$ g/mL (INH) + 6.25  $\mu$ M of peptide against MDR-TB. Linking the effect of D-LAK in the permeability of the cell membrane which facilitates the entrance of INH (Lan et al. 2014). Moreover, CAMPs usually present cytotoxicity to the host and sensibility to protease degradation. Jiang and co-works found that incorporation of D-enantiomers into LL37 resulted in less haemolytic effect (Jiang et al. 2011).

In general, CAMPs have shown bactericidal activity even though the acquisition of resistance towards CAMP as been observed, this is unlike to happen since drastic modifications of the bacterial membrane compromise its role.

**Table 2 - Examples of AMPs showing in vitro or in vivo activity against *M. tuberculosis* and respective mechanisms of action.**

CAMPs		Procedures/MIC determination	Activity	Cytotoxicity		References
W-R rich peptide PL – (A-D):	PL-A SPOT technology PL(B-D) standard manual Fmoc SPPS	Medium: MB 7H9 modify (without cations) PL-(A-C) REMA PL-D luciferase-based assay	MIC90: MTB range 1.1 – 141 $\mu$ M	TPH-1 cells	IC50: range 24,3 – 197,2 $\mu$ M	(Ramón-García et al. 2013)
D-LAK family	Standard manual Fmoc solid state chemistry	Medium: MB 7H9Broth+10%OADC Broth microdilution method Incubated 37° 4 up to 6 weeks. Visualized with Light microscope.	MIC90: Mtb(SLMS): 25 $\mu$ M MDR(GB2): 5 $\mu$ M XDR(WYC-I1): 100 $\mu$ M Combinatory treatment MIC90: MDR:10 $\mu$ M(INH)+6.25 $\mu$ M	TPH-1 cells differentiated into macrophage-like	14.4-32.3 $\mu$ M	(Lan et al. 2014)
VpAmp (peptide from <i>Vaejovis punctatus</i> )	Purchased (no data)	Medium:MB 7H9+10%OADC Peptide concentration: 0,4-96,4 $\mu$ g/mL Incubated 37° for 5 days. REMA	MIC90: Mtb: 5.4-21.4 $\mu$ M MDR: 4.8-30.5 $\mu$ M	Blood sample Erythrocytes	9.2-167 $\mu$ M	(Ramírez-Carreto et al. 2015)
Synthetic (LLKK) <sub>2</sub>	Purchased (GL biochem)	Medium: MB 7H9+10%ADC+ 0.05%Tween+ 0.2%glycerol Broth microdilution method (3.9-500 mg/L) of peptides spectrophotometrically	Mic99: Mtb: 125-500mg/L MDR(CSU87): 62.5-500mg/L	rRBCs	>1000 mg/L	(Khara et al. 2014)
Lassomycin	Isolated from actinomycetes	Medium: MB 7H9+10%ADC Broth microdilution method Incubated 37° for 5-7 days SynergyMX plate reader	MIC99: Mtb: 0.41-0.83 $\mu$ M and 0.83-1.65 $\mu$ M MDR: 0.83-1.65 $\mu$ M XDR: 0-41-165 $\mu$ M	NIH 3T3, and HepG2	350 $\mu$ g/mL	(Gavriš et al. 2014)

D-V13K, D- and L- LL37	Standard solid-phase peptide synthesis t- Boc	Medium: MB 7H11  Incubated 37° 7 days CFU/mL	MIC99: D(1-5) Mtb: 35.2-200µg/mL MDR: 49-100µg/mL D-LL37 Mtb: 200µg/mL	erythrocytes	D(1-5): 3.5 - 421.5µg/mL L-LL37: 43.4 µg/mL D-LL37: 125 µg/mL	(Jiang et al. 2011)
Peptoid 1 1-C134mer 1- Nssb, 14mer, 1-11mer, 1-Pro9	Standard solid-phase peptide synthesis	MABA by NIH/NIAID-contracted laboratory	MIC99: Mtb: 1-C134mer more active 6.6 µM and 1-Nssb infective >100µM	RAW 264.7 and J774 mouse macrophage cell line	1-C134mer: >100µM 1-11mer, 1-Pro9: 50µM Peptide 1: 20µM 1-Pro9, 14mer: non toxic	(Kapoor et al. 2011)
11 Tic-Oic family peptides	Purchased Standard solid-phase peptide synthesis	Medium: MB 7H12 Broth Broth microdilution method (0.5-100µg/mL) of peptides MIC: Visualise	MIC99: Mtb: 4.92-40.75µM MDR(CSU45): 4.92-49.26µM Mtb(oflo): 4.92-49.26µM	-----	-----	(Hicks 2016)
PG-1 from porcine leukocytes, HBD-1	Standard solid-phase peptide synthesis, (automated Milligen 9050 peptide synthesizer)	Medium: MB 7H9 Broth microdilution method 2-fold dilution (0- 128µg/mL) of peptides CFU/mL	PG-1 Mtb: 128µg/mL (96.7%) MDR(RM22): 128µg/mL HBD-1(45.1%) Mtb: 128µg/mL (49.9%) MDR(RM22): 128µg/mL (45.1%)	----	-----	(Fattorini et al. 2004)
Callyaerins Cyclic, Peptides	Extraction and Isolation from <i>Callyspongia aerizusa</i>	Medium: MB 7H9+ 0.5%glycerol+ 0.05%Tyloxapol+10% ADS Incubated 6 days REMA	MIC90 Mtb: 2-40µM MIC100 Mtb: 6µM-100µM	THP-1 and MRC-5 cell lines	THP-1: 30-100µM MRC-5: 2->100µM	(Daleto et al. 2015)
lactacin 3147 nisin A	Purified	Medium: MB 7H9GC broth Broth microdilution method 0.5 dilution (0.11- 60mg/mL) of peptides MABA	MIC90 lactacin 3147 Mtb: 7.5mg/mL nisin A Mtb: >60mg/mL	-----	-----	(Carroll et al. 2010)

HNP-(1-3) sNP-1 PG-1	All Purified exception of sNP-1 synthesize by Fmoc chemistry	Medium: MB 7H9  Incubated 37° for 48 hours Standard colony count assay	HNP-(1-2),sNP-1 Mtb: 50µg/mL (99%) HNP-3 Mtb: 50µg/mL (98%) PG-1 Mtb: 50µg/mL (91,6%) HNP-1, sNP-1, PG-1 Mtb(ci): 50µg/mL (86.3 to 99%)	-----	-----	(Miyakawa et al. 1996)
LL-37 CRAMP E2(Bac8c) E6(Sub3) CP26	Standard solid-phase peptide synthesis (tBOC)	Medium: MB7H9+ 10%OADC Two-fold serial dilution (0.4–12.8 _g/mL) Incubated 37° for 5 days REMA	MIC99 CP26 Mtb: 2.1µg/mL E2 Mtb: 2.6µg/mL E6 Mtb: 3.2µg/mL LL37 Mtb: ~5µg/mL CRAMP Mtb: ~4µg/mL In vivo Mtb: ~53% killing at 32µg/mouse (3xper week, 28- day treatment) In vivo MDR: ~45% killing a 32 µg/mouse (3x per week, 28-day treatment)	-----	-----	(Rivas-Santiago et al. 2013)
Magainin I Mastoparan Cecropin B MIAP	standard solid-phase peptide synthesis	Medium: MB 7H9+ 10%ADC  Two-fold serial dilution (6,4-1200ug/mL) of Peptides Incubated 37° for 4 days  MTT assay	MIC99 Cecropin B, Mastoparan Mtb: 600µg/mL Magainin I Mtb: 1200µg/mL Mtb(clinical isolates): MIAP Mtb: 300µg/mL	-----	-----	(Santos et al. 2012)
vgf-1	Isolated from <i>Naja atra</i> <i>venon</i>	Medium: MB 7H12 TB  Bactec TB-460	MIC99 MDR (clinical isolates): 8.5 mg/mL	-----	-----	(Xie et al. 2003)
Ecumicin	Isolated from actinomycete extracts	Medium: 7H12+ glycerol+ Casitone+ OADC MABA	MIC99 Mtb: 0,16-0,36 µM Mtb(MR): 0.12-0.31µM MDR(clinical isolates): 0.31- 0.62µM	Vero cells (ATCC CRL-1586) J774.1 macrophage cell line	Vero cells: >63µM J774cells: >32µM	(Pearson et al. 2016)

IK8-all D IK8-2D IK12-all L	Purchased (GL Biochem)	Two fold dilutions (3.9-500mg/L) of peptide	Mtb(clinica isolates): 15.6-62.5mg/L	RAW264.7 and WI-38 cells	HC10: >125 to >2000 mg/L	(Ong et al. 2014)
PR-39	Isolated from porcine intestine Rest Synthetic	Medium: MB 7H12 BACTEC radiometric assay and Standard colony count assay activity of PR-39 Incubated 37° for 21 days	PG-39 Mtb: 50mg/L 80% MDR(P1380/94): 100mg/L 50%	-----	-----	(Linde et al. 2001)

### 1.13. Cinnamic acids

Cinnamic acids (example for trans-cinnamic acid in Figure 9) belong to the class of phenolic acid and it's considered one of the most secondary metabolites in plants (Xu et al. 2009). These secondary metabolites are crucial to plant growth, development, reproduction and disease resistance. From spice cinnamon, *Cinnamomum zeilanicum* derives the denomination of cinnamic, use as food condiment, stimulant and antibacterial and antifungal compound. Not only is present in cinnamon but also is present in a diversity of aliments such as coffee, apples, berries, potato and more. Recently, the research on the potential proprieties of cinnamic acids has increased, and more articles are being published with potential application in cancer, malaria, diabetes and tuberculosis. In addition, molecular hybridization of cinnamic acid with a selective drug has been used in order alter the spectrum of potency and activity.

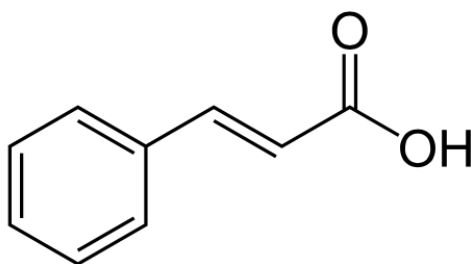


Figure 9 - Molecular structure of trans-cinnamic acid.

### 1.14. Cinnamic acids against *Mtb*

In 1893, Landerer discovered the therapeutic potential of cinnamic acid in TB conducting an experiment by injecting emulsion form of cinnamic acid in TB patients. Intravenous injections were administrated twice a week for 3 months. Landerer work showed no effect on acute TB in young adults. Although, in cases of chronic TB patients a gradual improvement of the symptoms was observed. Landerer reported, from the 50 patients treatment, a 58 percentage of cure and 20 percentage of improvement and 20 percentage of death (Warbasse 1894).

More recent studies tested natural and synthetic cinnamic acid derivates against *Mtb* (Tanachatchairatana et al. 2008). For example, studies conducted by Andrade-Ochoa and co-workers reported the capacity of cinnamic acid and cinnamaldehyde against *Mtb* with associated MICs of 8.16  $\mu\text{g}/\text{m}$  and 3.12  $\mu\text{g}/\text{mL}$ , respectively (Andrade-ochoa et al.



2015).

Yoya et al. 2009, observed the consequences of punctual additions synthetic cinnamic acid derivatives against TB. Was noticed that some modifications contributed to the decrease of activity and other had significant improvements such as the introduction of geranyl chain attributing a MIC of 0.6  $\mu\text{g/mL}$  (Yoya et al. 2009).

Molecular hybridization of cinnamic acid with a selective drug is presented as a solution in order to achieve a more efficient compound (Guzman 2014; Slavchev et al. 2014). For example, the molecular hybridization of INH with trans-cinnamic acid against *Mtb* resulted in MIC of 3.12  $\mu\text{g/mL}$  (Carvalho et al. 2008). Patel et al. at 2014, used a molecular hybridization of piperazine ring into cinnamic acid derivate which leads to increase on bioavailability and the antitubercular activities (Patel et al. 2014).

## 1.15. Solid Phase Peptide Synthesis (SPPS)

Merrifield, in 1963 introduced Solid Phase Peptide Synthesis (SPPS), a brand new method of synthesizing peptides that have enormous advantages relative to the previously known. The SPPS methodology has proved to be faster, simpler, cheaper and more efficient.

The peptide is synthesized on an insoluble solid support being one of the most determinant factors to build the desired peptide sequence. The reaction vessel is connected with a vacuum system which allows the removal of side products and excess of reagents and solvents through washing with Dichloromethane (DCM) and Dimethylformamide (DMF) and filtration.

Briefly, SPPS starts with the coupling of an amino acid N- $\alpha$  protected into the solid support (resin). The remaining  $\alpha$ -amino acids (AAn) of the sequence are sequentially linked together through the formation of an amide bond (peptide bond). After each coupling, the reactivity of the  $\alpha$ -amino group is protected by a temporary protecting group (usually 9-fluorenylmethoxycarbonyl (Fmoc)) and the other reactive functional groups in the amino acid are blocked by "permanent protection (tert-butyl, tBu). The carboxyl group of the amino acid is blocked by the bond linking the solid support or by the peptide bond.

SPPS is characterised by a group of coupling reactions favoured with activation of the carboxyl group through coupling agent and deprotection reactions with deprotection of the reactive  $\alpha$ -amide group of the already linked amino acid. Otherwise, in the coupling reaction an unwanted acid-base reaction will happen resulting with the formation of a salt, instead of bonding the two amino acids with amide bond.

Another particularity of SPPS, is the sequence order of amino acids, assembled through C<sub>t</sub>  $\rightarrow$  N<sub>t</sub> which is the opposite of biosynthetic route for peptides synthesis observed in nature (N<sub>t</sub>  $\rightarrow$  C<sub>t</sub> sense). The resin not only serves as a peptide support but also as protective group of carboxyl amino acid C-terminal.

The elongation of peptide chain occurs through repetitive cycles of coupling reactions of protected amino acid and subsequent deprotection of the temporary protecting group (Figure 10).

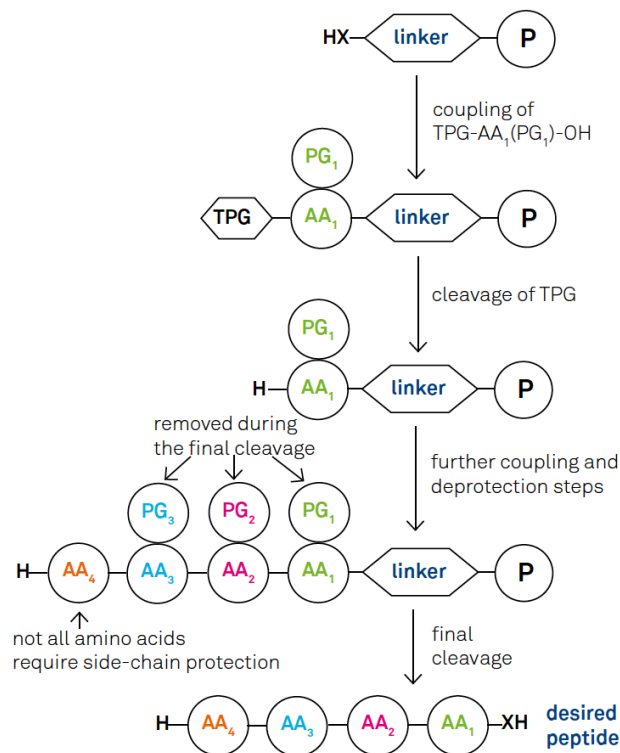


**Fig. 1.**  
**General scheme of SPPS.**  
X = O, NH  
AA = Amino Acid  
PG = Protecting Group  
P = Polymer Support  
TPG = Temporary Protecting Group

**Figure 10 - General scheme of SPPS. X=O,NH; AA= amino acid; PG=protecting group; TPG=temporary group; P - resin.**

When the sequence is completed all permanent groups are removed and the peptide is cleaved from by chemical solution capable of breaking the bond with the solid support. Nowadays, the SPPS methodology was quickly and easily automated and new equipment were developed in order to produce fast and more efficiently. One example of these equipment's is the Symphony X Multiplex Peptide Synthesizer, developed by Protein Technologies, Inc.<sup>®</sup>, which is a 24-channel peptide synthesizer that can run different sequences, scales and protocols on multiple reactors all at the same time, or run up to 12 reaction vessels with preactivation (BACHEM 2014; Behrendt, White, and Offer 2016).

## 2. Materials and Methods

### 2.1. Reagents, Solvents and Equipment

In this work the reagents and solvents were acquired from Novabiochem (Fmoc-Rink Amide MBHA resin and Fmoc-amino acids), Sigma-Aldrich (coupling agents, piperidine, N, N-Diisopropylethylamine (DIAE)), Resazurin (n-1-naphthylethylenediamine dihydrochloride), Merck (TFA, solvents).

Peptides were characterized by mass spectrometry (LC/MS), on Finnigan Surveyor LCQ-DECA XP MAX. The purification step of peptides achieved by Reverse Phase Medium-Pressure Liquid Chromatography (RP-MPLC), using a C18 Vydac<sup>®</sup> 218TP stationary phase, by Grace Vydac. The purity of the peptides was determined by high-performance liquid chromatography (HPLC) on a Merck-Hitachi LaChrom Elite equipment, with a quaternary pump, automatic and thermostated by Peltier effect injector and a diode detector. A reverse phase Purospher star RP C-18 (octadecylsilane) column (125 x 4.0 mm), with a particle diameter of 5 µm, was used. The elution was performed with a variable gradient of acetonitrile (ACN) in water containing 0.05% trifluoroacetic acid (TFA), at a 1 mL/min flow.

The purified peptides were lyophilized in a BenchTop Pro 9L with omnitronics from SP Scientific (Department of Chemistry and Biochemistry of Faculty of Sciences of University of Porto).

### 2.2. Peptide Synthesis by SPPS

#### 2.2.1. Manual Synthesis developed in this Project

The SPPS reactor consisted in a cylindrical vessel (polypropylene syringe) with a polyethylene porous filter adapted to a vacuum system essential for removal of the excess of reagents from the wash, deprotection and coupling steps. A Teflon rod used to manually stir the resin beads (Figure 11).

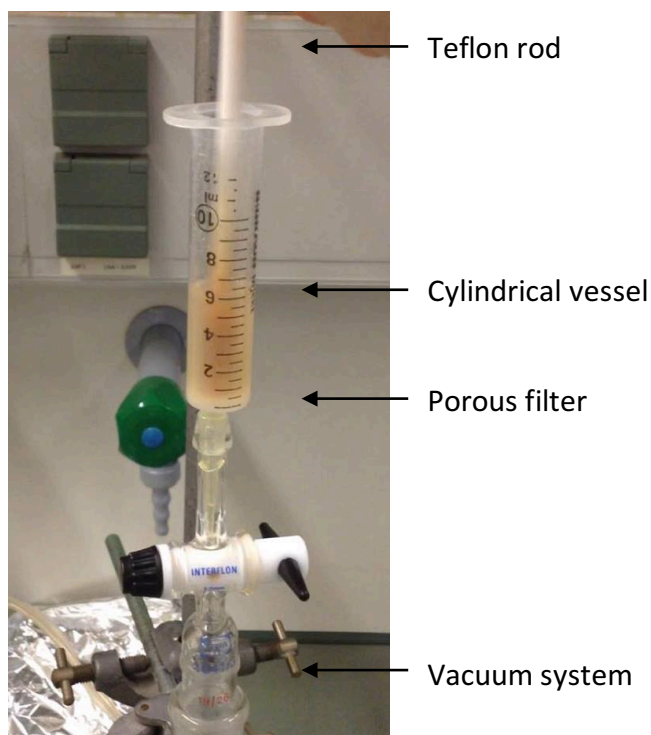


Figure 11 - Manual SPPS development in this project.

### 2.2.2. Preparation of the resin

The resin chosen as a support for the manual synthesis was the Rink Amide MBHA resin LL (100-200 mesh), a polystyrene-based polymer functionalized with 4-methylbenzhydrylamine (MBHA) groups, further modified with an N Fmoc protected (R,S)-2-{4-[amino(2,4 dimethoxyphenyl)methyl]phenoxy} acetic acid linker (Rink-amide linker). The loading capacity of the resin was 0,38 mmol/g and syntheses was performed at 0.2 mmol scale, so 0.526g of resin was weigh and transferred into the syringe. The swelling step of the resin was made by the addition of N,N-dimethylformamide (DMF) with continuous stir. After 20 min, DMF was rejected, and followed by the addition of dichloromethane (DCM) for 15 min. Before the peptide synthesis, initial removal of Fmoc group was performed using 20% piperidine in DMF (3mL, 1x1min + 1x20min). After deprotection, the resin was washed with DMF (3mL,3x1 min) and DCM (3mL, 3x1 min) and a Kaiser test was performed.

A Kaiser test positive (dark blue resin beads and solution) indicate that the construction of the peptide sequence can be initiated.

### 2.2.3. Kaiser Test

The Kaiser Test is used to detect the presence of primary amines, determining if coupling or deprotection reactions are complete. Ninhydrin (yellow) reacts with the deprotected N- terminal amine group leading to the formation of an intense blue chromophore known as Ruhemann's purple (Figure 12). The tests were performed by transferring few beads to a small glass tube which was added 6 drops of reagent A and 2 drops of B (3:1). The reagent A consisted in a solution of phenol (40 g) in 10 mL of ethanol mix with a solution of aqueous KCN (16.5 mg/25 mL) in 100mL distilled pyridine. The reagent B consisted of a solution of 5 g of ninhydrin in 100 mL of ethanol. After homogenization, the test tube was incubated at 110°C for 3 min. When N-Fmoc protected amino-acid is present after coupling step ninhydrin, and the result should remain yellow (negative test). When the test indicated a step wasn't completed, that step was repeated (Kaiser et al. 1980).

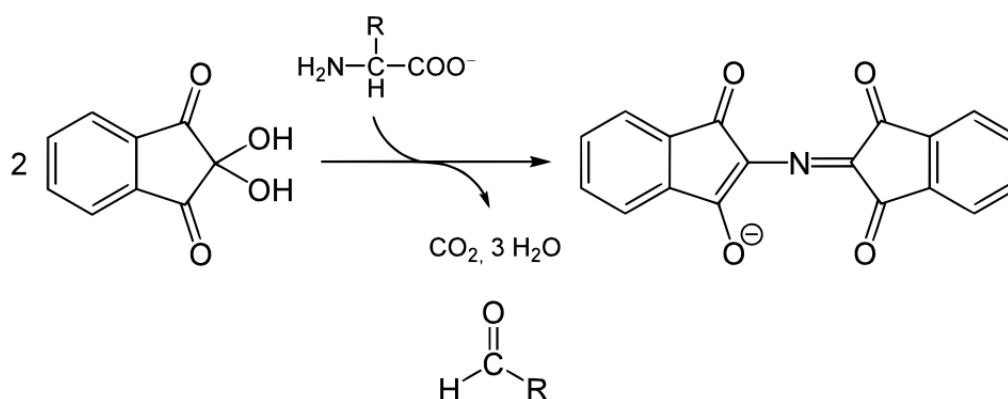


Figure 12 - Ninhydrin reaction with primary amines, resulting in the formation of chromophore (deep blue).

#### 2.2.4. Coupling of Amino Acids and Deprotection Cycles

The Elongation step is characterized by the coupling of an amino acid to the peptidyl-resin. Before being transferred to the syringe vessel the amino acids were activated for 5 min by a solution of Fmoc-AA-OH (5 eq.), coupling agent O-(benzotriazol-1-yl)-N,N,N',N'-tetramethyluronium hexafluorophosphate (HBTU, 5 eq.) and base DIEA (10 eq.) in DMF. The activated amino acid solution was transferred to the syringe to react with the previously deprotected resin or peptidyl-resin for 1 hour with continuous stirring. Once the coupling was completed, the peptidyl-resin was washed with DMF (3 mL, 3 x 1 min) and DCM (3 mL, 3 x 1 min) and Kaiser test was performed. When the test result came negative (yellow) was followed by the deprotection step applying the deprotection solution consisted in 20% of piperidine in DMF (3 mL, 1 x 1 min + 1 x 20 min). After this time, the resin was washed with DMF (3 mL, 3 x 1 min) and DCM (3 mL, 3 x 1 min) and another Kaiser test was made. Confirmed positive (dark blue) the next Fmoc-AA-OH was coupled following the previously described method. The peptide sequence was achieved by repeating the cycles of coupling of N-Fmoc amino acids and deprotection steps.

#### 2.2.5. Structural modification of CAMPs

After the peptide sequence completed, the peptidyl-resin for each peptide was divided into two fractions. The fraction CAMP(n) remained untouched and the fraction Cin+CAMP(n) was modified/coupled with cinnamic acid derivate. Deprotection of the Fmoc-AA-OH of the fraction Cin+CAMP(n) with 20% of piperidine in DMF (3mL, 1 x 1 min + 1 x 20 min). When finished cinnamic acid derivate was coupling to the sequence through activated solution of coupling agent cinnamic derivate, N,N,N',N'-Tetramethyl-O-(benzotriazol-1-yl)uronium tetrafluoroborate (TBTU,) and base DIEA (10 eq.) in DMF for 3 hours with continuous stirring. The Kaiser test was performed and with a negative result, peptide modification was completed.

### 2.2.6. Cleavage and deprotection of side chains of the peptide

When the peptide was completed and with a final deprotection step, the peptidyl-resin was subjected to a cleavage cocktail in order to break the bond linking the peptide to the resin support. In the hood was prepared a cleavage cocktail, containing 95 % TFA, 2.5% TIS (Triisopropylsilane) and 2.5% H<sub>2</sub>O. Then the dry peptidyl-resin was transferred to 15 mL Falcon tubes in 100 mg portions and 1 mL of cleavage cocktail was added to each Falcon. The tubes were left under orbital stirring for 2h at room temperature. When finished, the contents of tubes were filtered on funnel previously rinsed with TFA, and the resin beads were washed with TFA. The filtrate, containing the soluble peptide, was transferred to new 15 mL Falcon tubes in 1 mL portions and 14 mL of cold tert-butyl methyl ether were added to each tube. The peptide containing tubes were stored at -22 °C for 30 min. After this time the tubes were centrifuged at 3500 rpm for 5 minutes at -5 °C then the ether was rejected and other 14 mL of cold ether was added. The addition of ether and centrifugation were repeated 3 more times and finally, the tubes were left in a vacuum desiccator until the crude peptide was dry. Dry peptide pellets were then solubilized in 10% aqueous acetic acid and analysed by HPLC and LC-MS.

## 2.3. Purification of the conjugates

CAMP(n) and CAMP(n) conjugates (Cin+CAMP(n)) were solubilized in 10% aqueous acetic acid and purified by RP-MPLC, using ACN in water with 0.05% TFA as eluent, in gradient mode (15 – 35%). The collected fractions were analysed by HPLC to determine which contained the conjugate with a purity greater than 92%. These fractions were subsequently pooled, lyophilized and stored at -22°C until use.

### 2.3.1. Antimicrobial peptides

Peptide amino acid sequences were based on peptides with 9 amino acid of length previously describe and analysed in Ramon-Garcia (2013) study which included peptides enriched W and R for higher activity against *Mtb* (Ramón-García et al. 2013). 5 structurally similar CAMP(n) (Table 3) were synthesized using standard manual Fmoc



SPPS by above methodology already described. In order to improve CAMP(n) activity, a modification in the N-terminal side was performed with the coupling of a cinnamic acid derivate (Table 4).

Peptides were weighed and diluted in sterile distilled water to obtain the final stock concentration and then store 4°C until use.

**Table 3 - Sequence of synthesized CAMP(n) in this project.**

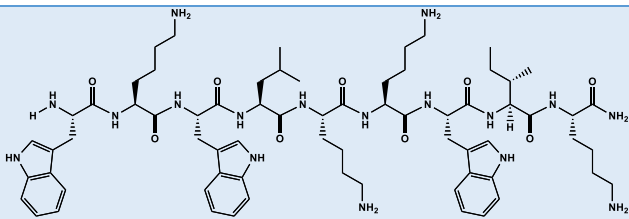
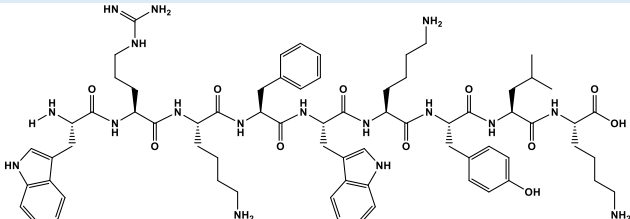
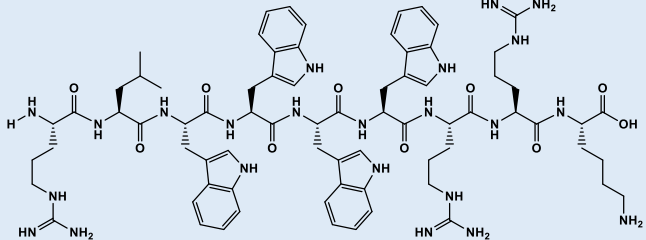
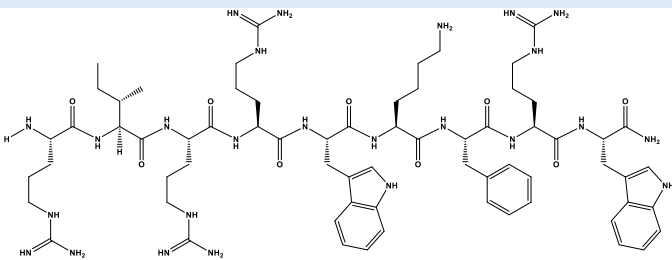
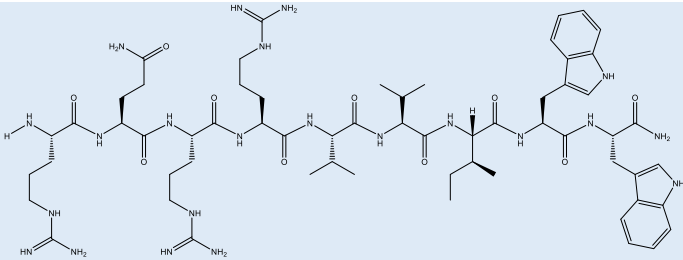
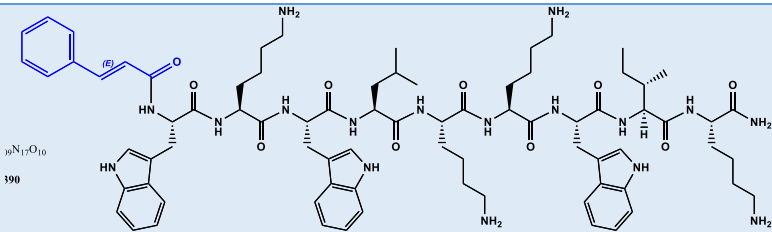
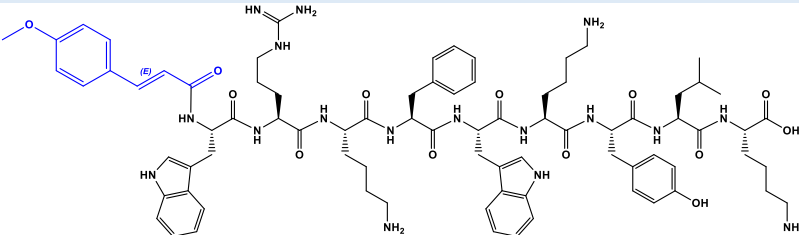
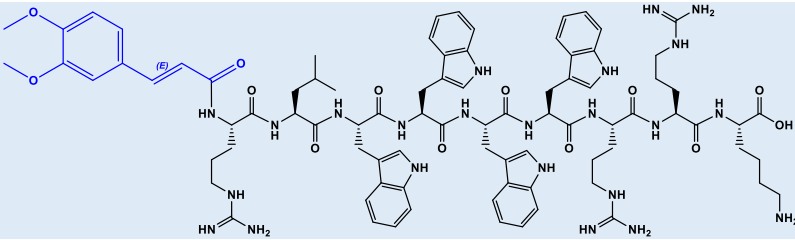
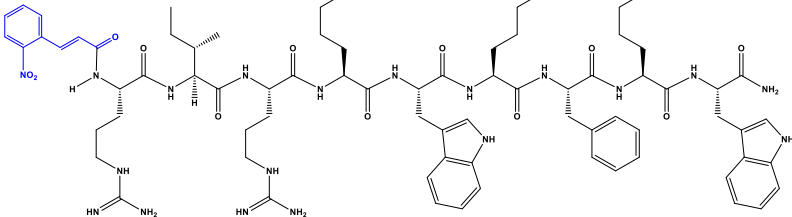
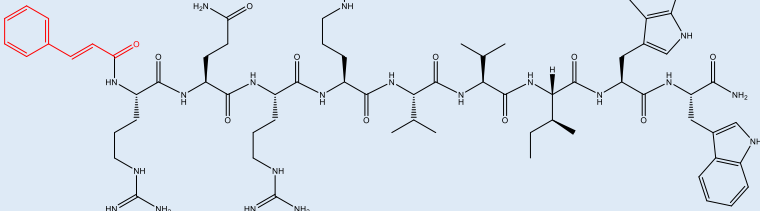
CAMP(n)	Sequence	Structure
CAMP1	WKWLKKWIK	
CAMP2	WRKFWKYLK	
CAMP3	RLWWWRRK	
CAMP5	RIRRWKFRW	
CAMP7	RQRRVVIWW	

Table 4 - Sequence of synthesised Cin+CAMP(n) in this project.

Cin+CAMP(n)	Sequence	Structure
Cin+CAMP1	trans cinnamic +WKWLKKWIK	
Cin+CAMP2	p-methoxycinnamic +WRKFWKYLK	
Cin+CAMP3	3,4-Dimethoxycinnamic+RLWWWWRRK	
Cin+CAMP5	o-Nitrocinnamic+RIRRWKFRW	
Cin+CAMP7	trans cinnamic +RQRRVVIWW	

## 2.4. *In vitro* assays

### 2.4.1. Mycobacterial strains, growth conditions and inoculum preparation

*M. tuberculosis* H37Rv susceptible strain and resistant clinical isolate MDR-Tb (resistance to INH, RIF and STR) were used at Instituto Nacional De Saúde Dr Ricardo Jorge (INSA) reference laboratory, all studies conducted in a laboratory of level 3 of biosecurity based on international procedures of manipulation this class of microorganisms.

Cultures were grown in Lowenstein-Jensen (LJ) medium for 21 days at 37°C.

The inoculum was prepared by scraped bacteria from different parts of LJ medium slants in order to ensure diverse population (Woods et al. 2011). Then the scraped bacteria were transferred into a tube containing 15-20 glass beads and were vortexed for 1-2 min. Right away was added sterile distilled H<sub>2</sub>O into the tube, vortexed for 1-2 min and solubilize bacteria was transferred into a new tube. The turbidity of the supernatant was adjusted to McFarland 1.0 (approximately  $3 \times 10^8$  CFU/mL).

### 2.4.2. Preparation of Resazurin

Resazurin powder (n-1-naphthylethylenediamine dihydrochloride) was dissolved in sterile distilled water to a final concentration of 0.05 mg/mL and stored at 4 °C until use.

### 2.4.3. Anti-Mycobacterium tuberculosis assays

The antibacterial activities of 5 CAMP(n) and 5 Cin+CAMP(n) against *Mtb* were assayed by the Resazurin Microtiter Assay Plate (REMA) method. Two different clinical isolates were used: (i) drug susceptible strain H37Rv; (ii) MDR strain patient clinical isolate. Their antibiograms were determined using the BD BACTEC™ MGIT™ method at INSA. 155 µL (peptides and positive control) and 180µL(negative control) of modify Middlebrook 7H9 médium (BD BBL™ MGIT™) supplemented with 10% Middlebrook OADC (oleic acid 0.6g, bovine albumin 50g, dextrose 20g a catalase 0.02g (BD BBL™ MGIT™ OADC) was added in each well of 96 well-plate (polystyrene, Sigma-Aldrich). Serial two-fold

dilutions of the peptides were prepared in 25  $\mu$ L of sterile distilled water (0.25  $\mu$ g/mL to 128  $\mu$ g/mL) and 20  $\mu$ L of bacterial suspensions were added to the well making a final volume of 200  $\mu$ L. Negative control with untreated bacteria, and positive control with INH (1.04  $\mu$ g/mL) MDR-TB strain used INH+STR (10.38  $\mu$ g/mL) were used (Figure 13). The plates of *Mtb* h37Rv and MDR-tb were incubated for 7 and 14 days, respectively, at 37°C. The growth of *Mtb* in the presence of peptides was visualized on a light microscope. After, 25  $\mu$ L of the resazurin solution were added per well, followed by another incubation overnight at 37°C. A change of color of resazurin from blue to pink indicated its reduction to resorufin, and therefore the growth of microorganisms. The MIC that inhibited 50 and 90% of bacterial growth compared with the growth control, was determined for each peptide by visual inspection and by further assure with resazurin reaction. All peptide concentrations were tested by duplicate.

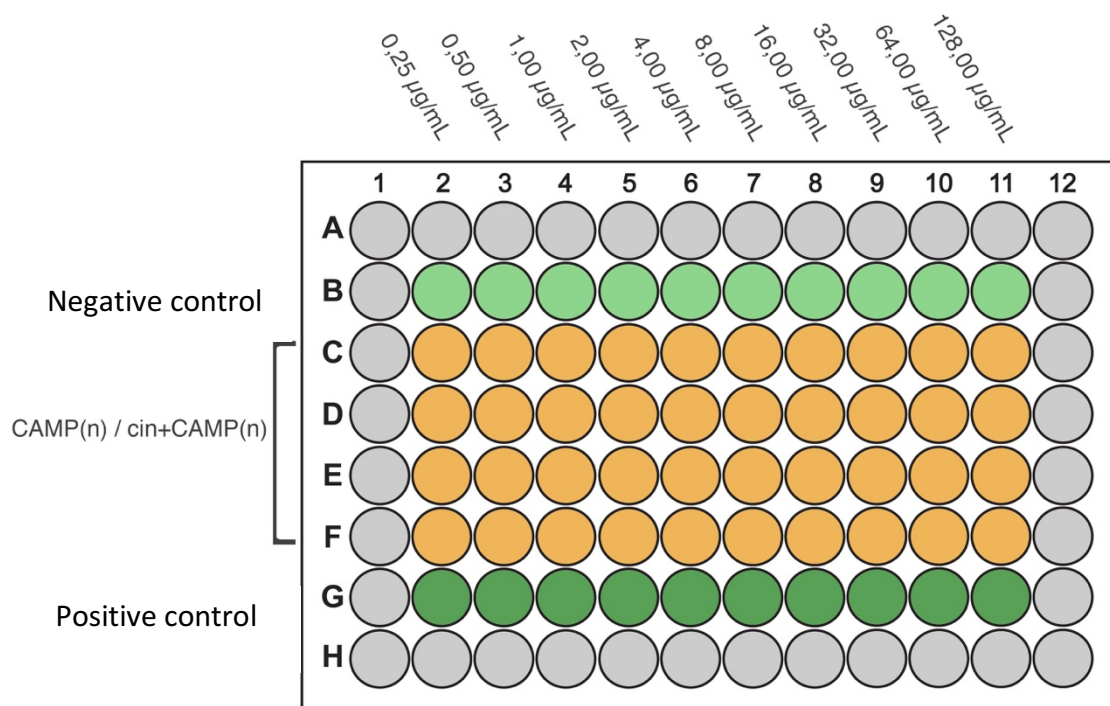


Figure 13 - schematized the 96 well-plate, was performed serial two-fold dilutions (0,25-128  $\mu$ g/mL); CAMP(n): CAMP without modification N-terminal; Cin+CAMP(n), CAMP with modification in N-terminal coupling cinnamic acid; Positive control (180 $\mu$ L medium + 20 $\mu$ L bacterial suspension + 1.04  $\mu$ g/mL).

## 2.5. Cell culture

THP-1 human monocyte cell line were used as a macrophage model. Undifferentiated THP-1 cells were maintained in RPMI-1640 medium supplemented with 10% fetal calf serum (FCS) and posterior differentiated into adherent macrophages by exposure to 80 ng/mL phorbol-myristate actate (PMA) for 24 h prior to experiment.

## 2.6. Cytotoxicity assay

The cytotoxicity of the 5 CAMP(n) and 5 Cin+CAMP(n) was determined by the MTS (3-(4,5-dimethylthiazol-2-yl)-5-(3-carboxymethoxyphenyl)-2-(4-sulfophenyl)-2H-tetrazolium) Tetrazolium assay, which measured the cell viability, based on article (Ramón-García et al. 2013). The differentiated THP-1 cells were seeded in 96-well plates at a cell density of  $4 \times 10^3$  cells/well. The peptides were diluted (concentration range 0.0156  $\mu$ g/mL-256  $\mu$ g/mL) in RPMI-1640 medium supplemented with 10% FCS and then were incubated with differentiated THP-1 cells at 37 °C, 5% CO<sub>2</sub> for 24 h. Then the cells were incubated with MTS solution containing phenazine ethyl sulphate (0.21 mg/mL) per well for 4h at 37° to convert the tetrazolium to the soluble formazan product. The experiments were performed two times (Riss et al. 2013).

## 2.7. Statistical analysis

All data presented in this study were statistically analysed using program Prism (GraphPad Software). One way or two-way ANOVA. All experiments were performed at least twice.

## 3. Results

### 3.1. Peptide synthesis and characterization

#### 3.1.1. CAMP1

Once crude of CAMP1 was dried in the vacuum desiccator and then solubilized in 10% aqueous acetic acid, was analysed by HPLC (Figure 14) and LC-MS (Figure 15). HPLC analysis demonstrated a distinct main compound (retention time ( $r_t$ )=11.7 min)

The exact and observed molecular mass of CAMP1 were 1313.8 Da and 1314.67 g/mol, respectively confirmed the target peptide (Table 5) as [peptide + H]. It is possible to observe several peaks in the mass spectrum, corresponding to different protonation states of the peptide.

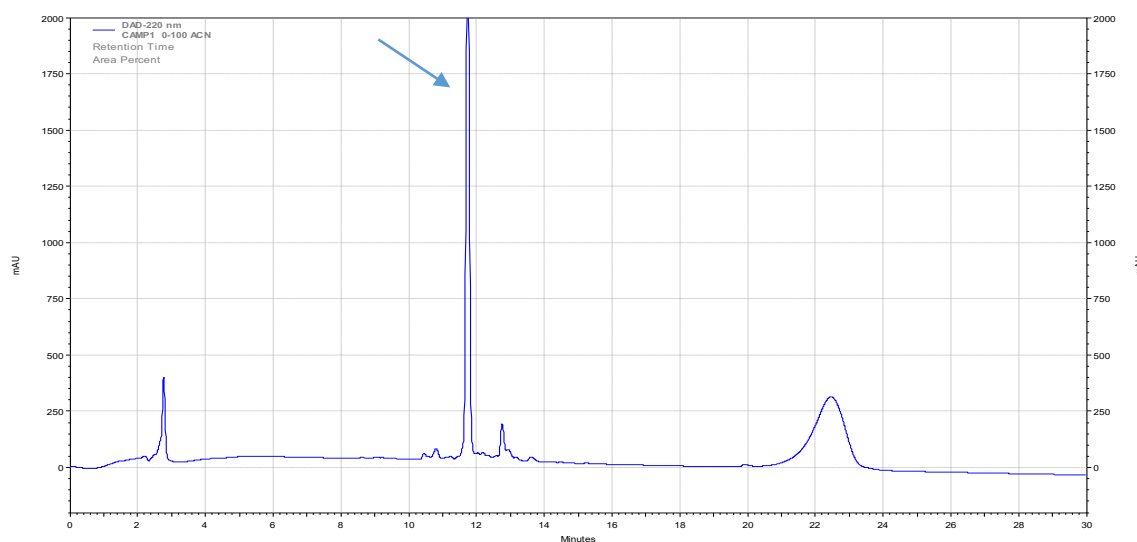


**Figure 14 – Chromatogram of the product of the manual synthesis of the peptide CAMP1, acquired with a HPLC system, with a C18 column, using ACN in water with 0.05% TFA as eluent, in gradient mode (0 – 100%), for 30 minutes, at a flow of 1 mL/min and detection at  $\lambda = 220$  nm.**

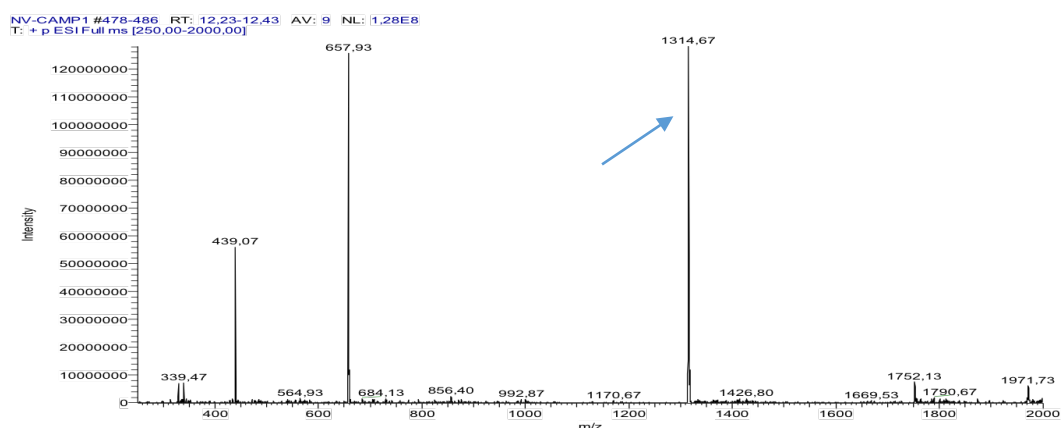


Figure 15 - Mass spectrum (LC-ESI/Orbitrap MS, positive mode) of the peptide CAMP1 (manual synthesis).

### 3.1.2. CAMP2

The synthesis of compound CAMP2 was carried out as described in the Experimental Section. The isolated product was analysed by HPLC and by LC-MS. The resulting chromatogram and mass spectrum are represented in Figure 16 and Figure 17, respectively. The HPLC chromatogram revealed the formation of a major product, with a  $t_r$  of 11.3 min, LC-MS analysis confirmed this product to have the molecular mass expected for compound of 1354,73 g/mol (Table 5).

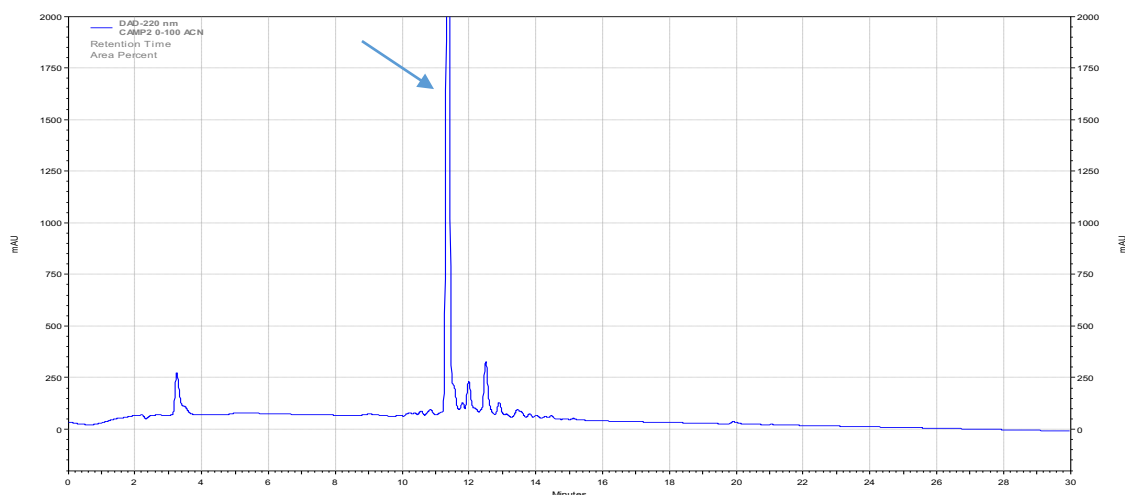


Figure 16 - Chromatogram of the product of the manual synthesis of the peptide CAMP2, acquired with a HPLC system, with a C18 column, using ACN in water with 0.05% TFA as eluent, in gradient mode (0 – 100%), for 30 minutes, at a flow of 1 mL/min and detection at  $\lambda = 220$  nm.

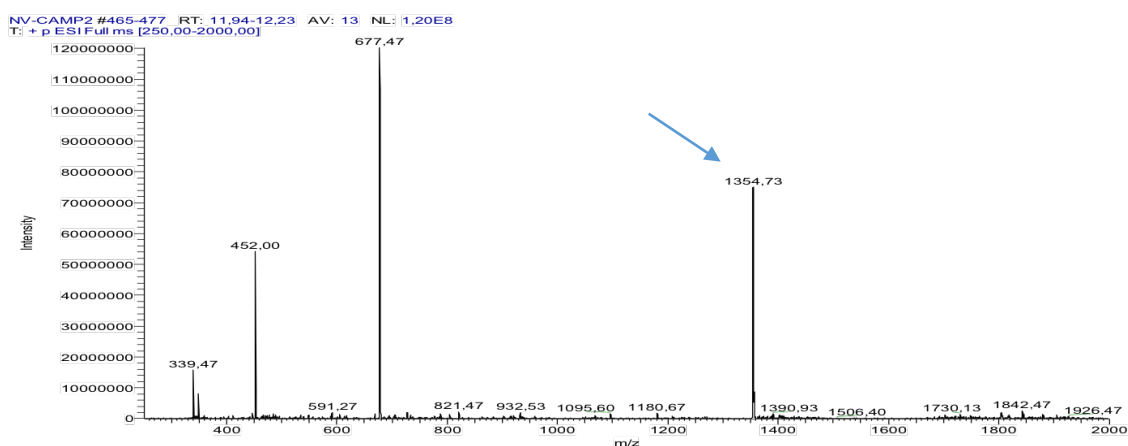


Figure 17 - Mass spectrum (LC-ESI/Orbitrap MS, positive mode) of the peptide CAM2 (manual synthesis).

### 3.1.3. CAMP3

The sequence and exact mass of the peptide CAMP2 by LC-MS (Figure 18). The HPLC chromatogram confirmed the formation of a main product, with  $t_r = 12.3$  min (Figure 19), which was identified as the target peptide CAMP3 by LC-MS analysis presenting the expected molecular mass of 1471.80 g/mol (Table 5).

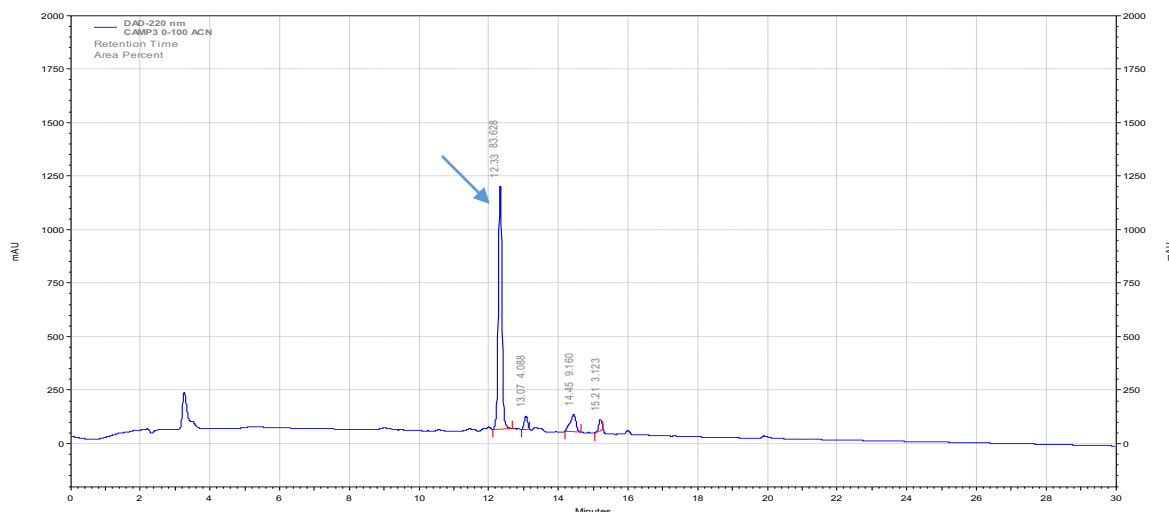


Figure 18 - Chromatogram of the product of the manual synthesis of the peptide CAMP3, acquired with a HPLC system, with a C18 column, using ACN in water with 0.05% TFA as eluent, in gradient mode (0 – 100%), for 30 minutes, at a flow of 1 mL/min and detection at  $\lambda = 220$  nm.



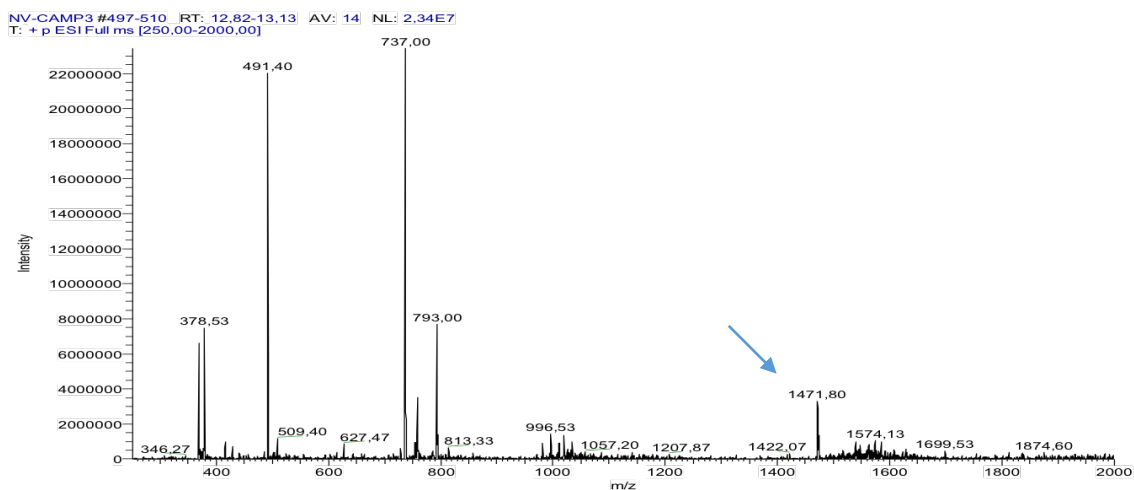


Figure 19 - Mass spectrum (LC-ESI/Orbitrap MS, positive mode) of the peptide CAMP3 (manual synthesis).

### 3.1.4. CAMP5

HPLC analysis revealed a light complex crude compound although the main peak (rt = 11.2 min), whose LC-MS analysis confirmed as the target peptide, which has an exact mass of 1401,8 Da (Table 5) (Figure 20 and 21).

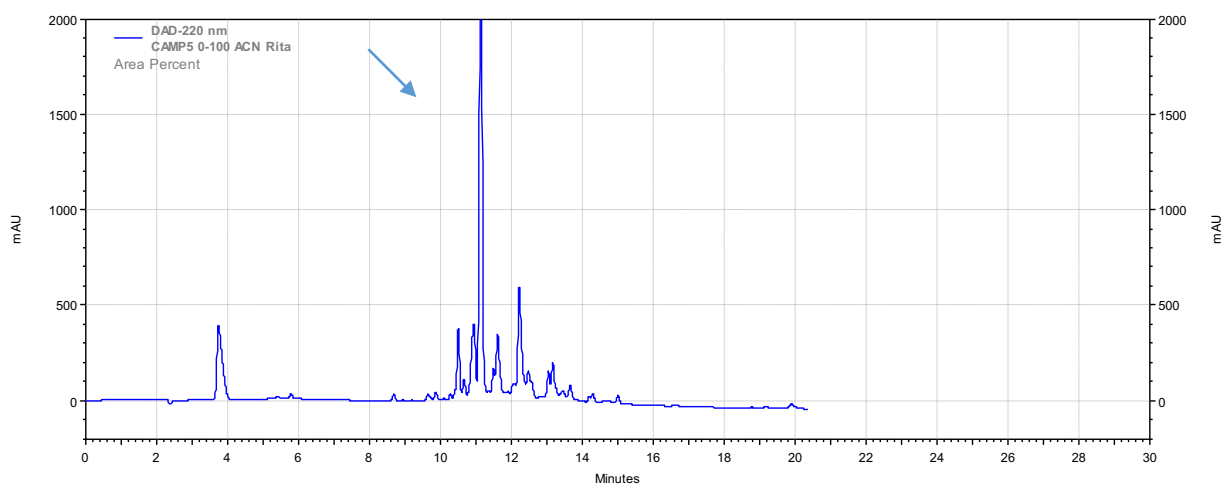


Figure 20 - Chromatogram of the product of the manual synthesis of the peptide CAMP5, acquired with a HPLC system, with a C18 column, using ACN in water with 0.05% TFA as eluent, in gradient mode (0 – 100%), for 30 minutes, at a flow of 1 mL/min and detection at  $\lambda = 220$  nm.

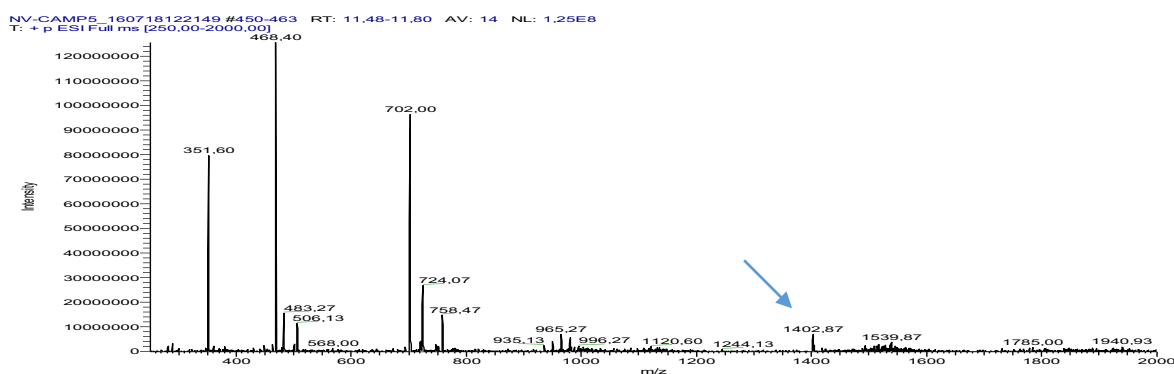


Figure 21 - Mass spectrum (LC-ESI/Orbitrap MS, positive mode) of the peptide CAMP5 (manual synthesis).

### 3.1.5. CAMP7

The isolated product was analysed by HPLC and by LC-MS, yielding the chromatogram and mass spectrum presented in Figure 22 and Figure 23, respectively. Results obtained confirmed that CAMP7, whose molecular weight is 1297.80 g/mol, was the larger peak of this synthesis ( $r_t = 12.9$  min) (Table 5).

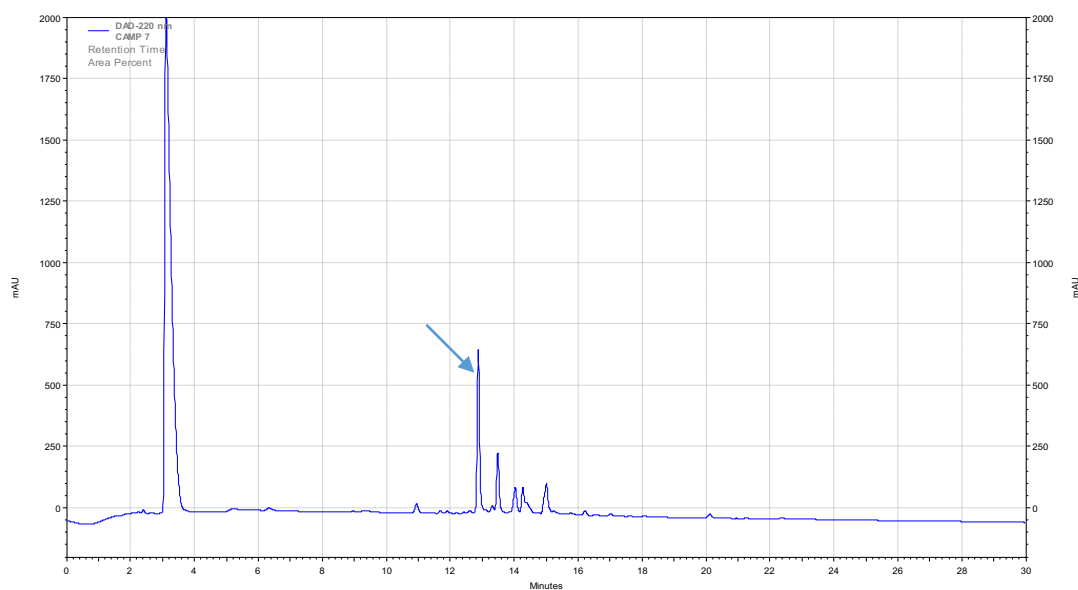


Figure 22 - Chromatogram of the product of the manual synthesis of the peptide CAMP7, acquired with a HPLC system, with a C18 column, using ACN in water with 0.05% TFA as eluent, in gradient mode (0 – 100%), for 30 minutes, at a flow of 1 mL/min and detection at  $\lambda = 220$  nm.

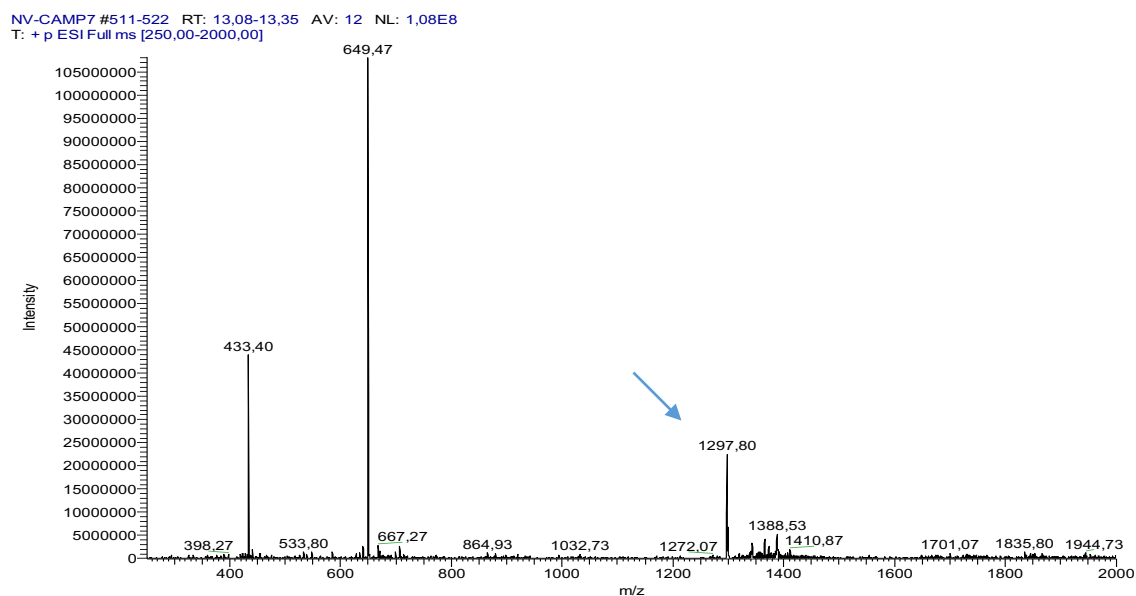


Figure 23 - Mass spectrum (LC-ESI/Orbitrap MS, positive mode) of the peptide CAMP7 (manual synthesis).

The general peptide products obtained by manual synthesis were a success, it was decided to carry out their purification.

Peptide	Exact mass (Da)	Molecular mass observed (g/mol)	Retention time, $r_t$ (min)
CAMP1	1313.8	1314.7	11.7
CAMP2	1353.8	1354.7	11.3
CAMP3	1471.8	1471.8	12.3
CAMP5	1401.8	1402.8	11.2
CAMP7	1296.8	1297.8	12.9

Table 5 - The exact mass and molecular mass observed of the CAMP(n) peptides detected by LC-MS and retention time determined by HPLC.

### 3.2. Structural modification of CAMP with cinnamic derivatives

After synthesizing the target peptides, CAMP(n) were modified with an cinnamic acid derivate in N-terminal side, as described in the experimental procedure section. Results from the syntheses of compounds Cin+CAMP(n) are next described.

#### 3.2.1. Cin+CAMP1

Once dried in vacuum desiccator and then solubilized in 10% aqueous acetic acid, Cin+CAMP1 was analysed by HPLC (Figure 24) and LC-MS (Figure 25). HPLC analysis demonstrated a distinct main compound ( $r_t=15.5$  min).

The exact mass and observed molecular mass of Cin+CAMP1 were 1443.9 Da and 1444.7 g/mol, respectively confirmed the target peptide (Table 6).

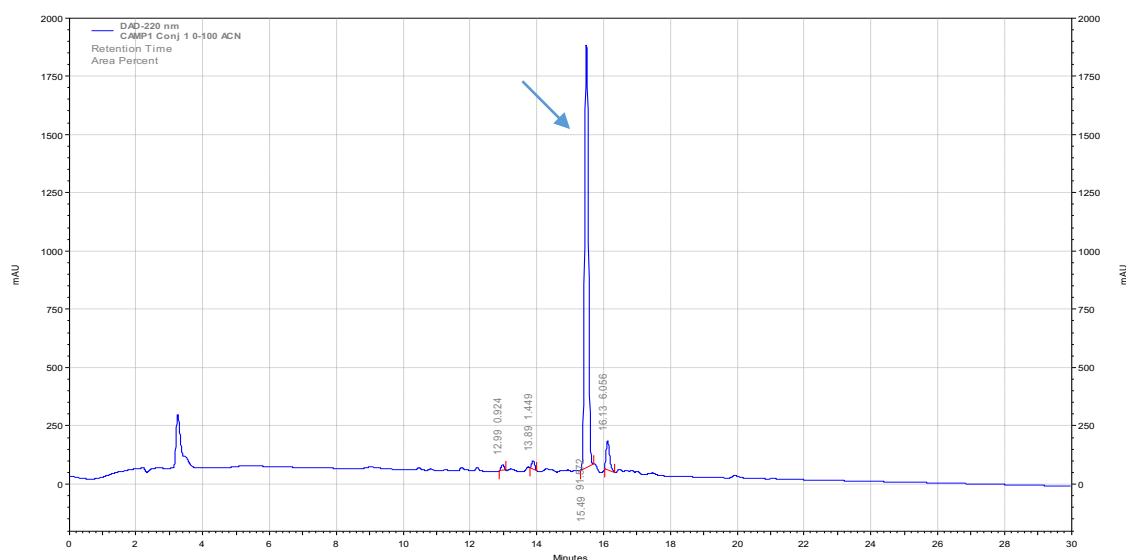


**Figure 24 - Chromatogram of the product of the manual synthesis of the peptide Cin+CAMP1, acquired with a HPLC system, with a C18 column, using ACN in water with 0.05% TFA as eluent, in gradient mode (0 – 100%), for 30 minutes, at a flow of 1 mL/min and detection at  $\lambda = 220$  nm.**

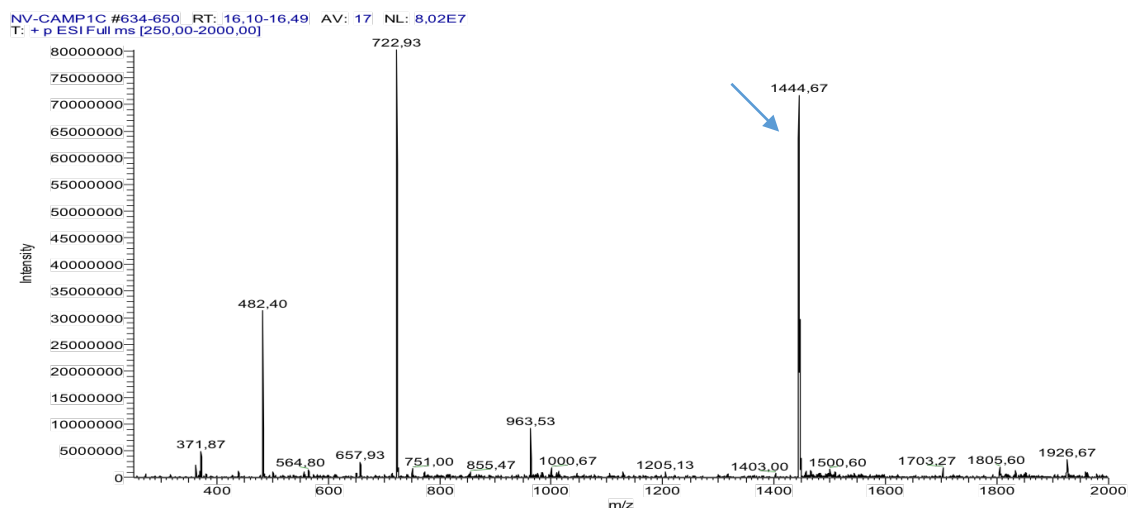


Figure 25 - Mass spectrum (LC-ESI/Orbitrap MS, positive mode) of the peptide Cin+CAMP1 (manual synthesis).

### 3.2.2. Cin+CAMP2

The isolated product was analysed by HPLC and by LC-MS, yielding the chromatogram and mass spectrum presented in Figure 26 and Figure 27, respectively. Results obtained confirmed that Cin+CAMP2, whose molecular weight is 1515.7 g/mol, didn't correspond to the larger peak of this synthesis ( $r_t = 14.6$  min) (Table 6).

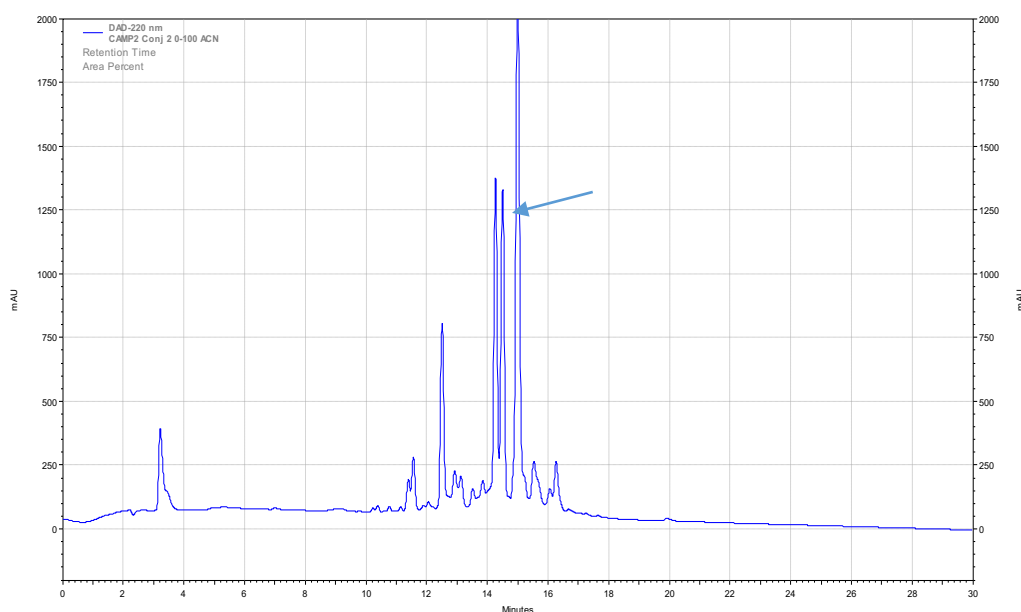
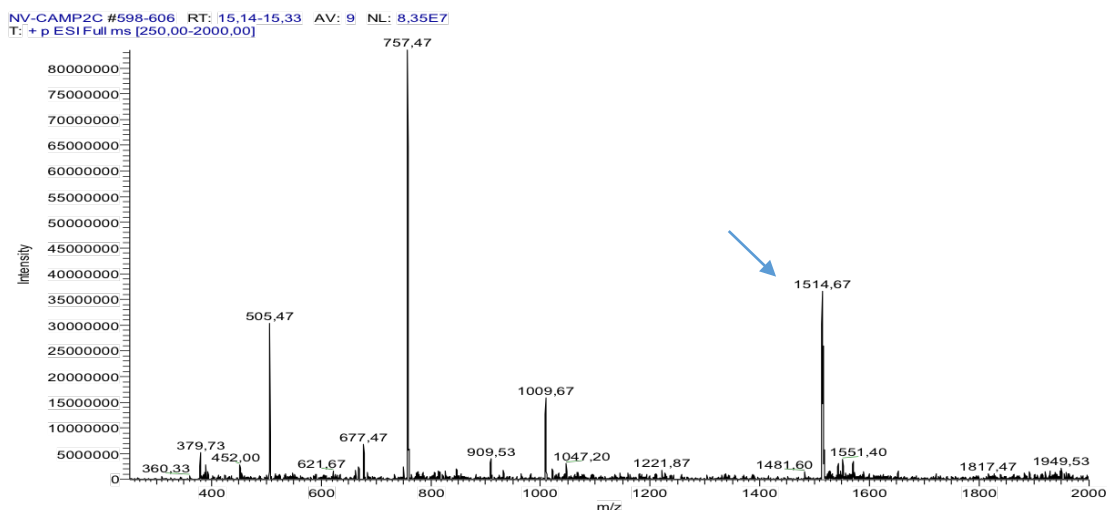


Figure 26 - Chromatogram of the product of the manual synthesis of the peptide Cin+CAMP2, acquired with a HPLC system, with a C18 column, using ACN in water with 0.05% TFA as eluent, in gradient mode (0 – 100%), for 30 minutes, at a flow of 1 mL/min and detection at  $\lambda = 220$  nm.



**Figure 27 - Mass spectrum (LC-ESI/Orbitrap MS, positive mode) of the peptide Cin+CAMP2 (manual synthesis).**

Together, these results show that the manual synthesis of Cin+CAMP2 results in a very complex combination of different products. The Automated MW-assisted Synthesis in the CEM Liberty1 peptide synthesizer of this peptide was performed, but similar results (not shown) were obtained. In the purification step was able to isolate the Cin+CAMP2 into three fractions, the first fraction consisted 100% of p-methoxycinnamic acid without double bond, second fraction composed by 50% with double bond and 50% without double bond of p-methoxycinnamic acid and last fraction was mainly constituted by 70.2% with double bond. The quality of the product p-methoxycinnamic acid was found to be the problem. Fraction 1 was choose to further antimicrobial test assays.

### 3.2.3. Cin+CAMP3

The HPLC chromatogram confirmed the formation of a major product of Cin+CAMP3, with  $t_r = 14.2$  min, whose LC-MS analysis confirmed as the target peptide, which has an exact mass of 1660.9 Da (Table 6) (Figure 28 and 29).

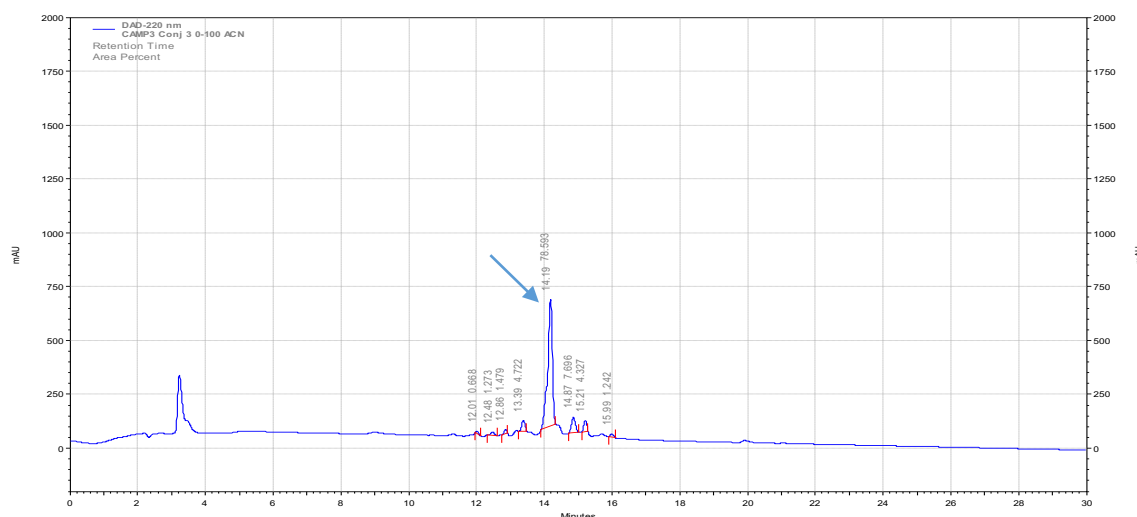


**Figure 28 - Chromatogram of the product of the manual synthesis of the peptide Cin+CAMP3, acquired with a HPLC system, with a C18 column, using ACN in water with 0.05% TFA as eluent, in gradient mode (0 – 100%), for 30 minutes, at a flow of 1 mL/min and detection at  $\lambda = 220$  nm.**

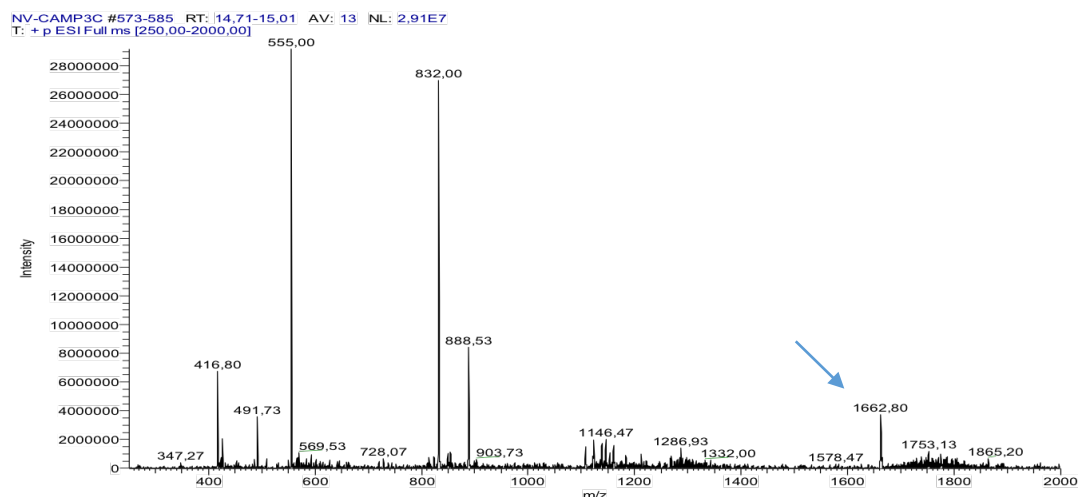


**Figure 29 - Mass spectrum (LC-ESI/Orbitrap MS, positive mode) of the peptide Cin+CAMP3 (manual synthesis).**

### 3.2.4. Cin+CAMP5

The synthesis of compound Cin+CAMP5 was carried out as described in the Experimental Section. The isolated product was analysed by HPLC and by LC-MS. The resulting chromatogram and mass spectrum are represented in Figure 30 and Figure 31, respectively. The HPLC chromatogram revealed the formation of a major product, with a  $t_r$  of 12.8 min, LC-MS analysis confirmed this product to have the molecular mass expected for compound of 1578.5 g/mol (Table 6 and Figure 31).

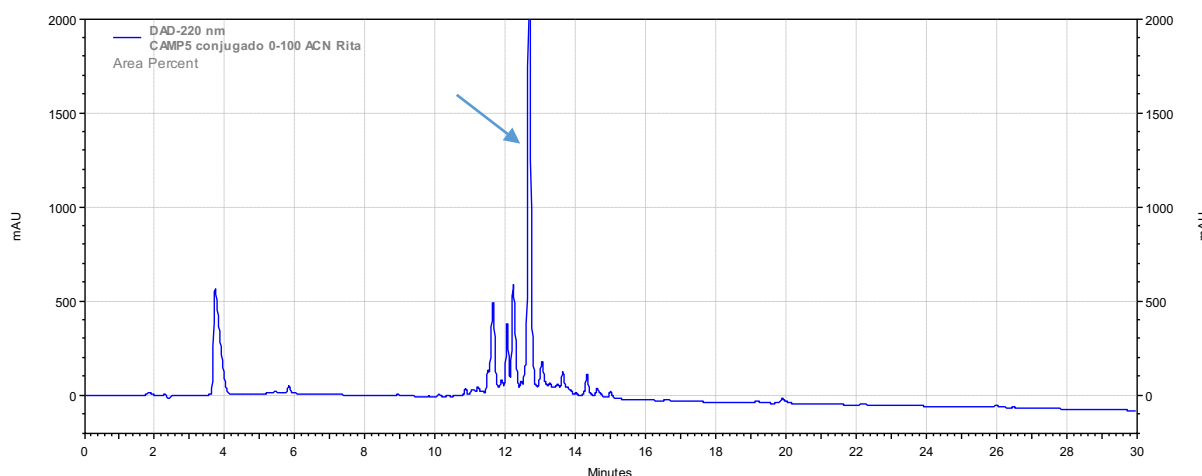


**Figure 30 - Chromatogram of the product of the manual synthesis of the peptide Cin+CAMP5, acquired with a HPLC system, with a C18 column, using ACN in water with 0.05% TFA as eluent, in gradient mode (0 – 100%), for 30 minutes, at a flow of 1 mL/min and detection at  $\lambda = 220$  nm.**

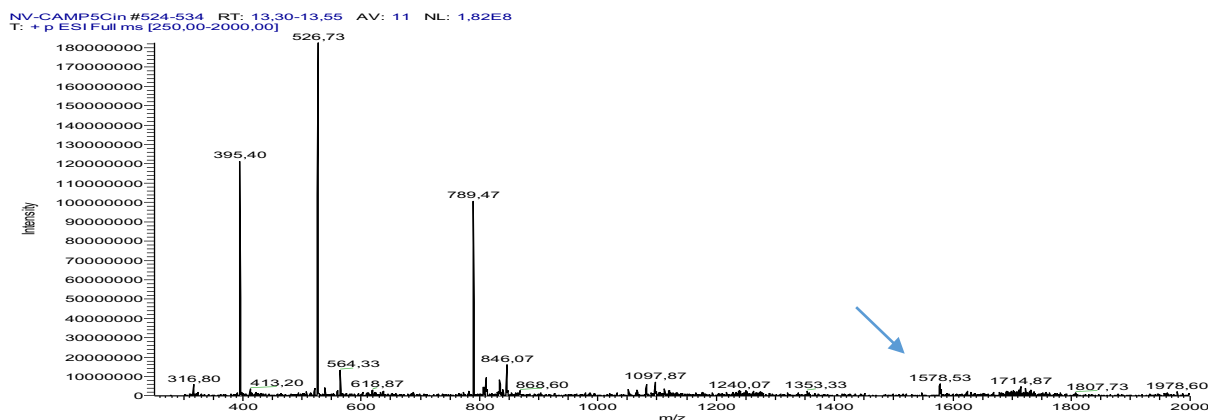


**Figure 31 - Mass spectrum (LC-ESI/Orbitrap MS, positive mode) of the peptide Cin+CAMP5 (manual synthesis).**



### 3.2.5. Cin+CAMP7

The sequence and exact mass of the peptide Cin+CAMP7 was obtained by LC-MS (Figure 33). The HPLC chromatogram confirmed the formation of a main product, with  $t_r$  = 14.2 min (Figure 32), which was identified as the target peptide CAMP3 by LC-MS analysis presenting the expected molecular mass of 1426.8 g/mol see in Table 6.

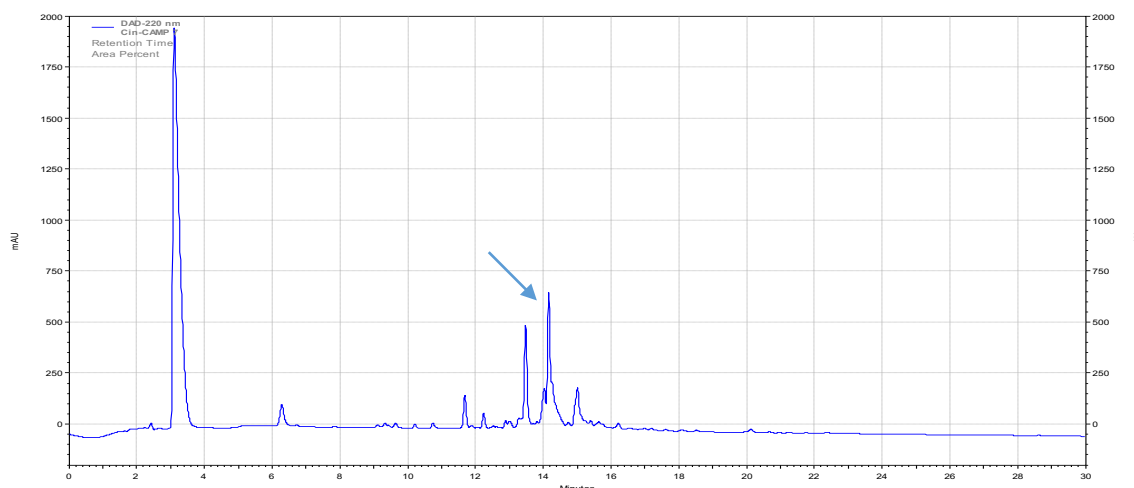


**Figure 32 - Chromatogram of the product of the manual synthesis of the peptide Cin+CAMP7, acquired with a HPLC system, with a C18 column, using ACN in water with 0.05% TFA as eluent, in gradient mode (0 – 100%), for 30 minutes, at a flow of 1 mL/min and detection at  $\lambda$  = 220 nm.**

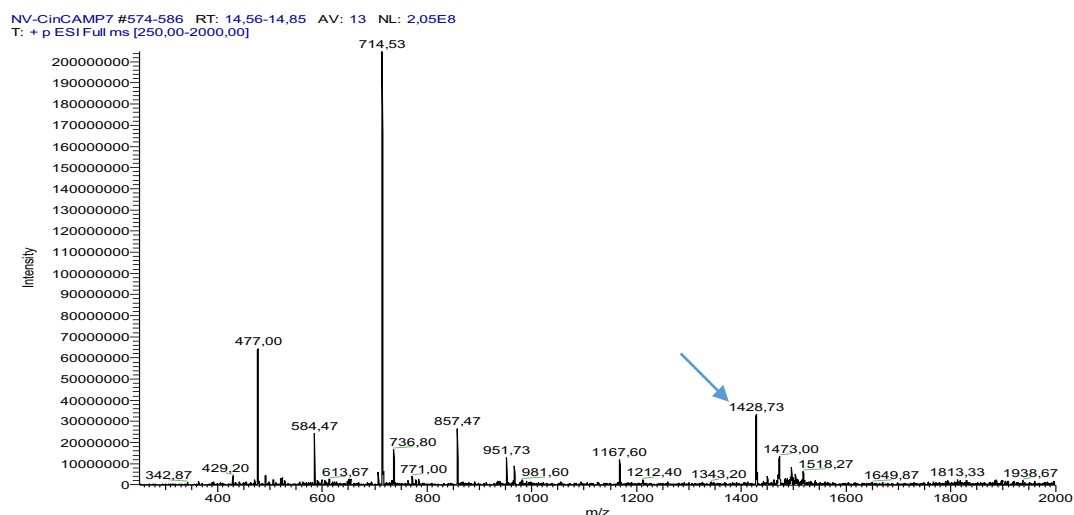


**Figure 33 - Mass spectrum (LC-ESI/Orbitrap MS, positive mode) of the peptide Cin+CAMP7 (manual synthesis).**

In Table 6 we can observe the exact mass, molecular mass observed and the retention time for each peptide obtained, using HPLC.

**Table 6 - The exact mass and molecular mass observed of the Cin+CAMP(n) peptides detected by LC-MS and retention time determined by HPLC.**

Peptide	Exact mass (Da)	Molecular mass observed (g/mol)	Retention time, $r_t$ (min)
Cin+CAMP1	1443.8	1444.8	15.6
Cin+CAMP2	1513.8	1514.7	14.7
Cin+CAMP3	1661.9	1662.8	14.2
Cin+CAMP5	1576.9	1578,5	12.8
Cin+CAMP7	1426.8	1428.7	14.2

### 3.3. Peptide Purification values.

Each peptide synthesized (CAMP(n) and Cin+CAMP(n)) were purified through RP-MPLC (previously described), the results obtained are displayed in Table 7 and graphic of purification analysis present in Supplementary information.

**Table 7 - Percentage of purification and amount of the manual synthesis CAMP(n) and Cin+CAMP(n). Purification step was performed as previously described in Experimental Procedures by RP-MPLC (purification analysis and quantification was made by HPLC, results in Supplementary information).**

<b>CAMPs</b>	<b>% of Purification</b>	<b>Amount (mg)</b>
CAMP1	99	17.1
Cin+CAMP1	96.1	24.1
CAMP2	98	28.4
Cin+CAMP2 Fraction 1	100	4.4
Cin+CAMP2 Fraction 2	50	2.3
Cin+CAMP2 Fraction 3	70.2	3
CAMP3	97	7.8
Cin+CAMP3	87.9	3.7
CAMP5 (1)	79.9	28.4
CAMP5 (2)	92.2	10.7
Cin+CAMP5	98	7.7
CAMP7	100	6.2
Cin+CAMP7	95.85	6.8

### 3.4. In vitro anti-tuberculosis assay

The in vitro anti-tuberculosis assay of the CAMP(n) and Cin+CAMP(n) were screened by visually comparing the growth and the morphology of the mycobacterial colonies with the control samples by light microscopy and through REMA method.

All ten peptides tested in this study showed concentration-dependent antibacterial activity against two clinical strains of *Mtb* (H37Rv and MDR). The results demonstrated that the peptides efficiently inhibited bacterial growth at varying MICs, summarized in Table 10. In general, all modified CAMPs demonstrated an enhance of the potency when compared with CAMP(n) peptides. The peptides with most pronounced activity against susceptible *Mtb* were Cin+CAMP 1 and 3 having a MIC of 44.33 and 38.51  $\mu\text{M}$ , respectively, resulting in a 45% increase in the peptide activity (Figure 34) (Table 10).

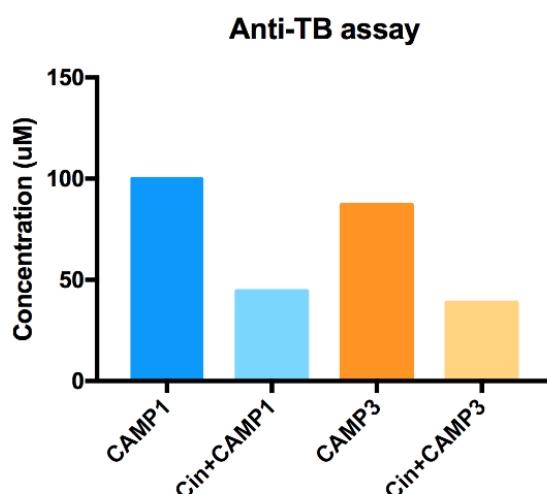


Figure 34 - MIC activities of CAMP1, Cin+CAMP1, CAMP3, Cin+CAMP3 against susceptible *Mtb* expressed in  $\mu\text{M}$ .

In contrast, Cin+CAMP5 appeared to be the least potent modified peptide, with a presence of bacterial growth even at 81.17  $\mu\text{M}$  ( $>128\mu\text{g/mL}$ ). For the CAMP(n) with exception of CAMP3, none was capable to stop the bacterial growth even in more than 90  $\mu\text{M}$  ( $>128\mu\text{g/mL}$ ).

At low concentrations of peptide is denoted inhibition of growth with a decreased of 50% when compared to the control wells. MIC50 of the most active peptide was 0.69  $\mu\text{M}$  (Cin+CAMP1) followed by 2.41  $\mu\text{M}$  (Cin+CAMP3) when compared to the respective CAMP1 and CAMP3 the MIC50 was 6.09  $\mu\text{M}$  and 5.44  $\mu\text{M}$ , respectively (Figure 35) (Table 8).

Table 8 - Reduction of MIC50 of Cin+CAMP(n) compared with IC50 of parental CAMP(n) against *Mtb*.

Peptides	Cin+CAMP1	Cin+CAMP2	Cin+CAMP3	Cin+CAMP5	Cin+CAMP7
% of Reduction	88.7	55.3	55.7	55.7	54.6

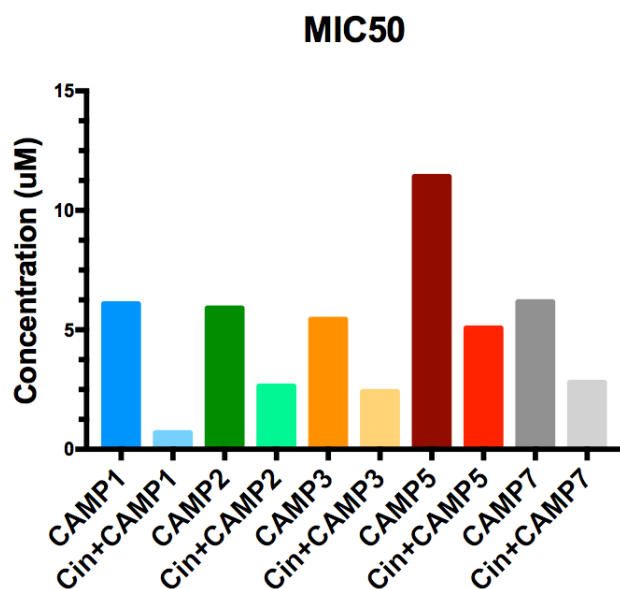
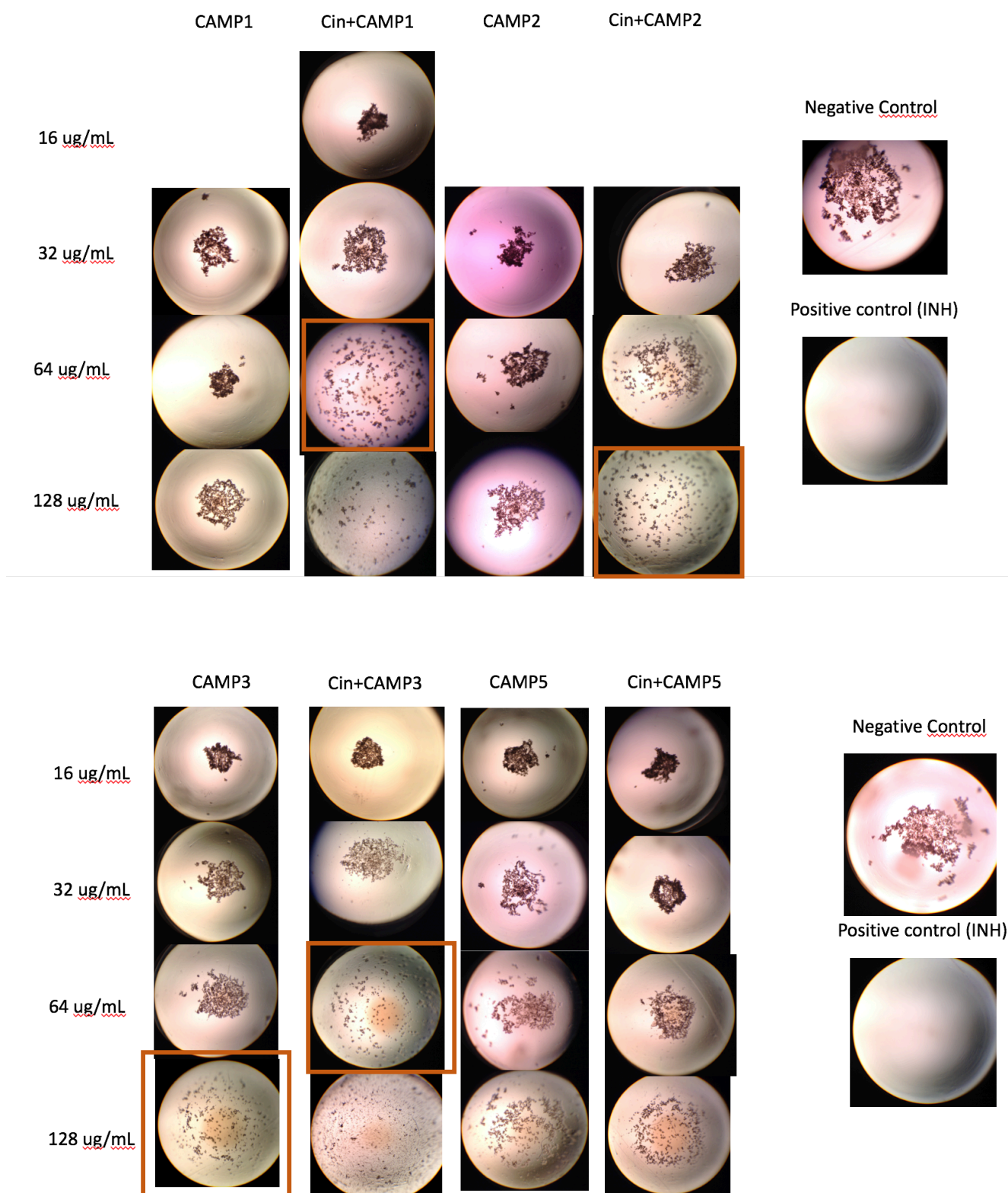
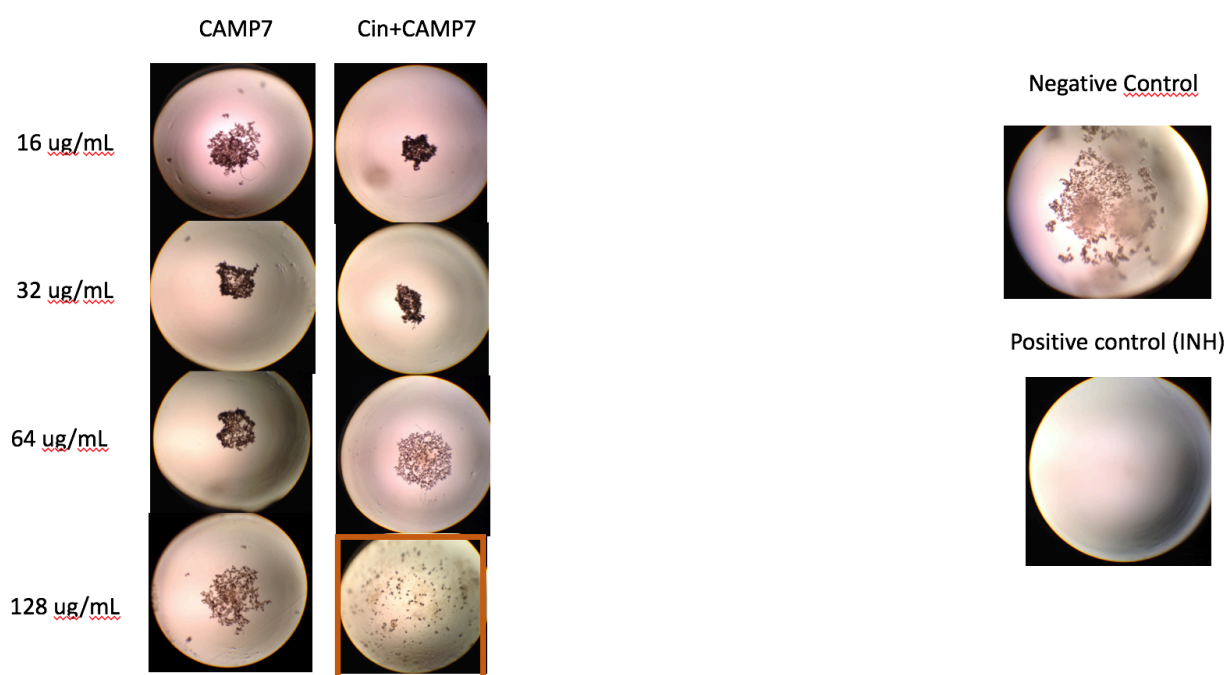


Figure 35 - MIC50 activities of CAMP(n) and Cin+CAMP(n) against susceptible Mtb expressed in uM.

With the increased concentration of peptide, the growth of mycobacteria was further inhibited and the improvement of antimicrobial activities was observed through microscope. The potential inhibited growth effect exhibited were characterised by a presence of disperse bacillus instead of remaining as colonies of aggregated mycobacteria seen in the control wells, see Figure 36.





**Figure 36 - In vitro anti-TB screening of D-AMPs activity against *Mtb* clinical isolates susceptible strain H37Rv; Representative light microscope images show the growth condition of the bacteria at various concentrations of CAMP(n) and Cin+CAMP(n) after 7 days of incubation. The framed images indicate the lowest concentrations of each peptide to inhibit 95% of bacterial growth compared with the growth control and further confirmed through REMA assay.**

Notably, against resistant strain of *Mtb* the antimicrobial potential of the Cin+CAMP1 was preserved with MIC of 44.33  $\mu$ M. The same pattern of improvement in activity with cin+CAMP(n) treatment over CAMP(n) treatment was observed, however, CAMP5 was the exception reflecting in a considerable increase of antimicrobial activity with 45.7  $\mu$ M. Despite that, Cin+CAMP3 showed the most effective inhibition of growth at low concentrations with an MIC50 of 0.6  $\mu$ M (Figure 37) (Table 9 and 10).

**Table 9 - Reduction of MIC50 of Cin+CAMP(n) compared with IC50 CAMP(n) against MDR-TB.**

Peptides	Cin+CAMP1	Cin+CAMP2	Cin+CAMP3	Cin+CAMP7
% of Reduction	94.3	55.3	77.9	8.3

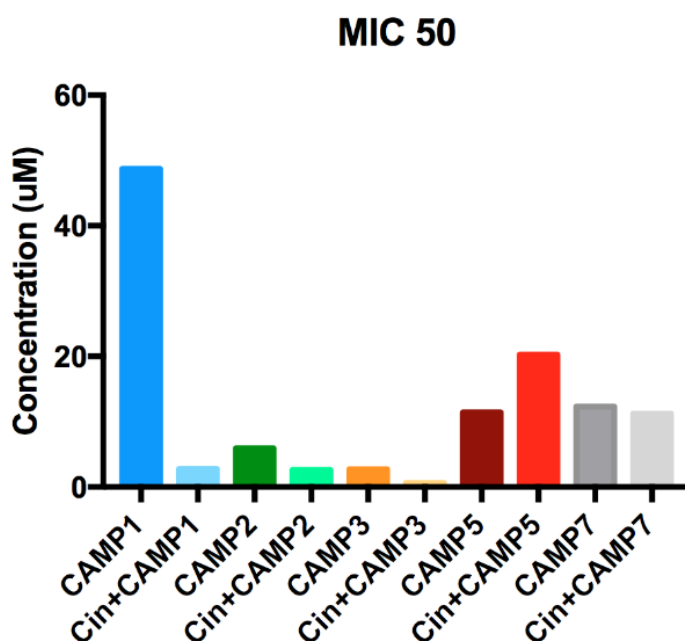


Figure 37 - MIC50 activities of CAMP(n) and Cin+CAMP(n) against Resistance Mtb MDR (INH,RIF and STR) expressed in µM.

Table 10 - Minimum inhibitory concentrations (MIC) of synthetic peptides against *Mtb* H37Rv and MDR *Mtb* (resistant to INH, RIF and STR) expressed in µg/mL and µM.

	MIC 50		MIC 95		MIC 50		MIC95	
	µg/mL	µM	µg/mL	µM	µg/mL	µM	µg/mL	µM
CAMP1	8	6.09	>128	>97.43	64	48.71	128	97.42
Cin+CAMP1	1	0.69	64	44.33	4	2.77	64	44.33
CAMP2	8	5.91	>128	>94.55	8	5.91	128	94.50
Cin+CAMP2	4	2.64	128	84.56	4	2.64	128	84.56
CAMP3	8	5.44	128	86.97	4	2.72	128	87.00
Cin+CAMP3	4	2.41	64	38.51	1	0.60	128	77.02
CAMP5	16	11.41	>128	>91.31	16	11.41	64	45.66
Cin+CAMP5	8	5.07	>128	>81.17	32	20.29	>128	>81.17
CAMP7	8	6.17	>128	>98.74	16	12.32	>128	>98.55
Cin+CAMP7	4	2.80	128	89.71	16	11.21	128	89.71



### 3.5. Determination of peptide cytotoxicity

The MTS assay was used to assess the cytotoxicity of the CAMPs. Initial cytotoxicity studies were carried out using macrophage-like THP-1 cells and all peptides showed a concentration-dependent cytotoxic effect. Previously tested CAMP(n) IC<sub>50</sub> values were applied in this study from the reference (Ramón-García et al. 2013). Comparison of the EC<sub>50</sub> values reveals the Cin+CAMP(n) have a substantially higher cytotoxicity than CAMP(n) (Table 11). Significant cytotoxic effects were observed at concentrations of 7.74 $\mu$ M for Cin+CAMP1 and 17.08 $\mu$ M for Cin+CAMP2 (Table 11) (Figure 38).

**Table 11 - Summary of IC<sub>50</sub> of CAMP(n) and Cin+CAMP(n) of the MTS assay performed in THP-1 cells. Results are an average of two independent repeated experiments. (1) Value of reference previously describe in (Ramón-García et al. 2013).**

CAMP	IC <sub>50</sub>	
	$\mu$ g/mL	$\mu$ M
CAMP1	48.04	24.3 <sub>(1)</sub> /36.57
Cin+CAMP1	11.17	7.74
CAMP2	-----	47.31 <sub>(1)</sub>
Cin+CAMP2	25.85	17.08
CAMP3	-----	87.0 <sub>(1)</sub>
Cin+CAMP3	40.37	24.29
CAMP5	-----	182.5 <sub>(1)</sub>
Cin+CAMP5	64.33	40.80
CAMP7	-----	197.2 <sub>(1)</sub>
Cin+CAMP7	61.23	42.91

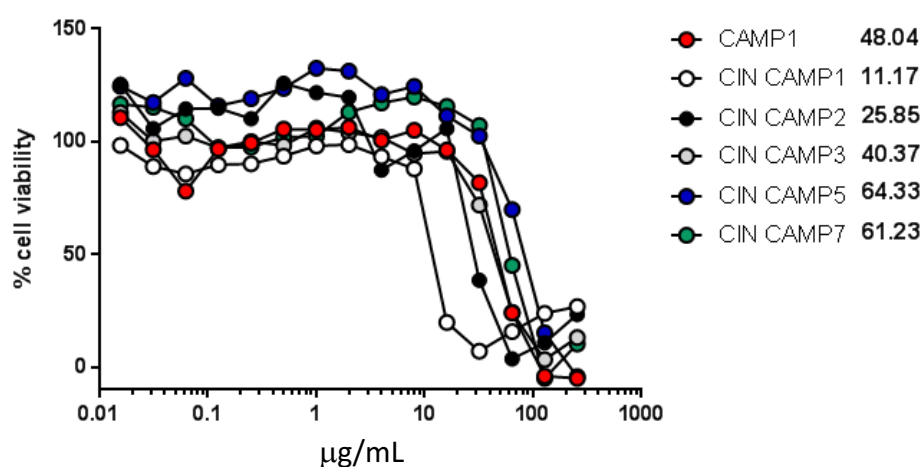


**Figure 38 - Cytotoxicity of CAMP1 and Cin+CAMP(n) on THP-1 cells. Values expressed in  $\mu$ g/mL, in collaboration with University of Minho.**

## 4. Discussion

The current increase of resistant *Mtb* strains to conventional antibiotics and poor patient compliance for the long and intense treatment has boosted the development of new active and less toxic compounds.

CAMPs arise as a potential candidate of drug-resistant TB for clinical use. This study intends to determine and optimize the properties of CAMPs already tested from (Ramón-García et al. 2013) in order to improve antimicrobial agents, specifically against resistant *Mtb* strains. After the crescent research on cinnamic acid, its antimicrobial activity and previous administration as a potential treatment of *Mtb* in late 19s (Warbasse, 1894), was decided to modify CAMPs with the addition of a cinnamic acid derivate in order to enhance the antimicrobial potential against *Mtb*. Briefly, in this study was synthesised and determined the antimycobacterial activity of 10 CAMPs which 5 have attached a cinnamic acid derivate.

In the article of the sequence peptide reference, Ramon-Garcia 2013 determined a MIC value of 1.1  $\mu\text{M}$  for the most effective and 24.7  $\mu\text{M}$  for the lowest effective of chosen peptides. Although with excellent results, the authors recur to modified MB 7h9 medium with no salts present ( $\text{Ca}^{2+}$ ,  $\text{Mg}^{2+}$  and  $\text{Na}^{+}$ ) known to inhibit the activity of cationic peptides at physiologic concentration. In the present work antimicrobial assay was performed with unmodified medium with present of cations in order to achieve the physiological condition as possible. The *in vitro* growth and MIC values were obtained by visual inspection and REMA assay to assure the results. In general, our results indicated that the presence of cations in the medium as a vast consequence on CAMP antimicrobial effect. Nevertheless, the copulation of cinnamic acid lend to an improvement on Cin+CAMP(n) activities, Cin+CAMP 1 and 3 were the most effective with total inhibition of cell growth. MIC50 and MIC90 values observed for those peptides were 0.69  $\mu\text{M}$  and 44.33  $\mu\text{M}$  for Cin+CAMP1 and 2.41 $\mu\text{M}$  and 38.51 $\mu\text{M}$  for Cin+CAMP3. For instances the MIC values determined for CAMP1 were 6.09  $\mu\text{M}$  and >97.43  $\mu\text{M}$  and for CAMP2 were 5.44  $\mu\text{M}$  and 86.97  $\mu\text{M}$ , an almost two-fold increase in concentration level is present. Another positive observation was that Cin+CAMP1 and Cin+CAMP3 appear to be equal effective against MDR strain. Unfortunately, the incorporation of cinnamic acid derivate into the CAMP(n) affect the cytotoxicity towards THP-1 cells and may be associated with a reduction of bacterial membrane selectivity after modification. Even though some of the peptide tested weren't effective in complete eradication of *Mtb*, some observational features in cell culture and MIC50 values make Cin+CAMP(n) still a promising compound.

Normally, in cell culture, the morphology of *Mtb* appears as aggregated clumps of

colonies. The reason is largely because of the widely complex mycobacterial cell wall rich in mycolic acids. In this study was observed that all Cin+CAMP(n) and some of CAMP(n) which not allows the formation of aggregates of colonies. A dispersion and scattered like effect was observed in all treated cultures with the exception of INH and STR. This behaviour may be explained due to the amphipathic properties of CAMPs. Which appears to affect the composition of the cell envelope and reduce virulence of *Mtb* in high concentrations of CAMP. Another two studies (Lan et al. 2014; Vermeer et al. 2012) described the same physiologic behaviour by antimicrobial peptides.

This should be taken in consideration due to the considerable differences in cell wall thickness which appears to be thicker in XDR strains. Also this can explain the partial increase of MIC values in presence of MDR strain.

In conclusion, was demonstrated that Cin+CAMP(n) can successfully inhibit the growth of both clinical isolates *Mtb* and MDR in vitro. The characteristic proprieties of CAMPs may also be effectively used to separate the aggregated *Mtb* by interacting with surface of mycobacteria. Cin+CAMP1 and Cin+CAMP3 hold, for now, a promising usage as drug adjuvant due to its effect on mycobacteria growth.

## 5. Conclusions and Future perspectives

At the end of this dissertation, we concluded that all proposed goals were accomplished. Both CAMP(n)s and Cin+CAMP(n)s were successfully synthesized by manual SPPS with high purification level.

The MIC value and inhibition of growth against *Mtb* and MDR-TB clinical isolate was proved enhance in modified CAMPs (Cin+CAMPs) when compared with CAMPs. The exception was Cin+CAMP5 which demonstrated the same MIC of CAMP5 against *Mtb* and for MDR-TB CAMP5 was observed with enhance activity over Cin+CAMP5.

In general, the coupling of cinnamic acid was proved to enhance the Cin+CAMP(n) activities. Unfortunately, the incorporation of cinnamic acid derivate into the CAMP(n) was also associated with loss of microbial selectivity demonstrating high levels of cytotoxicity towards THP-1 cells. Even though, observation features in cells culture and MIC50 values demonstrated an effective inhibition potential of Cin+CAMP(n) with the possible use adjuvant drug in the future.

Overall, this investigation project demonstrated the prospective value of Cin+CAMP(n) as new therapeutically approach against *Mtb* and MDR-TB.

In the future of this project, the next steps will require further optimization of Cin+CAMP(n) with the possible association with nanoparticles or Polyethylene glycol (PEG) delivery systems in order to lower the cytotoxicity observed. Moreover, possible evaluation of the synergy activity between Cin+CAMP(n) and conventional antibiotic.

## 6. Supplementary Information

### 6.1. Work Plan

The first phase of the project occurred in the Department of Chemistry and Biochemistry of Faculty of Sciences, University of Porto, for development the cationic antimicrobial peptides (CAMPs):

1. Five CAMPs with similar structure composed by 9 amino acids were synthesized using standard manual Fmoc SPPS. From the final volume of mass obtained, half was stored as CAMP without N-terminal modification (CAMP (n)) and the remainder was modified with N-terminal modification with the coupling of one cinnamic derivative.
2. Analysis and subsequent purification of the peptides was carried out by High Pressure Liquid Chromatography (HPLC) and Medium Pressure Liquid Chromatography (MPLC)
3. The product characterization was confirmed by Liquid chromatography-mass spectrometry (LC-MS/MS).
4. Final product obtained by lyophilization to remove the solvents present in the solution.

After peptide synthesis, the *Instituto Nacional de Saúde Dr. Ricardo Jorge* (INSA) in Porto was fundamental for the determination of the minimum inhibitory concentration (MIC) of the ten CAMPs against *Mtb*. The tasks were:

1. Antimicrobial activity for the ten CAMPs against MTB was determined through broth microdilution assay on a 96-well plate against *Mtb* H37Rv (standard strain and for quality control) and resistant clinical isolate MDR-Tb (resistance to INH, RIF and STR).
2. CAMPs were diluted in modify Middlebrook Broth 7H9 (BD BACTEC™ MGIT™) supplemented with 10% Middlebrook oleic albumin, dextrose and catalase (OADC) growth supplement (BD BACTEC™ MGIT™ OADC). Serial dilutions of peptide (from 128 µg / ml to 0.25 µg / ml) were prepared in a volume of 180 µl of medium and 20 µl of bacterial suspension (Mc Farland n°1) added to the 96-well plates making a final volume of 200 µl. Plates were sealed and incubated at 37 ° for 7 days. For the negative control 180 µl of medium plus 20 µL of suspension added without peptides, for the positive control was used isoniazid and streptomycin (INH and STR) as reference drugs.

3. After 7 days at 37° C, the growth of *Mtb* were screened by visually comparing the growth and the morphology of the mycobacterial colonies with the control samples by light microscopy and through REMA method.

In University of Minho was performed the cytotoxicity assay of the 5 Cin+CAMP(n) in order to determine the IC50 of the peptides against THP-1 human monocyte cell line:

1. IC50 determined by the MTS assay previously describe in the article (Ramón-García et al. 2013).

Finally, all data were statistically analysed using program Prism (GraphPad Software). One way or two-way ANOVA. All experiments were performed at least twice.

## 6.2. Peptides purification analysis.

HPLC analysis of all peptide purified (Figure 39 – 48).

### Camp1

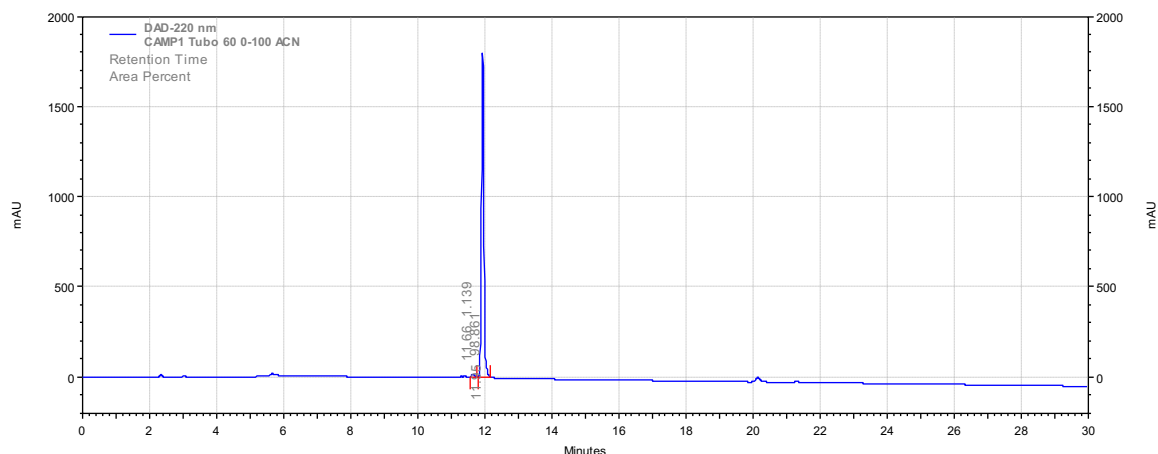


**Figure 39 - Chromatogram of the CAMP1 purified peptide, acquired with a HPLC system, with a C18 column, using ACN in water with 0.05% TFA as eluent, in gradient mode (0 – 100%), for 30 minutes, at a flow of 1 mL/min and detection at  $\lambda = 220$  nm.**

### Cin+CAMP1

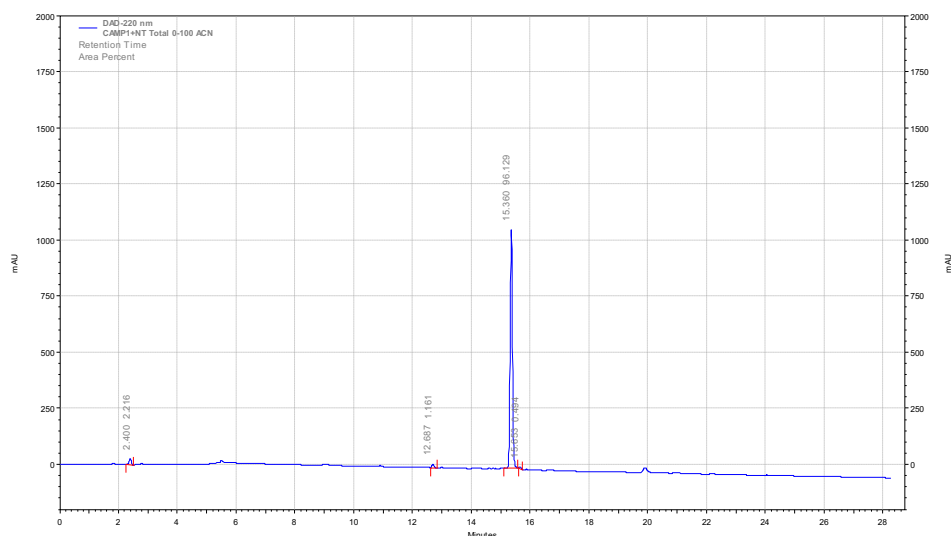


**Figure 40 - Chromatogram of the Cin+CAMP1 purified peptide, acquired with a HPLC system, with a C18 column, using ACN in water with 0.05% TFA as eluent, in gradient mode (0 – 100%), for 30 minutes, at a flow of 1 mL/min and detection at  $\lambda = 220$**

## CAMP2

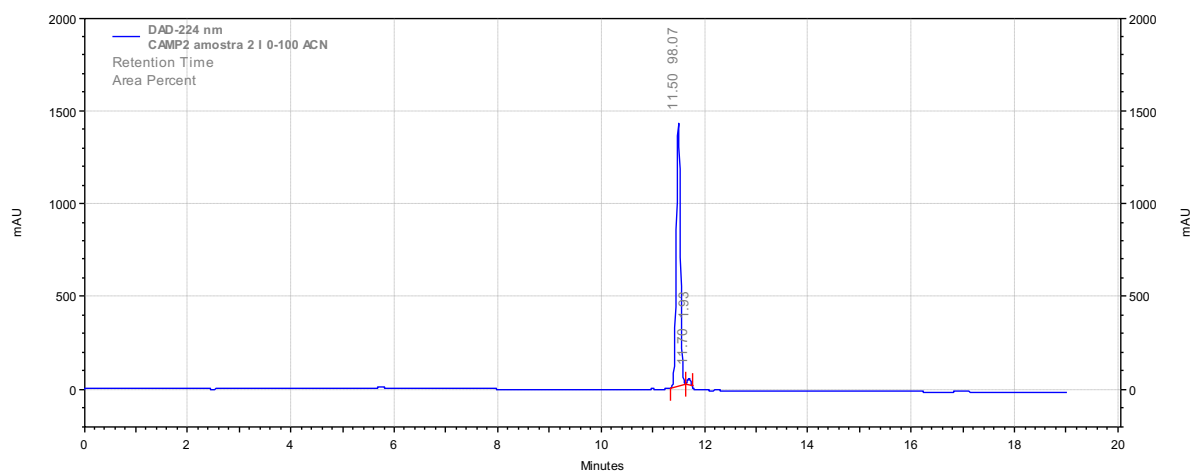


**Figure 41 - Chromatogram of the CAMP2 purified peptide, acquired with a HPLC system, with a C18 column, using ACN in water with 0.05% TFA as eluent, in gradient mode (0 – 100%), for 30 minutes, at a flow of 1 mL/min and detection at  $\lambda = 220$ .**

## Cin+ Camp 2

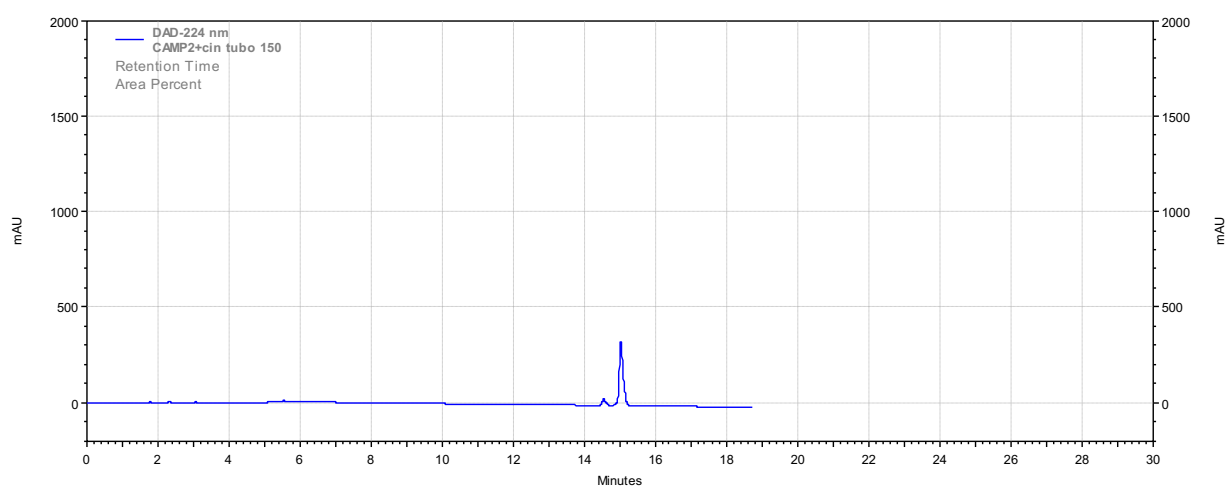


**Figure 42 - Chromatogram of the Cin+CAMP2 purified peptide, acquired with a HPLC system, with a C18 column, using ACN in water with 0.05% TFA as eluent, in gradient mode (0 – 100%), for 30 minutes, at a flow of 1 mL/min and detection at  $\lambda = 220$**



## CAMP3

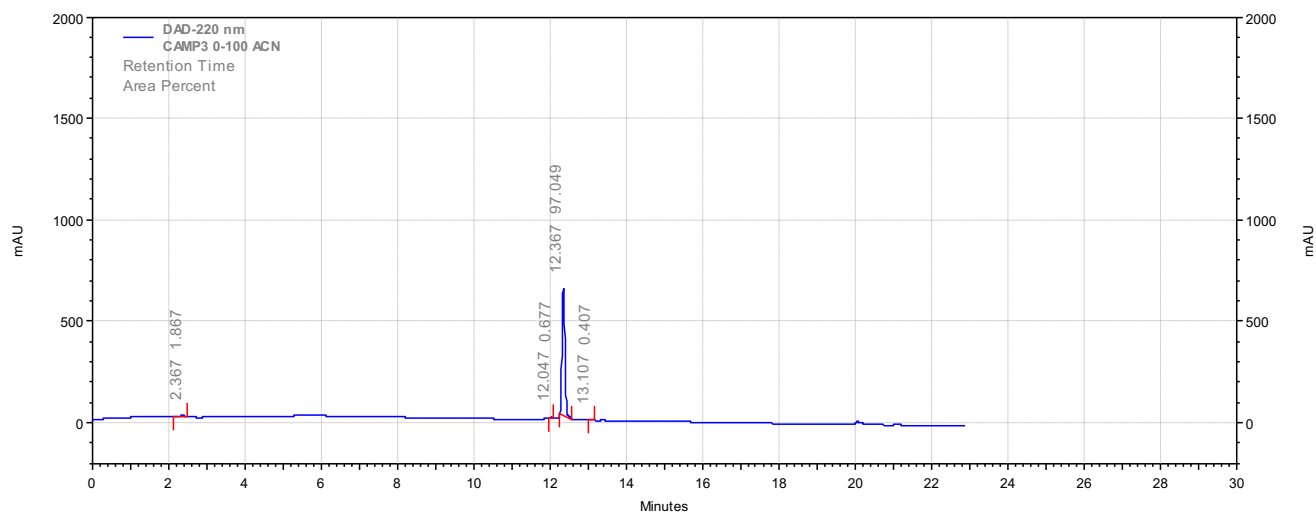


**Figure 43 - Chromatogram of the CAMP3 purified peptide, acquired with a HPLC system, with a C18 column, using ACN in water with 0.05% TFA as eluent, in gradient mode (0 – 100%), for 30 minutes, at a flow of 1 mL/min and detection at  $\lambda = 220$ .**

## Cin+CAMP3

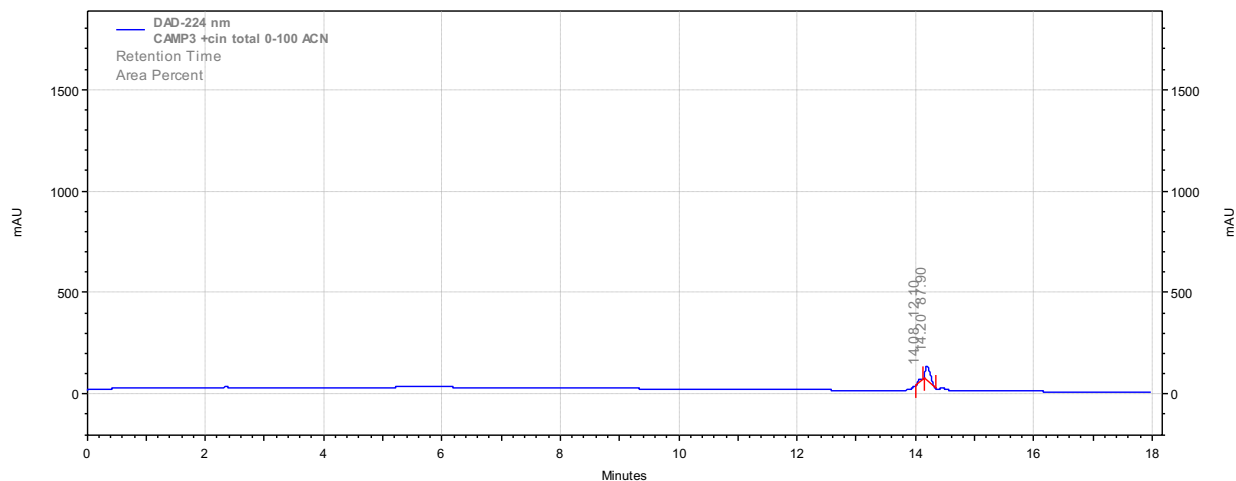


**Figure 44 - Chromatogram of the Cin+CAMP3 purified peptide, acquired with a HPLC system, with a C18 column, using ACN in water with 0.05% TFA as eluent, in gradient mode (0 – 100%), for 30 minutes, at a flow of 1 mL/min and detection at  $\lambda = 220$**

## CAMP5

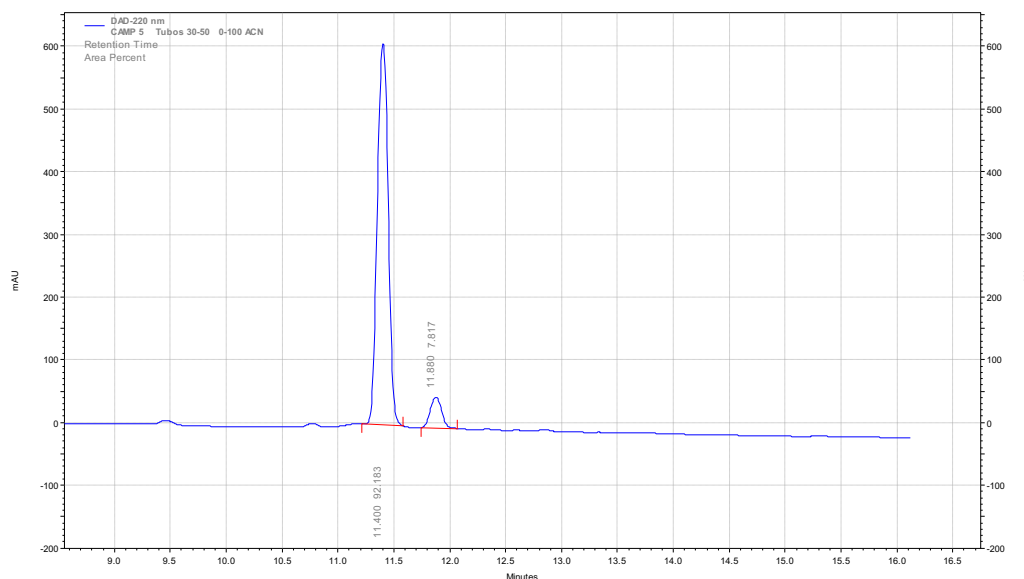


**Figure 45 - Chromatogram of the CAMP5 purified peptide, acquired with a HPLC system, with a C18 column, using ACN in water with 0.05% TFA as eluent, in gradient mode (0 – 100%), for 30 minutes, at a flow of 1 mL/min and detection at  $\lambda = 220$**

## Cin-CAMP5

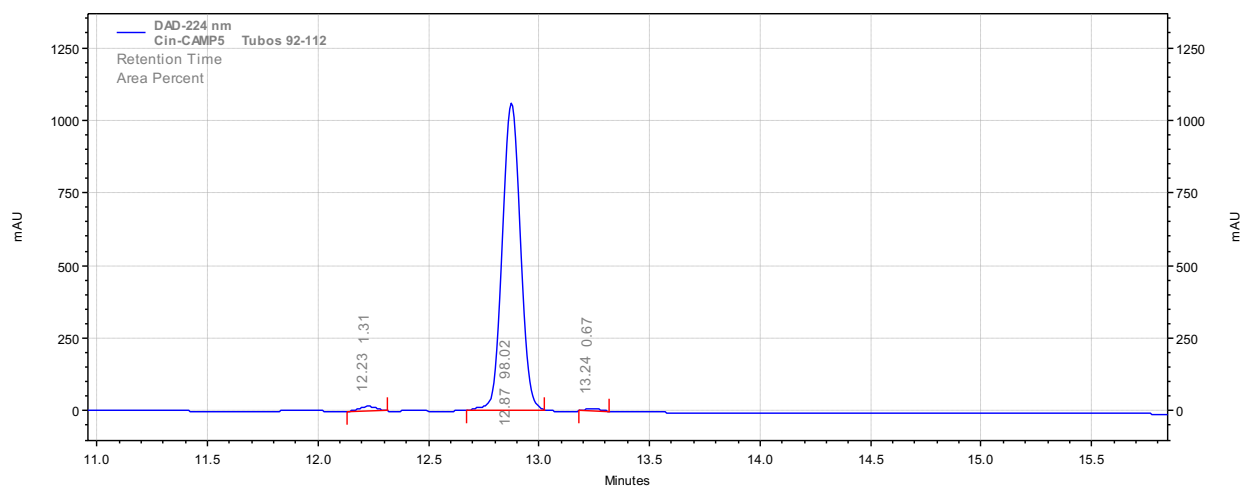


**Figure 46 - Chromatogram of the Cin+CAMP5 purified peptide, acquired with a HPLC system, with a C18 column, using ACN in water with 0.05% TFA as eluent, in gradient mode (0 – 100%), for 30 minutes, at a flow of 1 mL/min and detection at  $\lambda = 220$ .**

## Camp 7

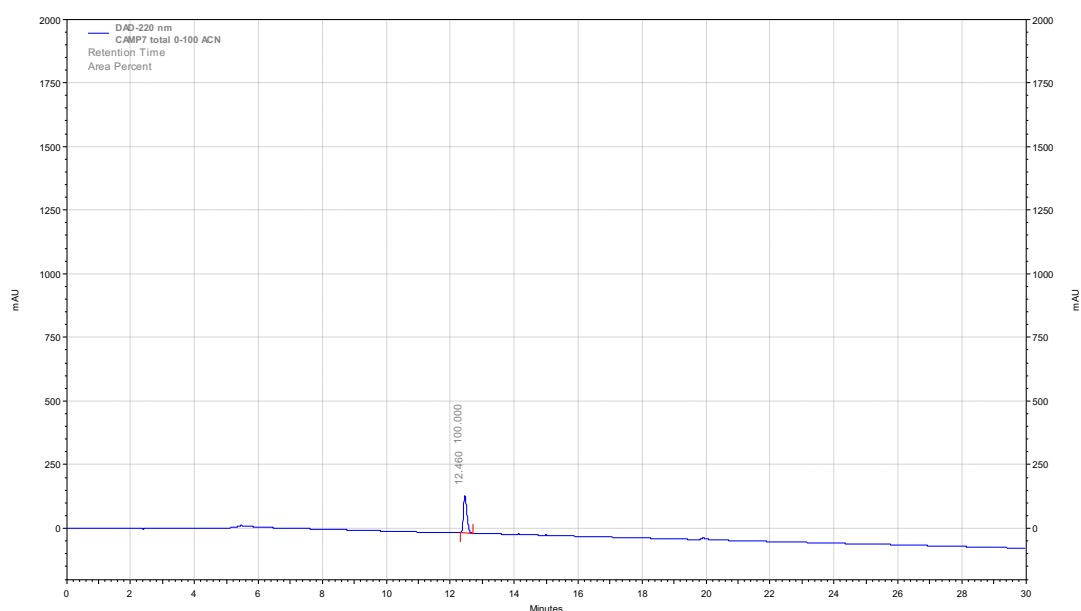


**Figure 47 - Chromatogram of the CAMP7 purified peptide, acquired with a HPLC system, with a C18 column, using ACN in water with 0.05% TFA as eluent, in gradient mode (0 – 100%), for 30 minutes, at a flow of 1 mL/min and detection at  $\lambda = 220$**

## Cin+camp7

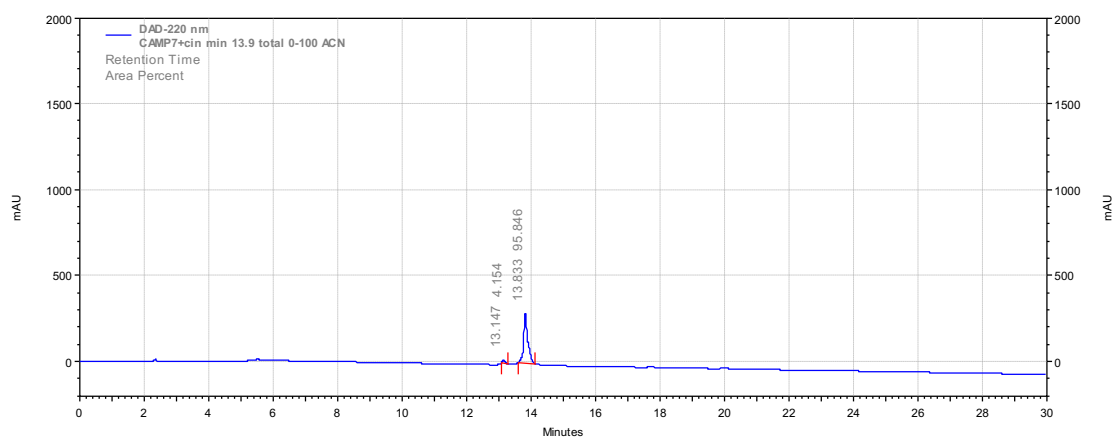


**Figure 48 - Chromatogram of the Cin+CAMP7 purified peptide, acquired with a HPLC system, with a C18 column, using ACN in water with 0.05% TFA as eluent, in gradient mode (0 – 100%), for 30 minutes, at a flow of 1 mL/min and detection at  $\lambda = 220$**

## 7. References

- Andrade-choa, Sergio et al. 2015. "Quantitative Structure-Activity Relationship of Molecules Constituent of Different Essential Oils with Antimycobacterial Activity against Mycobacterium Tuberculosis and Mycobacterium Bovis." *BMC Complementary and Alternative Medicine*: 1–11.
- Andries, Koen et al. 2005. "A Diarylquinoline Drug Active on the ATP Synthase of Mycobacterium Tuberculosis." *Science* 307: 223–27.
- BACHEM. 2014. "Solid Phase Solid Phase Peptide Synthesis." : 1–55.
- Behrendt, Raymond, Peter White, and John Offer. 2016. "Advances in Fmoc Solid-Phase Peptide Synthesis." *Journal of Peptide Science* 22(1): 4–27.
- Brogden, Kim A. 2005. "Antimicrobial Peptides: Pore Formers or Metabolic Inhibitors in Bacteria?" *Nature reviews. Microbiology* 3(3): 238–50.
- Brown, Lisa, Julie M Wolf, Rafael Prados-Rosales, and Arturo Casadevall. 2015. "Through the Wall: Extracellular Vesicles in Gram-Positive Bacteria, Mycobacteria and Fungi." *Nature reviews. Microbiology* 13(10): 620–30.
- Canadian Thoracic Society and The Public Health Agency of Canada and Licensor. 2014. "Chapter 2, Transmission and Pathogenesis of Tuberculosis." *Canadian Tuberculosis Standards, 7th Edition 2013*: 1–16.
- Carroll, James et al. 2010. "Comparison of the Activities of the Lantibiotics Nisin and Lacticin 3147 against Clinically Significant Mycobacteria." *International journal of antimicrobial agents* 36(2): 132–36.
- Carvalho, Samir A. et al. 2008. "Synthesis and Antimycobacterial Evaluation of New Trans-Cinnamic Acid Hydrazide Derivatives." *Bioorganic and Medicinal Chemistry Letters* 18(2): 538–41.
- Chevalier, Fabien Le et al. 2014. "Mycobacterium Tuberculosis Evolutionary Pathogenesis and Its Putative Impact on Drug Development." *Future microbiology* 9: 969–85.
- Cole, S T et al. 1998. "Deciphering the Biology of Mycobacterium Tuberculosis from the Complete Genome Sequence" *Nature* 393(6685): 537–44.
- van Crevel, Reinout, Tom H M Ottenhoff, and Jos W M van der Meer. 2002. "Innate Immunity to Mycobacterium Tuberculosis." *Clinical microbiology reviews* 15(2): 294–309.
- da Cunha, Nicolau B. et al. 2017. "The next Generation of Antimicrobial Peptides (AMPs) as Molecular Therapeutic Tools for the Treatment of Diseases with Social and

- Economic Impacts.” *Drug Discovery Today* 22(2): 234–48.
- Daletos, Georgios et al. 2015. “Callyaerins from the Marine Sponge *Callyspongia Aerizusa*: Cyclic Peptides with Antitubercular Activity.” *Journal of Natural Products* 78(8): 1910–25.
- Delogu, Giovanni, Roberta Provvedi, Michela Sali, and Riccardo Manganelli. 2015. “Mycobacterium Tuberculosis Virulence: Insights and Impact on Vaccine Development.” *Future Microbiology* 10: 1–18.
- Fattorini, Lanfranco et al. 2004. “In Vitro Activity of Protegrin-1 and Beta-Defensin-1, Alone and in Combination with Isoniazid, against Mycobacterium Tuberculosis.” *Peptides* 25(7): 1075–77.
- Gavrish, Ekaterina et al. 2014. “Lassomycin, a Ribosomally Synthesized Cyclic Peptide, Kills Mycobacterium Tuberculosis by Targeting the ATP-Dependent Protease ClpC1P1P2.” *Chemistry and Biology* 21(4): 509–18.
- Gleeson, Todd D., and Catherine F. Decker. 2006. “Treatment of Tuberculosis.” *Disease-a-Month* 52(11–12): 428–34.
- Guzman, Juan David. 2014. 19 Molecules Natural Cinnamic Acids, Synthetic Derivatives and Hybrids with Antimicrobial Activity.
- Hancock, R E W, and H G Sahl. 2006. “Antimicrobial and Host-Defense Peptides as New Anti-Infective Therapeutic Strategies.” *Nature biotechnology* 24(12): 1551–57.
- Hancock, Robert E W, and Robert Lehrer. 1998. “Cationic Peptides: A New Source of Antibiotics.” *Trends in Biotechnology* 16(2): 82–88.
- Hicks, Rickey P. 2016. “Antibacterial and Anticancer Activity of a Series of Novel Peptides Incorporating Cyclic Tetra-Substituted C( $\alpha$ ) Amino Acids.” *Bioorganic & medicinal chemistry* 24(18): 4056–65.
- Hoagland, Daniel T., Jiuyu Liu, Robin B. Lee, and Richard E. Lee. 2016. “New Agents for the Treatment of Drug-Resistant Mycobacterium Tuberculosis.” *Advanced Drug Delivery Reviews* 102: 55–72.
- Jenssen, Håvard, Pamela Hamill, and Robert E W Hancock. 2006. “Peptide Antimicrobial Agents.” *Clinical Microbiology Reviews* 19(3): 491–511.
- Jiang, Ziqing et al. 2011. “Anti-Tuberculosis Activity of  $\alpha$ -Helical Antimicrobial Peptides: De Novo Designed L- and D-Enantiomers versus L- and D-LL-37.” *Protein and peptide letters* 18(3): 241–52.
- Kaiser, E., C.D. Bossinger, R.L. Colescott, and D.B. Olsen. 1980. “Color Test for Terminal Prolyl Residues in the Solid-Phase Synthesis of Peptides.” *Analytica Chimica Acta* 118(1): 149–51.
- Kang, Su-Jin, Sung Jean Park, Tsogbadrakh Mishig-Ochir, and Bong-Jin Lee. 2014. “Antimicrobial Peptides: Therapeutic Potentials.” *Expert review of anti-infective*

- therapy 12(12): 1477–86.
- Kapoor, Rinki et al. 2011. “Efficacy of Antimicrobial Peptoids against Mycobacterium Tuberculosis.” *Antimicrobial Agents and Chemotherapy* 55(6): 3058–62.
- Khara, Jasmeet S. et al. 2014. “Anti-Mycobacterial Activities of Synthetic Cationic  $\alpha$ -Helical Peptides and Their Synergism with Rifampicin.” *Biomaterials* 35(6): 2032–38.
- Kohanski, Michael A, Daniel J Dwyer, and James J Collins. 2010. “How Antibiotics Kill Bacteria: From Targets to Networks.” *Nature reviews. Microbiology* 8(6): 423–35.
- Lakshmaiah Narayana, Jayaram, and Jyh-Yih Chen. 2015. “Antimicrobial Peptides: Possible Anti-Infective Agents.” *Peptides* 72: 88–94.
- Lan, Yun et al. 2014. “Cationic Amphipathic D-Enantiomeric Antimicrobial Peptides with in Vitro and Ex Vivo Activity against Drug-Resistant Mycobacterium Tuberculosis.” *Tuberculosis* 94(6): 678–89.
- Leung, A N. 1999. “Pulmonary Tuberculosis: The Essentials.” *Radiology* 210(2): 307–22.
- Linde, Charlotte M A, Sven E Hoffner, Essam Refai, and Mats Andersson. 2001. “Susceptible and Multi-Drug-Resistant Mycobacterium Tuberculosis.” : 575–80.
- Matsumoto, Makoto et al. 2006. “OPC-67683, a Nitro-Dihydro-Imidazoazole Derivative with Promising Action against Tuberculosis in Vitro and in Mice.” *PLoS Medicine* 3(11): 2131–44.
- McPhee, Joseph, Monisha Scott, and Robert Hancock. 2005. “Design of Host Defence Peptides for Antimicrobial and Immunity Enhancing Activities.” *Combinatorial Chemistry & High Throughput Screening* 8(3): 257–72.
- Melo, Mn, Rafael Ferre, and Marb Castanho. 2009. “Antimicrobial Peptides: Linking Partition, Activity and High Membrane-Bound Concentrations.” *Nature Reviews Microbiology* 7(March): 245–50.
- Miyakawa, Y et al. 1996. “In Vitro Activity of the Antimicrobial Peptides Human and Rabbit Defensins and Porcine Leukocyte Protegrin against Mycobacterium Tuberculosis.” *Infection and immunity* 64(3): 926–32.
- Nguyen, Liem. 2016. “Antibiotic Resistance Mechanisms in M. Tuberculosis: An Update.” *Archives of Toxicology* 90(7): 1585–1604.
- Niederweiss, Michael. 2013. “Physiology of Mycobacteria.” 2911(9).
- Ong, Zhan Yuin et al. 2014. “Effect of Stereochemistry, Chain Length and Sequence Pattern on Antimicrobial Properties of Short Synthetic  $\beta$ -Sheet Forming Peptide Amphiphiles.” *Biomaterials* 35(4): 1315–25.  
<http://www.ncbi.nlm.nih.gov/pubmed/24211081> (February 26, 2016).
- Ormerod, L. P. 2005. “Multidrug-Resistant Tuberculosis (MDR-TB): Epidemiology,

- Prevention and Treatment.” British Medical Bulletin 73–74: 17–24.
- Patel, Kavithkumar N, and Vikas N Telvekar. 2014. “European Journal of Medicinal Chemistry Design , Synthesis and Antitubercular Evaluation of Novel Series of N - [ 4- ( Piperazin-1-Yl ) Phenyl ] Cinnamamide Derivatives.” European Journal of Medicinal Chemistry 75: 43–56.
- Pawelczyk, Jakub, and Laurent Kremer. 2014. “The Molecular Genetics of Mycolic Acid Biosynthesis.” Microbiology Spectrum 2(4): MGM2-0003-2013.
- Pearson, C Seth et al. 2016. “Combined Bioinformatic and Rational Design Approach To Develop Antimicrobial Peptides against Mycobacterium Tuberculosis.” Antimicrobial agents and chemotherapy 60(5): 2757–64.
- Powers, Jon Paul S, and Robert E W Hancock. 2003. “The Relationship between Peptide Structure and Antibacterial Activity.” Peptides 24(11): 1681–91.
- Ramírez-Carretero, Santos et al. 2015. “Peptides from the Scorpion Vaejovis Punctatus with Broad Antimicrobial Activity.” Peptides 73: 51–59.
- Ramón-García, Santiago et al. 2013. “Targeting Mycobacterium Tuberculosis and Other Microbial Pathogens Using Improved Synthetic Antibacterial Peptides.” Antimicrobial Agents and Chemotherapy 57(5): 2295–2303.
- Riss, Terry L et al. 2013. “Cell Viability Assays.” Assay Guidance Manual [Internet] 114(8): 785–96.
- Rivas-Santiago, Bruno et al. 2013. “Activity of LL-37, CRAMP and Antimicrobial Peptide-Derived Compounds E2, E6 and CP26 against Mycobacterium Tuberculosis.” International Journal of Antimicrobial Agents 41(2): 143–48.
- Rosada, Rogério Silva et al. 2012. “Effectiveness, against Tuberculosis, of Pseudo-Ternary Complexes: Peptide-DNA-Cationic Liposome.” Journal of colloid and interface science 373(1): 102–9.
- Santos, Paola et al. 2012. “Effect of Antimicrobial Peptides on ATPase Activity and Proton Pumping in Plasma Membrane Vesicles Obtained from Mycobacteria.” Peptides 36(1): 121–28.
- Sarathy, Jansy Passiflora, Véronique Dartois, and Edmund Jon Deoon Lee. 2012. “The Role of Transport Mechanisms in Mycobacterium Tuberculosis Drug Resistance and Tolerance.” Pharmaceuticals 5(11): 1210–35.
- Schluger, Neil W. 2005. “The Pathogenesis of Tuberculosis: The First One Hundred (and Twenty-Three) Years.” American Journal of Respiratory Cell and Molecular Biology 32(4): 251–56.
- Schmidtchen, Artur, and Martin Malmsten. 2015. “(Lipo)polysaccharide Interactions of Antimicrobial Peptides.” Journal of Colloid and Interface Science 449: 136–42.
- Slavchev, Ivaylo et al. 2014. “Antimycobacterial Activity Generated by the Amide

- Coupling of (-)-Fenchone Derived Aminoalcohol with Cinnamic Acids and Analogues." *Bioorganic and Medicinal Chemistry Letters* 24(21): 5030–33.
- Smith, Issar. 2003. "Mycobacterium Tuberculosis Pathogenesis and Molecular Determinants of Virulence." *Clinical microbiology reviews* 16(3): 463–96.
- Somoskovi, A, L M Parsons, and M Salfinger. 2001. "The Molecular Basis of Resistance to Isoniazid, Rifampin, and Pyrazinamide in Mycobacterium Tuberculosis." *Respiratory research* 2(3): 164–68.
- Tanachatchairatana, Tanud, John Barnard Bremner, Ratchanaporn Chokchaisiri, and Apichart Suksamrarn. 2008. "Antimycobacterial Activity of Cinnamate-Based Esters of the Triterpenes Betulinic, Oleanolic and Ursolic Acids." *Chemical & pharmaceutical bulletin* 56(2): 194–98.
- Vermeer, Louic S. et al. 2012. "Conformational Flexibility Determines Selectivity and Antibacterial, Antiplasmodial, and anticancer Potency of Cationic  $\alpha$ -Helical Peptides." *Journal of Biological Chemistry* 287(41): 34120–33.
- WHO. 2016. "Global Tuberculosis Report 2016." Cdc 2016 (Global TB Report 2016): 214.
- Woods, Gail L, Shou-yeen Grace Lin, and Edward P Desmond. "Susceptibility Test Methods: Mycobacteria,." 1(31): 1215–38.
- Xie, J. P. et al. 2003. "In Vitro Activities of Small Peptides from Snake Venom against Clinical Isolates of Drug-Resistant Mycobacterium Tuberculosis." *International Journal of Antimicrobial Agents* 22(2): 172–74.
- Xu, Zhanyou et al. 2009. "Comparative Genome Analysis of Lignin Biosynthesis Gene Families across the Plant Kingdom." *BMC Bioinformatics* 10(Suppl 11): S3.
- Yeaman, Michael R, and Nannette Y Yount. 2003. "Mechanisms of Antimicrobial Peptide Action and Resistance." *Pharmacological reviews* 55(1): 27–55.
- Yoya, Georges Koumba et al. 2009. "Synthesis and Evaluation of a Novel Series of Pseudo-Cinnamic Derivatives as Antituberculosis Agents." *Bioorganic and Medicinal Chemistry Letters* 19(2): 341–43.
- Zasloff, Michael. 2002. "Organisms." 415(January): 389–95.



